JRC Scientific and Technical Reports

An assessment of weather-related risks in Europe: maps of flood and drought risks

Interim report for ADAM FP6 Integrated Project

Elisabetta Genovese, Nicola Lugeri, Carlo Lavalle, José I. Barredo (JRC-IES)
Marco Bindi, Marco Moriondo (DISAT - University of Florence)

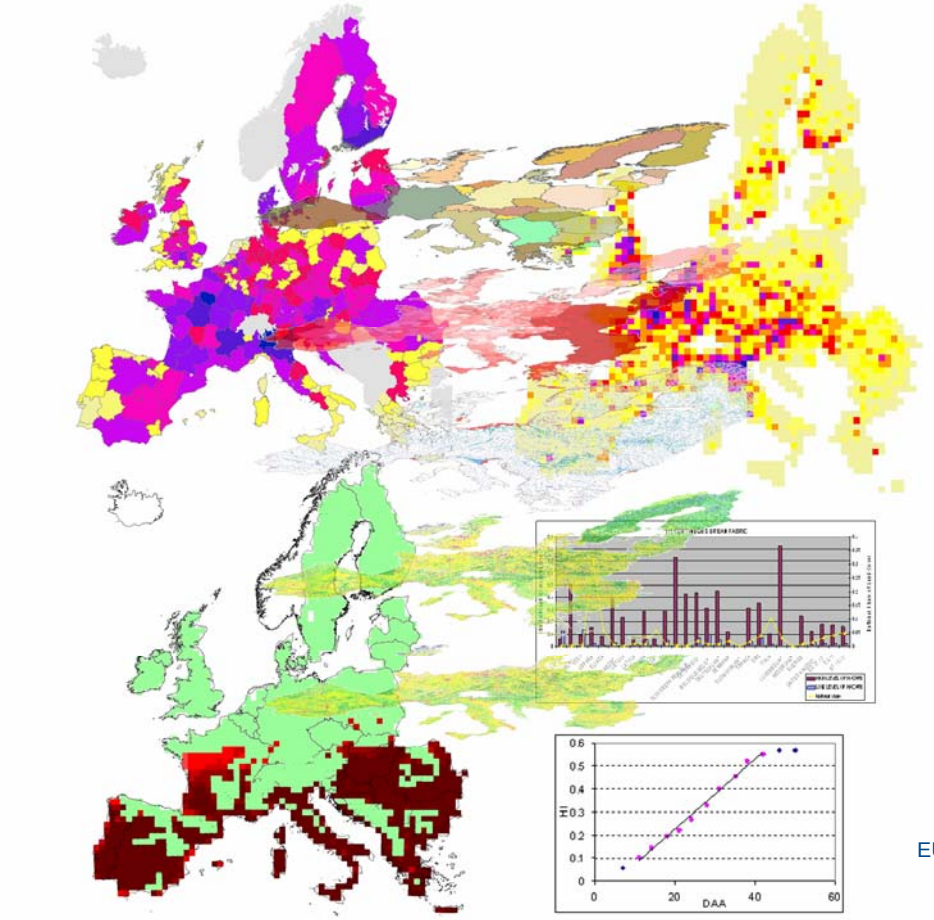

EUR 23208 EN - 2007

JRC
EUROPEAN COMMISSION

ies
Institute for Environment and Sustainability

The mission of the Institute for Environment and Sustainability is to provide scientific-technical support to the European Union's Policies for the protection and sustainable development of the European and global environment.

European Commission
Joint Research Centre
Institute for Environment and Sustainability

Contact information
Address: Nicola Lugeri
European Commission - DG JRC - Natural Hazards Action (NAHA)
IES-LMNH TP 261 Via E. Fermi 2749
21027 Ispra (Va) - Italy

E-mail: nicola.lugeri@jrc.it
Tel.: +39 0332 78 5187
Fax: +39 0332 78 9085

http://ies.jrc.ec.europa.eu/
http://www.jrc.ec.europa.eu/

JRC 42287

EUR 23208 EN
ISSN 1018-5593

Luxembourg: Office for Official Publications of the European Communities

Printed in Italy

Table of Content

Executive Summary

This technical report describes the adopted methodology and the outputs produced by task A2.1 during the first 18 months of life of the ADAM project.

The task 'A2.1 - An assessment of weather-related risks in Europe' has the following main objective:

"*Quantify and map weather-related extreme-event risks to public and private capital assets, human lives, and agriculture/forestry/tourism, and identify high-risk areas ("hot spots") on which to focus more detailed analysis.*"

The work benefits from the experience gained in several EU research projects, (such as EFAS, EFFIS, MICE, ESPON, MARS and ENSEMBLES) and is based on existing methodological approaches (e.g. Schelhaas, et al. 2003; Barredo et al. 2004, Moriondo et al. 2006) for the computation of impacts of extreme weather events.

The key innovative aspects of the work herein presented are manifold:

- the quantification of the **probabilistic monetary impact** of extreme events;
- the **combined use of modelling techniques and of observed data** to supply the lack of information at the various scales of relevance of the study;
- the **estimation of uncertainty** arising from limitations in data availability and modelling assumptions;
- the **geographical scale** (continental) of the exercise.

In short, the results herein presented, although still in a preliminary version, are unique because of their characteristics, format and way in which they have been produced.

The key outputs of task A2.1 are digital maps of risks from natural extremes at continental (i.e. European) scale identifying monetary/economic losses. The maps are furnished as input to other tasks of package A2 for successive modelling exercises and analysis.

As defined in the project work-plan, task A.21 has duration of 24 months. The 18-month deliverables are maps of flood and drought risks.

The report focuses on inland river flood damage to properties and infrastructures and on climatic stresses (drought and heat waves) in agriculture. Population exposure has only been addressed in a partial study and it's therefore not included in the final monetary losses assessment.

The work on floods has been carried out by the Institute for Environment and Sustainability of the Joint research Centre; the work on droughts and heat waves by the Department of Agronomy and Land Management – University of Florence.

The methodology is centred on the risk paradigm of the research community. The risk is defined as a product of hazard, exposure and vulnerability where:

- Hazard is the threatening natural event including its probability/magnitude of occurrence;
- Exposure is the values/humans that are present at the location related to a given event;
- Vulnerability is the lack of resistance to damaging/destructive forces (damage function).

This definition has been applied to extreme events such as floods and heat/water stresses, with the due adjustments required by data availability and specific modelling techniques (see Figure A).

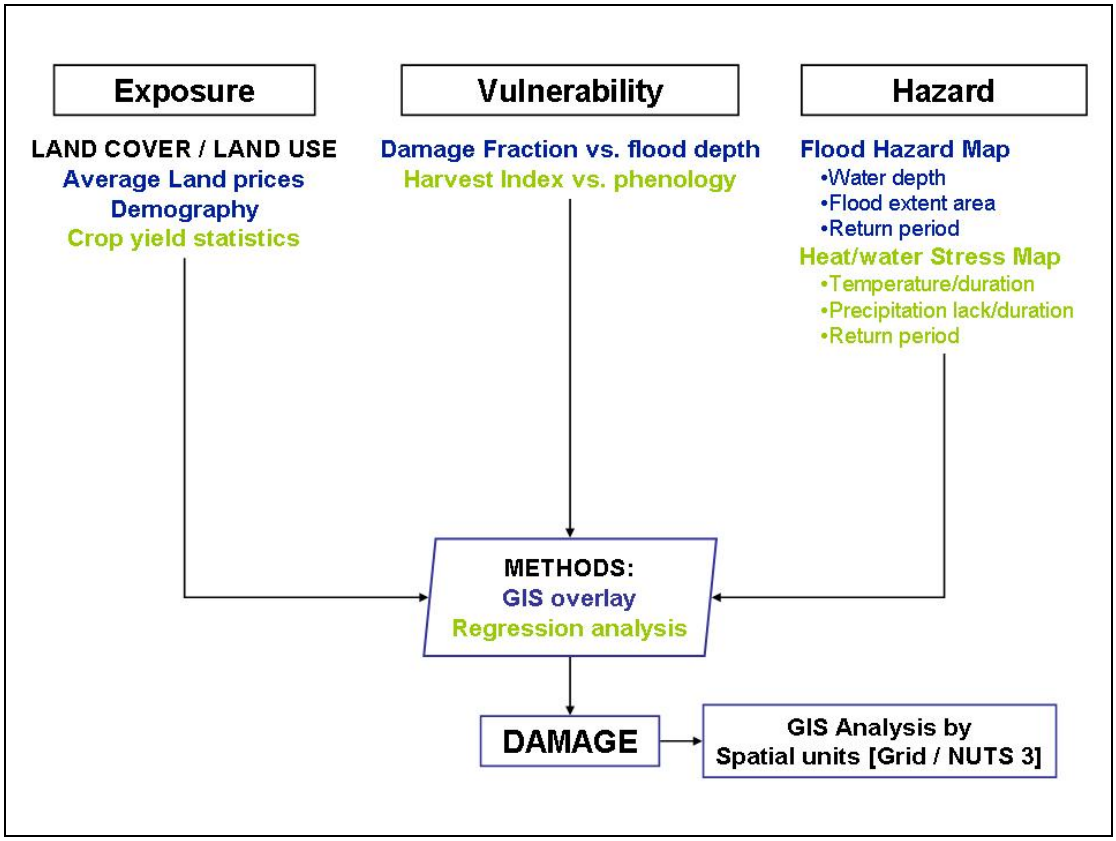

***Figure A**:Operational scheme for the application of the risk paradigm to floods (text in blue) and heat/water stresses (text in green).*

From the computational side, the methodology follows an approach based on the integrated assessment of information of the territory by using spatial analysis techniques. Such information can be derived from different sources and operational analyses (e.g. digital terrain models, land cover surveys, river network, etc.).

The collected datasets share the common location on the territory (geo-referencing). They may possibly have different degrees of resolution (grid size, minimum mapping unit) and in some cases accuracy (position, detail of information). The scale of the study and the data availability drive the choice on the datasets.

The grid-based final datasets are then further processed in terms of synthesis (aggregation, statistics) on wider territorial areas, which can be defined either physically (catchments, built-up areas….) or abstractly (administrative areas, geographical grids..).

The scale of the study is continental, so it falls into the so-called “Macro” scale risk assessment category.

The probabilistic aspect of the whole assessment process is included in the event-specific Hazard. As far as floods are concerned, the return periods for the maps of flood depth and flooded area extension are evaluated combining runoff statistics deduced from hydrological modelling (LISFLOOD, De Roo, 1999) and water levels calculated from the geomorphological characteristics of the catchment. LISFLOOD is a physically based and

spatially distributed model, integrated with a GIS (Geographical Information System) that provides an ideal environment for modelling processes in a landscape. The main advantage of LISFLOOD is that it uses input parameters that can be measured and can handle large databases. Additionally, it can run at different geographical scales and is therefore well suited to ingest data generated by regional climate models and/or to simulate runoff at catchment scale.

The general approach for the computation of potential monetary impact (direct risk) is centered on the definition of appropriate damage functions for floods and climatic-stresses respectively. The flood damage function takes into account only the flood depth as the cause of the damage and relates it to monetary damage for the assessment of direct damage as a consequence of flooding. The flood damage functions are specific for each land use type (e.g. residential, industrial, etc.) and for each of the 27 Member States of the European Union and are expressed per unit surface (e.g. hectare or square-meter). This approach represents a remarkable improvement with what was originally planned for A2.1, when the use of a single generalized damage function was envisaged for the whole of Europe. The new flood damage functions have been reconstructed in a dedicated study carried out by the JRC, outside the financing scheme of ADAM.

The final outcomes of the overall approach are maps of monetary damage computed for four return periods, with European coverage. For each return period, minimum and maximum values have been produced to highlight the range of uncertainty. These maps are further elaborated to produce the Average Annual Damage that allows comparison with economic indicators such as GDP and PPS.

Although it is difficult to find literature on studies performed at comparable scale and with comparable methodology, a preliminary evaluation of potential inaccuracies on the final damage figures has been performed by comparison with somewhat similar exercises carried out for Wales and England. The results are reasonably satisfactory, indicating that the computed values of damage fall within the respective uncertainty ranges. Indeed, the agreement would improve considerably when considering that a difference of values of about 30% is attributable to the exposure alone.

The financial damage affecting agriculture because of climatic stresses (drought and heat-waves) has been computed by converting the yield loss into monetary damage taking into account the average price paid to the farmer for a ton of yield averaged for the last 10 years. The Cropsyst model has been used to assess crop yield on the basis of the Regional Climate Model Cropsyst (Cropping Systems Simulation Model) is a multi-year, multi-crop, daily time step crop growth simulation model, developed with emphasis on a user-friendly interface (Stockle et al, 2003). The model simulates the soil water budget, the soil-plant nitrogen budget, crop canopy and root growth, crop phenology, dry matter production, yield, residue production and decomposition, and erosion.

On the basis of the monetary loss distribution over a period of 30 years, the frequency and return period of monetary loss has been assessed on the basis of a Gumbel distribution.

Digital maps of monetary loss in agriculture as consequence of droughts and heat-waves have been computed for the Guadiana Region and at European scale (limited to the Mediterranean area because of the analysed crop species) for two return periods.

With the aim to thoroughly describe the methodology, some results of European-wide analyses on exposure to floods are described in this report:

- Analysis of physical exposure (assets) based on land cover at Country level
- Historical trend (1990-2000) of physical exposure
- Potential exposure of population to floods in Europe

The final products of A2.1 are digital maps in GIS standard (ARC-Info GRID) and tabular (Excel-compatible tables) formats.

The detailed analysis of the produced results has not yet been performed and will be the subject of joint discussion with the other A2 tasks. However, a few considerations can be anticipated, hinting to the selection of hot-spots:

- there is an overall increase from 1990 of assets exposed to flood hazard in Europe. This is mainly due to new developments (e.g. new residential and industrial areas) in flood-prone areas;
- a group of Countries (namely: Slovenia, Luxembourg, Czech Republic, Hungary, Austria, Slovakia and Germany) presents higher exposure of urbanised land to floods;
- for 50 European NUTS-3 regions (e.g. provinces) the share of population potentially exposed to high flood risk is above 20% ;
- almost all of the newest Member States of the EU have a potential average annual damage due to floods higher than 1% of the respective GDP.

The remaining work to be carried out in months 19-24 will be mainly dedicated to the refinement of the products described in this report. In particular the following aspects of work will be considered:

- Extension to other hazards such as frost impacts on agriculture, forest fires and windstorms with contributions from other project partners.
- Improvements in data format following requirements from other tasks in A2. This aspect is essential to ensure that the data can be used as input into the micro and macro-economic models to be adopted in A2.3. However it is already envisaged that no further intensive data processing will be feasible.
- Quantification of inaccuracies and uncertainties. The proposed approach allows the quantification of direct impacts of extremes at continental scale but, due to the nature of the different data sets implied in the study, it does contain limitations coming mainly from the processes of geographical scale-conversion. The aim is to quantify such inaccuracies.
- The analysis performed for drought and heat-waves for Guadiana and the Mediterranean basin will be extended to the whole EU for the assessment of climate change impact in agriculture at continental level. The analysis will include major crops, and the economical losses as derived from this analysis will be weighted on the basis of relative importance of each crop
- Further pursue the calibration of the return period for flood events. Although it is considered that possible errors in the values of the return periods generally contribute to the final figures to a much lesser extent than the scale-conversion processes, it is envisaged to perform the calibration of selected test site (e.g. Tisza catchment and

possible other hot-spots) also making use of records of direct monetary losses for known flood events.

- Definition of ‘hot-spot’ following certain criteria such as loss/GDP, but this is not yet fixed at the current stage of the project and needs futher in coordination with other tasks in A2. Potential study areas are already identified in ADAM (e.g. Tisza and Guadiana catchments) and will be analysed in further detail. Other areas of potential interest are the Upper Danube, Austria and possibly some Mediterranean regions.

1 Introduction

1.1 State of the art

A great deal of knowledge exists on the risks (exposure, sensitivity and impacts) from sudden and slow-onset disasters due to extreme weather. The reinsurance industry (e.g., Munich Re), consulting firms (e.g., Risk Management Solutions), multi-lateral financial institutions (e.g., the World Bank), and NGOs (e.g. Red Cross and Red Crescent Societies) have worked together with the academic research community in estimating risks from extreme events across the globe. A number of EU research projects and services (MICE, ESPON, EFAS, MARS, ENSEMBLES) have focused on weather-related risks in Europe (see, for example, Maracchi, 2004; Parry, 2000; Moriondo, 2005). The impact of climate change on water-related anomalies (flood and drought) has been recently reviewed by the Commission of the EU Water Directors (2005).

However, there is still a lack of a European-wide consistent and probability-based approach for the quantification of impacts of extreme weather events. The need for such information as an aid to political and economic decision making is widely recognised (Berz et al., 2001).

This technical report describes the progresses of work and the results obtained thus far in WP A2.1 for the first project milestone (month 18).

Contributions from JRC and DISAT are hereby included. The work carried out by the JRC has dealt with the evaluation of flood risk in Europe, while DISAT focused on potential damages in agriculture by droughts and heat wave hazards.

The work benefits from experience gained in several EU research projects, and is based on existing methodological approaches (e.g. Schelhaas, et al. 2003; Barredo et al. 2004, Moriondo et al. 2006) for the computation of impacts of extreme weather events.

As far as flood hazard is concerned, the work is based on a methodological approach proposed by the JRC, with evaluation of physical losses and subsequent financial evaluation. The approach is based on the combination of land cover/flood hazard data in a GIS environment. The final output is the evaluation of potential financial losses at European level. A case-study (city of Prague) is also presented to further explain the procedure used to assess flood damage.

The evaluation of extreme climatic stresses (drought and heat waves) in agriculture is based on the use of crop growth models. These tools allow the quantitative assessment of yield loss and may be used for the simulation of the impact on final yield from extreme climate conditions.

The outputs, mainly database tables and maps, for floods and droughts are then ready to be interpreted and/or to be “injected” into further modelling processes, which in ADAM A2.2 concerns the projection of these risks to 2025 (quantitatively) and 2100 (qualitatively), and in A2.3 the assessment of present-day economic vulnerability to the risks of extreme weather in selected “hot spot” regions and sectors.

The key innovative aspects of the work herein presented are manifold:

- the quantification of the **probabilistic monetary impact** of extreme events
- the **combined use of modelling techniques and of observed data** to supply the lack of information at the various scales of relevance of the study;
- the **estimation of uncertainty** arising from limitations in data availability and modelling assumptions
- the **geographical scale** (continental) of the exercise.

In short, although the results herein presented are still in a preliminary version, they are unique because of their characteristics, format and way in which they have been produced.

1.2 Structure of the report

Chapter 2 defines the relevant terminology in the framework of natural hazards. Section 2.1 provides the theoretical basis for climate change impacts and emphasizes that, while natural hazards are caused primarily by natural events, they are also influenced by social, economic and political factors. A background on approaches to studying natural hazards is then developed (section 2.2), including a literature review and a definition of the terminology (section 2.3).

This is followed by an overview of the natural hazard types herein considered and their main characteristics (section 2.4).

Chapters 3 and 4 address the computation of the three components of the "risk triangle" (Fig. 2.1) for flood and water/heat stresses, respectively. The approach is methodological and operational. Therefore, the main issues driving the operational choices are discussed; firstly all the scale of the study and data availability. The impacts of weather-related risks are described, with the aim to establish an overall cost-estimate of losses, and the corresponding maps are presented. In particular, the work of JRC focuses on the economic aspects of flood damage by investigating the value of physical assets affected by the event. DISAT's approach focuses on the methods to assess the economical damage caused by yield losses due to extreme weather events. A territorial approach is pursued, in order to maintain as much as possible the direct link with the real, physical content of the places involved.

Analyses of exposure based on land use and hazard maps are performed at European level on a Country by Country basis and for a historical trend.

Chapter 5 concludes with an overview on advantages, major limitations and issues to be further explored.

2 Theoretical basis for natural hazards

In recent years, there has been an increase in extreme events such as river flooding and drought periods in several regions of Europe. The reasons for the increased risk are multiple and correlated. Potential climate changes are expected to cause a rise in the frequency as well as the intensity of extreme weather events, which may lead to more widespread and severe natural disasters. On the other hand, increased exposure, e.g. urban expansion along major rivers, causes increased damage.

A common approach is to focus upon natural hazards as predominantly or exclusively natural events. However, there are dangers in such an approach because hazard and disasters arise also from social reasons and backgrounds.

After discussing climate change impacts, we define the relevant terminology in the framework of natural hazards. This is followed by an overview of the natural hazard types here considered and their characteristics.

2.1 Climate change impacts

Climate change is one of the greatest environmental, social and economic threats faced by the planet. During the last century, the average temperature in Europe has increased by 0.95°C. In its Third Assessment Report, published in 2001, the UN Intergovernmental Panel on Climate Change (IPCC) projects that global average surface temperatures will rise by a further 1.4°C to 5.8°C by 2100.

According to the IPCC, “there is new and stronger evidence that most of the warming observed over the last 50 years is attributable to human activities, in particular to the emission of greenhouse gases” (IPCC, 2001a).

The magnitude of the impacts strongly depends on the nature and rate of future temperature increase. Consequences of climate change include an increased risk of flooding and drought, biodiversity losses, threats to human health and damage to economic sectors such as forestry, agriculture, tourism and the insurance industry (IPCC, 2001b).

Agricultural practices are weather dependent, and yields from a single crop vary significantly from year to year depending on each season’s weather. Therefore, any changes in climate may have repercussions on agriculture, e.g. warmer climate may cause winter-sown cereals to develop faster (Olesen and Bindi, 2002), emphasizing their vulnerability to spring frosts; drier and hotter summers may reduce water availability and increase the risk of heat stress for some crops.

The number of disastrous weather and climate-related events in Europe per year doubled over the 1990s compared with the previous decade, while non-climatic events such as earthquakes remained constant. Four of the five years with the largest economic losses have occurred since 1997 (EEA, 2004). In Europe these losses have increased substantially over the past 20 years to an average of EUR 10 billion in the 1990s.

Mitigating climate change is a key environmental priority for the European Union. The European Commission has recently launched a research project called PESETA (Projection of Economic impacts of climate change in Sectors of the European union based on botTom-up

Analysis) which is to contribute to a better understanding of the possible economic impacts induced by climate change in Europe over the 21st century (Feyen, 2006).

PESETA examines climate change impacts on the following sectors: coastal systems, energy demand, human health, agriculture, tourism, and river basin floods. This enables a comparison between them and therefore provides a notion of the relative severity of the damage inflicted. For each of these categories, a corresponding sector-based study is developed by the project partners.

Early results from PESETA show that the effects of climate change in Europe and the Arctic are already significant and measurable. Climate change will heavily affect Europe's natural environment and nearly all sections of society and the economy. Because of the non-linearity of climatic impacts and the sensitivity of ecosystems, even small temperature changes can have major effects.

In recent years, a number of research projects dealing with the impacts of climate change have been launched. Some projects have focused on specific sectors (e.g. ACCELERATE has pointed to investigate the relationship between land use and agriculture) or on wider themes (e.g. ATEAM has analysed the response of ecosystems to global changes). The project MICE has focused on the impacts of intensities and occurrence of extreme events in Europe. STARDEX has analysed statistical downscaling of extreme events looking at two variables: temperature and rainfall. PRUDENCE addressed the issues related to deficiencies in regional projection and to the quantification of confidence and uncertainties in prediction of future climate and its impacts. ENSEMBLE is developing a ensemble earth system prediction system.

ADAM workpackage 2.1 builds upon experiences matured in these projects and aims to fill the gap existing in the availability of European-wide consistent and probability-based information of the monetary impacts of extreme events (such as flood, drought and heat waves).

2.2 Background to natural hazard and study approaches

Although caused by natural events, natural hazards and disasters are products of an interaction between nature and the social, economical and political environment which “structures” and configures the lives of individuals and communities (Parker, 2000).

The “hazard paradigm” (White, 50s; Hewitt and Burton, 70s; Hewitt, 80s), in which flood and other hazards are primarily viewed as natural phenomena, has been a central and prevailing view in the hazards and disasters field for much of the twentieth century, although it has become increasingly criticized (Parker, 2000). This approach usually focuses upon the physical agents in the natural or human-modified environment, which cause a threat to society.

From this perspective, hazards are viewed as an objective condition present inside our environment to be investigated as a particular natural process. Therefore parameters such as flood probability, flood depth, rainfall-runoff lag times, flood hydrographs and the flood depth-damage relationship become the focus in order to make the event measurable.

The main competing approach is based upon the view that social, economical and political conditions are overcoming and gaining importance in the incidence and distribution of

disaster damage. Therefore natural disasters are not viewed as natural phenomena but as being produced by society. During the 1970s and 1980s, a number of studies reinforced the power of this explanation (Hewitt, 1983; Watts, 1983). Whereas in the "hazard paradigm" the hazards are viewed as external agents affecting society, in the "social agents" approach vulnerability to disasters is concerned with the internal state of society (Hewitt, 1997)

Central to this "social agents" approach are therefore the concepts of **Exposure** and **Vulnerability**. The first, is a measure of the human population, land uses and investment located in areas (in the case of floods) at risk of flooding; exposure is growing rapidly as human occupation of floodplains and flood-prone coastal zones intensifies and it's a prime, contributory cause of flood disasters. The second is viewed as essential to the origins and causes of flood disasters; vulnerability comes into play through various aspects: dwellings with little resistance to floods, the quality of buildings, lack of protection from floods, weaknesses of the population related to age, gender, health status and infirmity. Similar examples could be drawn up for droughts and heat-waves. Inability to avoid or recover from a disaster and low levels of protection or assistance are also contributing social factors.

2.3 Terminology for estimating natural disaster risk

It is of the highest importance to establish clear definitions and a common vocabulary in order to facilitate the definition of terms like *risk*, *hazard*, *exposure* and *vulnerability*. This paragraph defines the relevant terms in more detail.

The first step towards the definition of a strategy for the prevention of natural disaster is the definition and evaluation of the risk (Barredo, 2004).

Today, the term *risk* has a range of meanings and several dimensions connecting to safety, economic, environmental and social issues. These different meanings often reflect the needs of specific decision-makers and as a result there is no precise definition for risk. A difficulty with the terminology of risk is that it has been developed across a wide range of disciplines and activities, there is therefore potential for misunderstanding in technical terminology associated with risk assessment, since technical distinctions are made between words which in common usage are normally treated as synonyms. Most important is the distinction that is drawn between the words hazard and risk (Gouldby and Samuels, 2005).

A hazard does not automatically lead to a harmful outcome, but identification of a hazard does mean that there is a possibility of harm occurring, with the actual harm depending upon the exposure to the hazard and the characteristics of the exposed subject.

The term *risk* has been defined in several ways in the natural hazard literature. In chapters 3 and 4 are applied the standard definitions adopted by the disaster community as described in Chrichton, (1999) and Kron (2002): according to his theory, three variables determine the "risk": hazard, vulnerability and exposure.

Hazard: the threatening natural event including its probability/magnitude of occurrence;

Exposure: the values/humans that are present at the location involved;

Vulnerability: the lack of resistance to damaging/destructive forces.

Hence, based on mathematical calculations, risk is computed by combining hazard, exposure and vulnerability.

Based on this definition, the risk may be decreased by reducing the size of any one or more of the three contributing variables - the hazard, the elements exposed and/or their vulnerability. The reduction of any one of the three factors to zero would consequently eliminate the risk.

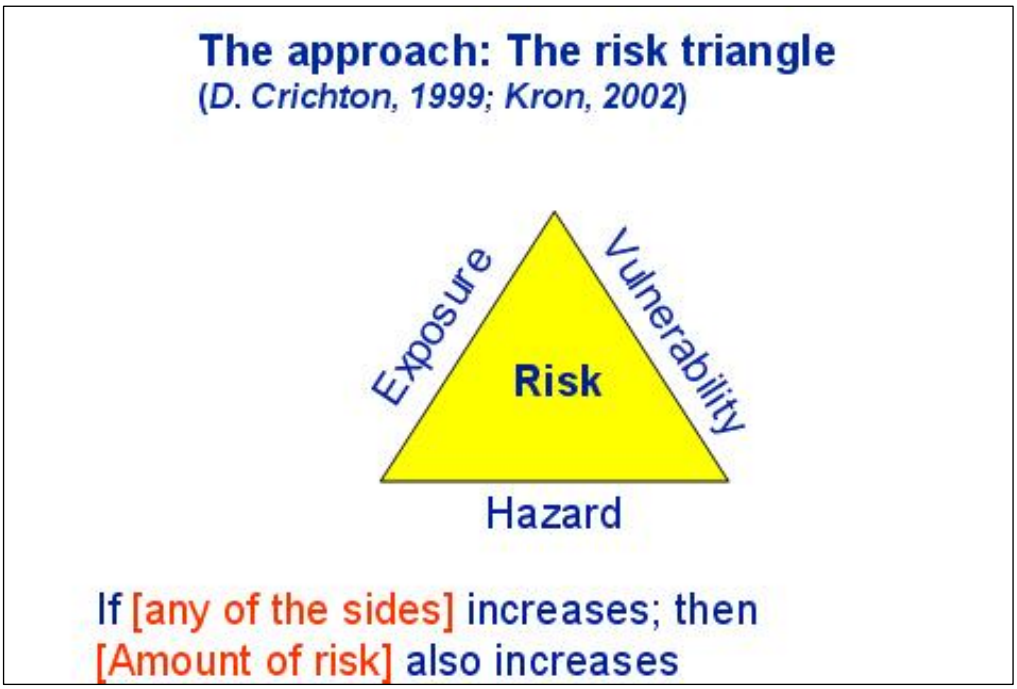

Figure 2.1*: The risk triangle.*

2.4 Different kinds of natural hazards

2.4.1 Floods

This section deals with the terminology adopted to differentiate flood typologies and to describe flood characteristics. Issues related to the link between land use trends and flood risk management are also briefly handled herein.

The term flood has been defined in a number of ways. Typically a flood is defined in hydrology in terms of a river's height of volume, which exceeds the river's average state over some length of time (Pielke, 2000). In insurance contracts it is defined as a "temporary covering of land by water as a result of surface waters (still or flowing) escaping from their normal confines or as a result of heavy precipitation" (Munich Re, 1997).

According to Kron (2002), there are three main type of flood:

- *Storm surges*: they can occur along the coasts of seas and big lakes;
- *River floods*: they are the result of intense and/or persistent rain for several days or even weeks over large areas, sometimes combined with snowmelt; river (or plain) floods develop relatively slowly, because the flood wave builds up with the water from the tributaries over a period of days. They are characterised by potentially widespread inundations covering up to hundreds of square kilometres. The time scale over which the flood develops and the area affected are, in general, inversely related (Compton, 2004).
- *Flash floods*: they sometimes mark the beginning of a river flood, but they are largely local events relatively independent of each other and scattered in time and space. They are

produced by intense rainfall and usually occur in a relatively small area, having a massive potential for destruction.

Floods have a number of measurable characteristics:

- *Flood depth* has a direct consequence for humans. Low velocity floodwaters of 1 meter depth or more are usually considered to be a threat to humans, and urban flood damage has been found to be correlated with flood depth.
- *Flood discharge* is another common index of flooding and provides the basis for most methods of predicting flood magnitude.
- *Flood duration* also has effects on flood damages, especially the length of flood disruption, and may be calculated from a flood hydrograph.
- *Rainfall-runoff lag time* is a measure of the time between the beginning of rainfall and the peak of flooding.
- *Seasonality* is a further flood characteristic: although floods may occur at any time of the year, they tend to be concentrated in wet seasons or when snow melts.
- *Floodwater velocity* and *flood extent* are associated to flood damage: they are a measure of importance on modelling the flow and effects of floods (Parker, 2000).
- *Floodplains* are “flood-prone” areas
- *100-year flood* describes an event with magnitude equal or higher than x (with x representing the parameter -usually discharge or water level at a certain gauging station- describing the hydraulic behaviour of the river) which has a probability of 1 percent to occur in any given year, or: P(X>=x)=1/100. This a probabilistic definition, so it is not expected to be exactly 100 years between two 100-year-floods, as the concept is often misunderstood (Petry, 2002). However, it assumes that occurrence and therefore flood probabilities are constant over time. The issue of how these probabilities may vary in terms of climate change is addressed in other workpackages of the project.

Floodplains have often been sought as sites for urban development because of the facilities they offer, including access to a source of water for a variety of uses. Cities have been permanently developing their water-related infrastructure and discharging their urban waters into the nearest water body (Andjelkovic, UNESCO, 2001). The development of urbanization and activities has continued, although this expansion represents a hazard if the vulnerability of those activities exceeds an acceptable level (Colombo and Vetere Arellano, 2002).

The possible interaction between human use of the floodplain and the onset of a flood event potentially creates a natural risk. In fact a disaster only exists once a flood occurs, depending on the amount of property damage, disruption and loss of lives. As urban areas grow, both geographically and demographically, the flood hazard and risk increase in part because there is more exposure, but also because the process of urbanization itself alters local hydrological characteristics (Montz, 2000).

In undeveloped areas such as forests and grasslands, rainfall and snowmelt collect and are stored on vegetation, in the soil column, or in surface depressions. When this storage capacity is filled, runoff flows slowly through soil as subsurface flow.

In contrast, urban areas, where roads and buildings cover much of the land surface, have less capacity to store rainfall and snowmelt (Konrad, 2003). Construction of roads and buildings

often involves removing vegetation, soil, and depressions from the land surface. The permeable soil is replaced by impermeable surfaces such as roads, roofs, parking lots, and sidewalks that store little water, reduce infiltration of water into the ground and accelerate runoff to ditches and streams. Development along stream channels and floodplains can alter the capacity of a channel to convey water and can increase the height of the water surface (Konrad, 2003). Bridges, in particular, reduce the natural carrying capacity of the river and provide barriers upon which debris can accumulate. In addition, development along the river can intrude on the river and restrict flow as a result.

Therefore, "once floodplains become urbanized, there follows an almost inevitable demand from the local community for flood protection" (Smith, 1996; in Parker, 2000).
In the methodology proposed for A2.1, issues such as increased exposure to land use developments and/or demographic distribution are key elements for the evaluation of direct flood risk. Flood occurrences and related return periods are also duly and extensively accounted for in the computations.

2.4.2 Droughts

Drought stress on plants occurs when a plant is not able to replenish the water lost by transpiration and is a major abiotic stress that severely affects agricultural systems and food production. Even intermittent water stress at critical stages of cereal crops may reduce yield.
Accordingly, water shortage is becoming a central issue in global change impact assessment in agriculture. Koustopoulou and Jones (2005) identified in the Mediterranean basin several sites which, in the last three decades, showed on the one hand an increasing trend in annual rainfall and on the other hand a decreased number of rainy days. Prolonged dry spells, as suggested in this analysis, and predicted by GCMs, result in a considerable water shortage that has a high impact on agricultural yield. In particular more frequent summer droughts may result in an exacerbation of yield losses for both summer and winter crops. Both types of crops are exposed to summer drought, (with different intensity according the latitude) during sensible stages of their growth cycle.

In fact, the phenological phases when the drought event occurs play a fundamental role in determining the crop yield loss. According to its timing, the risks of drought can be classed into two types: drought events during the vegetative phase that can be recovered during the rest season (depending on the duration of dry spell) and drought events during the reproductive stages (anthesis and post anthesis stages) resulting in a direct loss of yield biomass due to the low floret fertility and reduced seed-set.

Due to the high importance of water stress as reducing factor of crop yield, the effect of this stress on plant growth has been widely studied and the results of these studies have been implemented in the crop growth simulation model.

2.4.3 Heat Waves

The increase in extreme weather events, as already observed for Europe (Koustopoulou and Jones, 2005) and simulated by both Global and Regional Circulation Models (GCMs and RCMs respectively) for the future decades (2070-2100) (Moriondo et al. 2006), is a key element for crop yield assessment in future scenarios. These increases may determine

reductions in mean crop yields and farmer economic risk (i.e. higher number of years with crops yields below ‘zero-profit’ thresholds).

In fact, temperatures outside the range of those typically expected during the growing season, may have severe consequences for crops reducing significantly the yields (Porter and Gawit, 1999).

Both high and low temperatures decrease the rate of dry matter production and extreme episodes may cause a block of crop growth. In particular, climate extreme events during key development stages of the crop may have a dramatic impact on final production even in the case of favourable weather conditions for the rest of the growing season.

These effects were reviewed for wheat by Porter & Gawith (1999) and, for annual crops in general, by Wheeler et al. (2000). A general point that arose from these reviews was that temperature above a certain threshold adversely affects plant growth and development. in particular for wheat and sunflower, cardinal temperatures were identified underlying that, in the case of heat waves at anthesis, the formation of reproductive sinks, such as seeds and fruits were particularly disadvantaged. In particular, heat stress at anthesis stage was demonstrated to have a strong effect on the final yield (Ferris et al. 1998; Porter and Gawit, 1999; Wheeler et al. 2000; Wollenweber et al., 2003) because it decreases pollen and floret fertility as indicated in many studies (Chimenti and Hall, 2001, Challinor et al., 2005). The production and transfer of viable pollen grains to the stigma, germination of the pollen grains and growth of the pollen tubes down the style, and fertilization and development of the zygote are necessary for successful seed set. Although all these phases are temperature sensitive, some are more sensitive than others and high temperatures can cause both male and female sterility in wheat.

In contrast, the effect of higher temperatures during grain filling is limited to the shortening of this phenological phase.

Subsequently, climate impact assessments on crop yield should take into consideration, along with the average changes in climate conditions, the change in extreme events frequency during sensible crop developmental stages (e.g. anthesis).

Up to date, many problems limited the analysis of extreme temperature impact in the present and future scenarios as proposed by SRES.

Among the reasons that have limited these analyses there is the low capability of GCMs to reproduce extreme climate events. In fact, GCMs simulated climate variability is highly dependent on physical parameterization (convection scheme used to describe precipitation or land-surface scheme for maximum and minimum temperature).

Moreover, many of the crop simulation models available are not able to reproduce the impact of short-term climate extremes that can depress yields of major crops.

3 Flood risk assessment

3.1 Scale and data availability

When one has to deal with risk or damage assessment from flood hazard, the "ideal protocol" would require very detailed quantitative information about local morphology and assets of the territory. Although the nature of the hazard is non-deterministic, local communities demand that the knowledge of the potential losses (or the real ones) deriving from a flooding event should be as detailed as possible. This, in turn, requires a huge amount of reliable data on the river catchment properties and an accurate quantification of the accumulated value of the land involved (Büchele 2006, FLOODsite 2006). When one wants to broaden the view on a European scale, the idea to treat the problem according to the same scheme of local catchments is fairly unrealistic, because of a lack of consistent information and also because of the resources needed to process data at high resolution on such a wide geographical extension.

At EU level, the activity on policies of flood related issues is presently focused on the ongoing process of adopting the "Directive on the assessment and management of floods", which aims at building a common framework of policies and actions on floods prevention and mitigation at continental level. A systematic knowledge base, through the mapping of the territory (topography, flood hazard, flood risk, land use) and the gathering of information on past flood events is envisaged to be built-up as the basis of the management plans to be established by Member States, according to the directive guidelines. Such maps, as proposed in the most recent version of the common position adopted by the Council of Europe, should be made ready by the end of 2012. An EU-wide flood damage assessment procedure could therefore be built on top of a continental flood hazard database which should possibly include all the national contributions. This, in turn, would also require that a correspondingly detailed European database on exposure of assets and on vulnerability to floods be built up. The time horizon for this to happen is likely to be set beyond the above cited 2012. The methodology here presented is therefore based on what is now available in terms of official input data at EU scale.

In order to quantify the damages potentially caused by river floods at European scale we have followed a territorial approach for the computation of the three key parameters (hazard, exposure and vulnerability) of the risk triangle, following the scheme sketched in Fig. 3.1.

Hazard: flood hazard maps are generated from catchment characteristics. The main data component in this respect is the Digital Terrain Model (DTM), which allows an evaluation of the water depth in each location after a given flood extent. In a Europe-wide perspective, it is mandatory to work with consistent data sources, which means that, although certain nations are already provided with high or very-high resolution DTM's and river network information systems, the resolution of the analysis will be dictated by that of the data source which is consistent and validated throughout the whole continent. To put it into figures, we are dealing with a **spatial resolution (grid cell) of 1 km**.

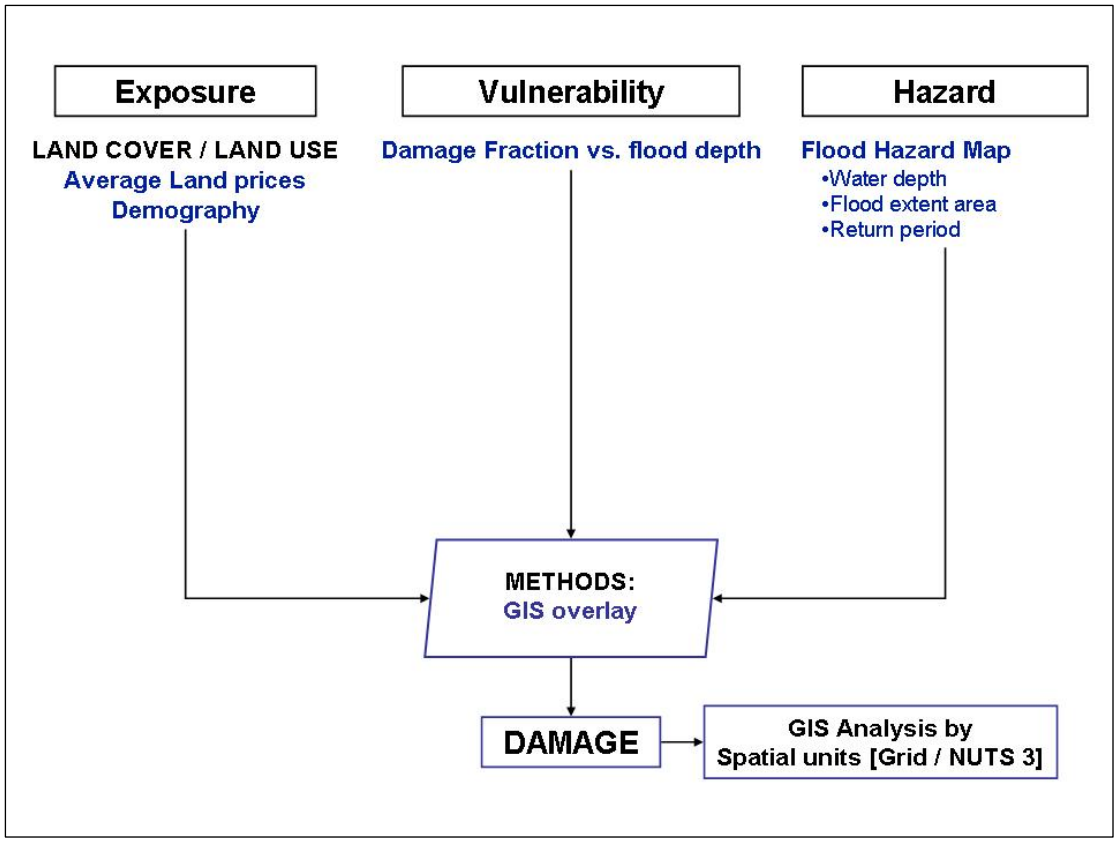

***Figure 3.1**: Operational scheme for the evaluation of the potential flood damage.*

Return periods for the flood hazard maps are evaluated from runoff statistics by coupling the hydrological model LISFLOOD with the regional climate model HIRHAM (Dankers at al., 2007) and by means of a trial and error analysis applied to some European river catchments. The two models run at different spatial resolution (grid cell size) so that the climate data are regridded down to the 5 km resolution of LISFLOOD. More details on this topic are given in sec. 3.2

Exposure: the main element for the computation of exposure is the CORINE Land Cover (CLC) map of the European natural and artificial landscape. The combination of hazard and land cover maps allows estimating the exposure to floods of physical assets which are in turn grouped according to the classes of the land cover map. CLC has a nominal scale of 1:100000, with minimum mapping unit of 25 hectares and has been operationally used in the raster version with 250 metres pixel size. More details, along with examples of analyses for policy-making, are given in sec. 3.3.

Vulnerability: as mentioned in sec. 2.4.1 and further elaborated in sec. 3.4, the damage caused by floods may depend on each one of its main characteristics. However, the only operational possibility to quantify these effects was to consider only the flood depth. Therefore, the vulnerability of the assets under threat is estimated by means of depth-damage functions for each land use class of CLC for all EU 27 countries. Such functions, are operationally expressed as a multiplying factor **V(h)** (with h the flood depth), where $0 \leq \mathbf{V(h)} \leq 1$.

The final digital maps represent the values of the potential monetary damage assessment for, respectively, four return periods and annually averaged in two geographical formats representing two different territorial units:

- Accumulated values over cell (grid) of 50 x 50 Km size and
- Accumulated values over administrative aggregation level (NUTS-2, sub national)

It is worth stressing that the monetary damage is computed assuming that for a given return period, the flood event is occurring **simultaneously** in the whole territorial unit. The maps must therefore be used and evaluated bearing in mind these characteristics.

The three components (hazards, exposure and vulnerability) of the risk triangle are in turn described in the following sections. In addition, the territorial analysis of exposure is given in more detail.

3.2 Flood Hazard Map

The flood hazard map (FHM) used in this analysis is obtained from a 1 km grid DTM and the 1 km European flow network (Hiederer and De Roo, 2003) developed by the Natural Hazard Action at the Joint Research Centre (De Roo, 2007). It provides quantitative information on both the expected extent of flooded area and on the water depth.

Hydrological processes such as flooding and soil erosion are determined by topographical parameters, and therefore digital elevation data plays a crucial role in modelling. An overview of hydrological applications of DTMs can be found in Gurnell and Montgomery (1999) and De Roo (1998). Wilson (2004) and Wilson and Atkinson (2003) showed the effect of data uncertainty on predictions of flood inundation and thus flood hazard, using the LISFLOOD-FP model (Bates & De Roo, 2000; De Roo et al. 2000). The accuracy of the DEM is of utmost importance for the accuracy of the final flood hazard map. Inaccuracies in the final predicted flood extent arise from unknown surface roughness values, or linear features on floodplains such as roads, ditches etc. that are not well incorporated in the DTM.

The map is solely based on topographic features: an algorithm has been developed to find the height difference between a specific grid-cell and its closest neighbouring grid-cell containing a river, while respecting the catchment tree-structure (Barredo 2005).

Details of the computations and examples of validation of the maps are given in (De Roo et al. 2007). The final output is presented in Figure 3.2

It is worth underlining that the flood hazard maps are produced in absence of flood defences. This feature and the spatial resolution of the map (1 km) cause a range of uncertainty in the results. In addition to this, the approach does not account for flood volume – this may result in an over-estimation of the flood in extensive flat areas.

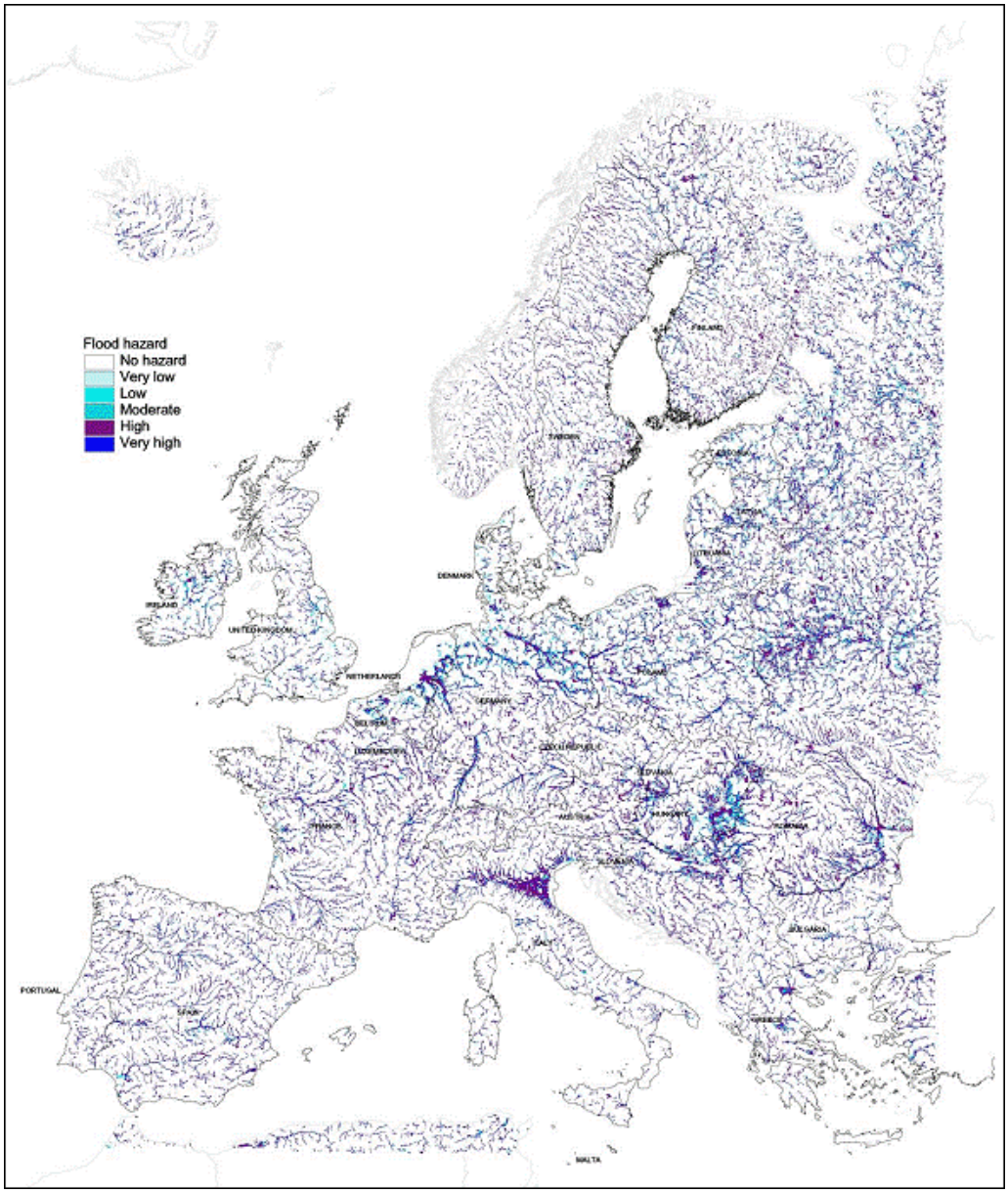

***Figure 3.2**: European Flood Hazard Map - elevation difference and the estimated extreme water level of the river determine the potential flood risk. The six classes of the legend match with the flood hazard classes reported in table 3.1.*

As already pointed out, the hazard flood map is based on elevation difference values with respect to the river in a catchment. The original hazard map legend therefore classifies the land according to 6 elevation groups; in addition to those classes, special groups were defined to describe coastal hazard and lakes. Table 3.1 displays the legend of the flood hazard classes corresponding to the elevation difference from the river.

It should be noticed, that the values corresponding to the class called “river itself” have been considered as a real hazard class. The reason for this is that a 1km-wide riverbed is seldom encountered in Europe. As briefly described above and more widely discussed in sec. 3.3, the exposure is evaluated by means of the CLC survey, which has a resolution 4 times higher (16 CLC pixel per 1 FHM pixel) than the hazard map and contains a class describing inland waters. The superposition of each 1km-wide pixel of the FHM representing a river onto the underlying land described by the CLC map, allows to distinguish which is the “true” river and

which is the land type lying close to it, thus likely to be inundated in a flood event. The CLC class corresponding to water is of course taken as "no exposure" land, so it does not contribute to the monetary damage assessment.

Elevation difference (m)	***Flood Hazard Class***
River itself	6 - Very High
< 0.0 m	5 - High
0.0 – 3.0 m	4 - Moderate
3.0 – 6.0 m	3 - Low
6.0 - 10 m	2 - Very Low
> 10 m	1 - No Hazard
Coastal areas, Lakes	Not considered

Table 3.1: *Flood Hazard Classes and elevation. The river level is taken as 0-metre level.*

Coastal hazard has been neglected, since the current focus is on inland river flood events. Discussion on the choices and the assumptions made to make the method operational will be shortly described.

The computation of the return periods for the flood hazard map described above is complex and is still subject of in-depth investigation for what concerns the calibration of the periods.

The frequency of flood events can usually be estimated by employing one the following three basic methods (Jones and Kay, 2007):

- Use of historical data
- Use of rainfall data
- Use of gauged data

The lack of systematic records of past river flows, with details and characteristics adequate to the geographical scale of the analysis performed in workpackage A2.1, does not allow adoption of a particular method, but has forced the development of a mixed approach based on the use of a rainfall-runoff model for the generation of floods frequencies and of historical records of damages for the subsequent evaluation of uncertainties.

The method evolves into two steps:

1. A first approximation of definition of return periods for the hazards flood map is based on the geomorphological characteristics of the river catchments and on statistics of estimated runoff. This first guess is carried out at European scale (i.e. all basins are included in the analysis) deducing water levels for four return periods from the analysis performed for the Upper Danube Catchment.
2. A further calibration is performed by employing additional datasets such as records of direct monetary losses in known flood events and on selected test areas where flooded areas and inundation water depths are computed with higher accuracy. This would allow the definition of a set of "control points" for a further detailed calibration. This step will be subject of analysis in the last phase of work in A2.1 and is therefore only marginally dealt with in this report.

A comparable approach, with different procedural steps and with the use of actual gauge data and higher spatial resolution, was adopted in 1996 to produce the Flood Risk Map for

England and Wales (Morris and Flavin, 1996), with good agreement between the modelled simulations and the actual flood maps.

The core of the proposed methodological framework is the hydrological model LISFLOOD, which transfers the climate forcing data into river runoff estimates. LISFLOOD (de Roo et al., 2000) simulates the spatial and temporal patterns of catchment responses in large river basins as a function of spatial information on topography, soils and land cover. LISFLOOD is a physically based and spatially distributed model, integrated with a GIS that provides an ideal environment for modelling processes in a landscape. The main advantage of this kind of models, as compared for example to other models such as TOPMODEL (Beven and Kirkby, 1979) and HBV (Bergstrom, 1995; Lindstrom et a. 1997), is that LISFLOOD uses input parameters that can be measured and can handle large databases.

LISFLOOD is one-way coupled with the regional climate model (RCM), i.e., there is no feedback from the hydrological model to the climate model. Hydrological simulations on the basin scale using LISFLOOD typically run with grid spacings of 1 to 5 km. After bias corrections and downscaling, the regional climate data serves as input to the LISFLOOD model. For both time slices (control and scenario), the hydrological model calculates daily discharges at each grid within the area of interest. For the purposes of Task A2.1 in ADAM, only the control period (years 1960-1990) is herein considered.

Runoff statistics are determined employing extreme value analyses. The statistics yield an assessment of the expected flood frequencies **expressed as a value of the discharge with certain (e.g., 100 years) return period** (Dankers et al., 2007)**.**

With a digital elevation model, stream water levels are readily transferred into flooded areas and inundation water depths (Feyen et al., 2006). The calibration of the return-periods for the European Flood Hazard Map is performed by comparison of water depths with those deduced by the hydro-climate modelling framework.

The method (see scheme in Figure 3.3) has been applied for the 30 year control period generated out of the experiment with the RCM HIRHAM (Christensen et al., 1996) at horizontal resolution of 12 km in the framework of the PRUDENCE project (Prediction of Regional scenarios and Uncertainties for Defining EuropeaN Climate change risks and Effects; Christensen et al., 2007)

The procedure is computationally heavy and requires considerable efforts for the calibration of climate data and the application of the hydrological model. It is therefore well suited to be applied for specific catchments, as demonstrated in the frame of the PESETA project (Feyen et al., 2006).

For the purpose of the calibration of the European Flood Hazard map, we have taken advantage of the detailed processing performed for the Danube Catchment upstream of Bratislava (130 000 km^2) situated in Austria, Germany, Switzerland, Slovak Republic and Czech Republic. Part of the processing was done in the frame of the PESETA project.
For this area, the RCM outputs for the control run were validated against observations from synoptic stations. The HIRHAM simulations of temperature, precipitation, solar and thermal radiation, humidity and wind speed data were used to drive LISFLOOD on a daily basis. Based on 30 years of daily discharge data, an extreme value distribution (in this case a Gumbel distribution) was fitted to the annual maxima, which was then used to estimate

extreme discharge levels with three return periods (20, 50 and 100 years respectively). Simulations for higher return periods were not performed because the extrapolation from the 30-year record would not have ensured a sufficient level of confidence. The procedure is described in (Feyen et al., 2006) and (Dankers et al., 2007).

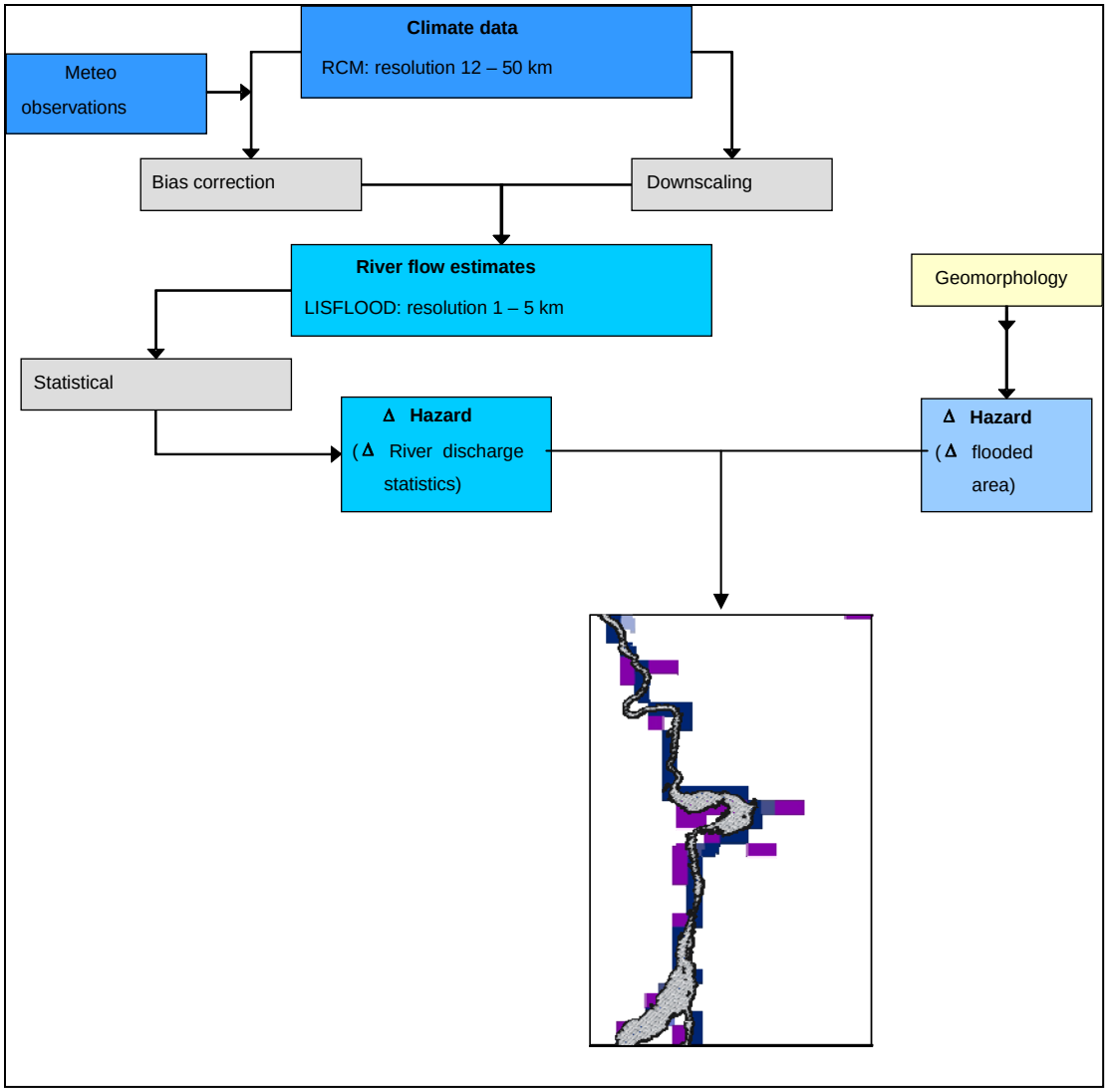

***Figure 3.3**: Procedural scheme for the determination of return periods from runoff statistics.*

Flood river water levels were subsequently derived with estimated river channel geometries. Figure 3.4 shows the water levels for the 100-year return period.

Water level statistics have been used to calibrate the water depths of figure 3.2 by attributing a return period for each hazard class.

The extreme water levels computed for the Upper Danube area were analysed to evaluate the range of values above the reference river level, which was adequately set as zero-level for both maps. The contributions from small rivers were not considered to be consistent with the

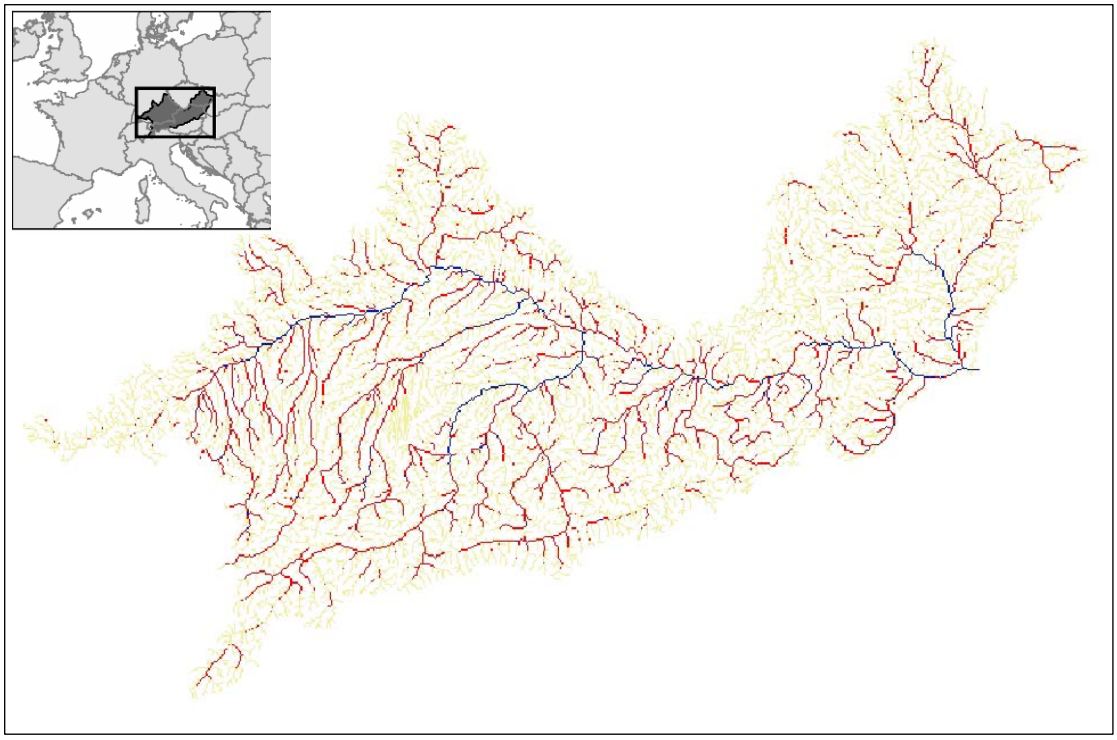

***Figure 3.4**: Water levels for the Upper Danube catchment area.*

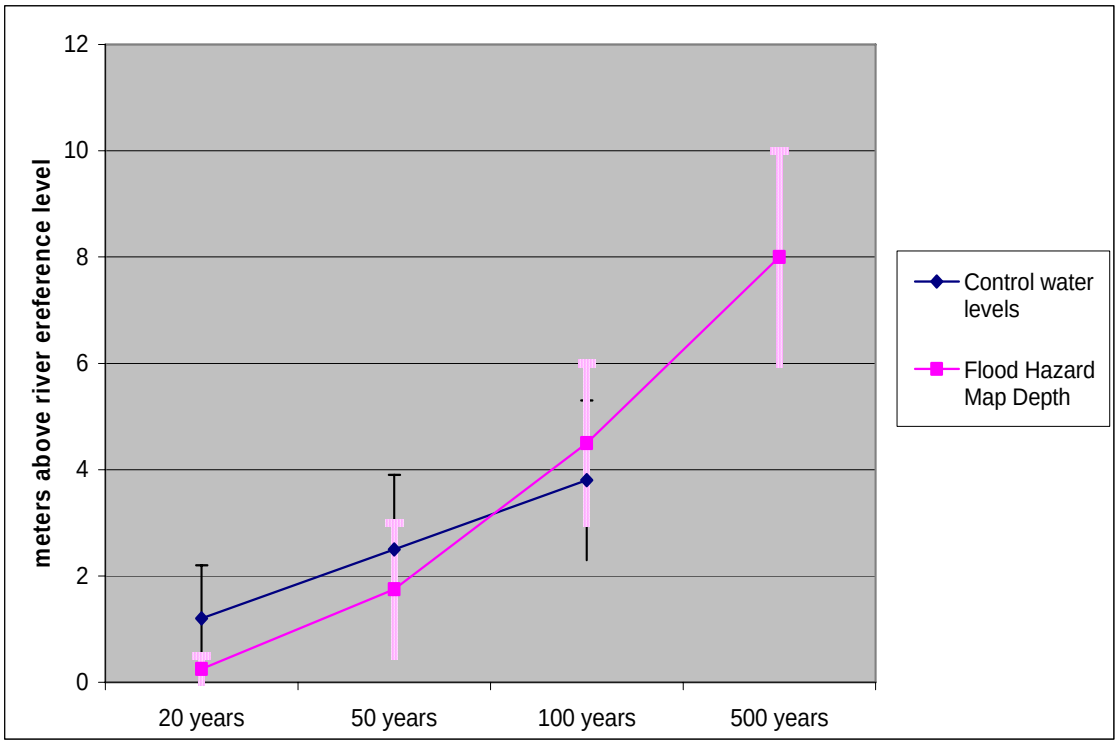

***Figure 3.5**: Water levels for the Upper Danube catchment as computed by the couple RCM-LISFLOOD model. The curve in blue represents the average value of extreme river levels for the three return periods considered in the analysis, as computed from the control period of the RCM. The standard deviation is also presented as a vertical error bar. The curve in red represents the water depths for the hazard- classes derived by the European Flood Hazard Map. These water depths will be taken as reference for the application of the flood damage functions (see Table 3.2).*

assumption made for the definition of hazard map. Figure 3.5 depicts the values for the 3 return periods:

For the 20-year flood the estimated range of extreme water level is: 0 – 2.2 metres

- For the 50-year flood the estimated range of extreme water level is: 1.1 – 3.9 metres
- For the 100-year flood the estimated range of extreme water level is: 2.5 – 5.5 metres.

As expected, the effects of hydro-geomorphological characteristics of the catchment produce a range of variability of extreme water levels computed along the river bed. In other terms, for a given return period there might be a different water level corresponding to different locations in the river catchment.

The ranges of extreme water levels were used to perform a first-guess evaluation of the return periods of the overall Flood Hazard Map, by means of a trial-and-error analysis applied to some European river catchments.

The flood hazard map has been finally calibrated by defining the correspondence between return periods, and both the ranges of water level values and the flooded areas extensions, as summarised in the following table:

Flood Hazard Class (FHC) and corresponding water level	**RETURN PERIOD (Years)**
6 (< 0.5 metres)	20
5+4 (0.5 – 3.0 metres)	50
3 (3.0 – 6.0 metres)	100
2 (> 6.0 metres)	500

Table 3.2*: The four return periods and the related flood hazard classes.*

The value of 0.5 metres arises from the resolution step of the damage functions to be explained in sec. 3.4. Starting from the 0m elevation difference of the corresponding class “6” (see tab. 3.1) and given the resolution of the data, this value has been chosen to express the minimum water level representing a flood event.

The water level at the river is then translated into water depth in the flooded area according to the elevation differences of tab. 3.1. Therefore, in a 20-year flood, the areas represented by class “6” are estimated to be inundated to a depth of 50cm, while in a 50-year flood, it is expected that the areas covered by water will be those belonging to classes 6, 5 and 4 (with flood depths varying according to their elevation ranges) and so on. It is assumed that the territorial extension of each return period includes the previous one (if any).

The water levels corresponding to the various return periods are reported in figure 3.5 above, for comparison with the values deduced from the coupled modelling approach.

It can be noted that the assumed value of the water level for the 20-year return period (0 - 0.5 meter) is at the extreme lower end of the range of values measured for the Upper Danube area (average value: 1.2 metres). The selected value is the result of the trial-and-error analysis which indicated an overestimation of the water level coming from the Upper Danube when applied to other catchments.

The lowest class of risk for water level higher than 6 metres has been attributed to a return period of 500-years. As previously mentioned this figure has not been calibrated and is

therefore to be used only as a nominal value. An attempt to quantify the highest return period will be performed in the remainder of the A2.1 activities.

The overall approach herein adopted presented a number of uncertainties still to be fully quantified. The validation exercises so far performed are indicating that the major cause of inaccuracy resides in the poor geographical resolution (1 km) which does not allow to properly account for detailed geomorphological features, thus resulting in an overestimate of the potentially flooded area. Conversely, the contribution from smaller rivers is not taken into account, either, thus underestimating the hazard. How these counter-acting limitations of the method are actually balancing or overtaking each other, is still to be assessed.

The use of more detailed elevation data would certainly increase the accuracy of the measurements but would in turn require more accurate data for calibration and validation. In addition, the application of high resolution data at continental scale would require increased and dedicated resources for data processing. Also, the application of calibration curve derived from a specific catchment to the whole European territory is questionable. However, the uncertainty deriving from the use of this generalised procedure can be reduced if the calibration uncertainty is quantified and taken into account for further statistical analysis (Jones and Kay, 2007).

The added value of this approach is that the map brings altogether information on water depth and flooded area extent – essential for the application of the flood damage function – with a probabilistic approach. A direct indication of the uncertainty is given by the range of values for the water-level corresponding to each return period.

Therefore, the proposed approach is believed to provide a unique and valid way of quantifying the flood hazard in the whole European continent. The issues related to uncertainty of the results will be further tackled in the conclusive remarks of this report and will be the subject of work for the remaining months of A2.1.

3.3 Land Cover-based analysis of exposure to floods

The CORINE (Coordinated Information on the European Environment) Land Cover project was launched by the European Commission, managed and maintained by the European Environmental Agency - EEA (1995, 2000, 2002), in order to provide support for the Commission in its efforts to use and develop advanced data-compilation and management techniques in carrying out its policies.

CORINE Land Cover (CLC) is a map of the European natural and artificial landscape based on interpretation of satellite images. It is intended to provide consistent localized geographical information on the land use of the Member States of the European Community. This is useful for environmental analysis and comparisons as well as for policy making and assessment. No other land cover information programme in the world embraces such a wide geographical area in such detail.

This EU-wide programme examines land cover using a standard methodology and nomenclature. The purpose of this project was to provide a baseline to examine future land cover changes and as an important research tool for a variety of environmental studies. The CLC data is based on a minimum mapping size of 25 hectares

CORINE coding is a hierarchical, three-level code, with five 1st level classes, fifteen 2nd level ones and forty-four 3rd level ones, according to the legend published by EEA (1995) and reported in Annex 1.

The CLC database was realized for two dates (1990 and 2000) with a nominal scale of 1:100,000. The product is basically a vector dataset, but two raster versions have been released, with 100 metres and 250 metres pixel size. The database CLC2000, version 8, released by EEA on March 2006, in the 250 metres pixel size version, has been used for this analysis. The more accurate 100 m pixel version was not used because it is too detailed as compared with the 1km pixel size of the current version of the flood hazard map. Nevertheless, an example presented below was based on the 100m dataset, because a pre-processing was made on this data and it was not possible to upscale them without corrupting the information.

The CLC provides a qualitative (type of land cover) and quantitative (extent of surface or area) description of the territory. In the operational framework herein presented, a monetary value in € has been found for the damages specifically caused by floods to each land cover class. The latter feature will be further explained in section 3.4 and exploited in Section 3.5 to evaluate the direct (monetary) damage of floods. The studies presented in the two following sub-sections were performed, before the database with land values and damage functions was made available; therefore only the basic land cover information was used to estimate the exposure of the European territory and population to floods. These applications can be seen as intermediate products deriving from the risk triangle approach: in fact, as mentioned in sec. 3.1, the maximum value for Vulnerability is 1, so that the combination of Hazard and Exposure can be considered as the maximum possible damage from floods, although not yet expressed in monetary terms. It can therefore be used to elaborate on indicators that are anyway very valuable for policy-making purposes.

3.3.1 Country-based analysis of artificial-surfaces exposure

This investigation aims at quantifying the exposure of assets to river floods through the overlay of the territorial information across the whole of Europe, in raster format, coming from the CLC surveys and related information and from the river flooding hazard map. For readout of the results in terms of management, planning and policies, the resulting information is aggregated by administrative boundaries at national (NUTS0), regional (NUTS2) and sub-regional (NUTS3) level[1]. Likewise, the hierarchical classification of the CLC suggested to include in the database the possibility to aggregate the results also onto the three CLC levels. In addition to this, a time dimension is added by the presence of two dates for the CLC survey, nominally stated as 1990 and 2000; although the true date of the observation varies slightly across the nations. Figure 3.6 sketches the overlay scheme suggesting the possible combinations of information detail from the datasets and the integration of the results.

[1] NUTS stands for “Nomenclature des Unités Territoriales Statistiques” (Nomenclature of Territorial Units for Statistics), see http://ec.europa.eu/comm/eurostat/ramon/nuts/introduction_regions_en.html

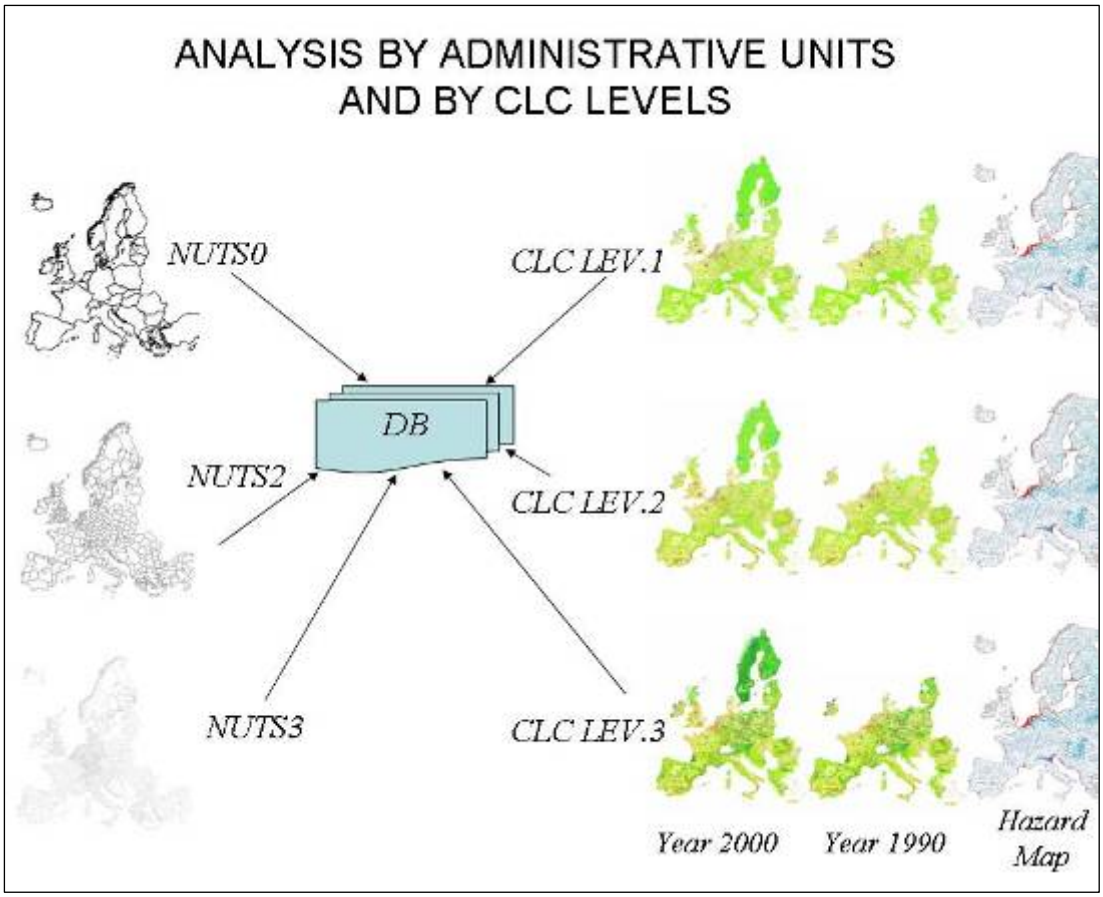

***Figure 3.6**: Scheme for the integration of information.*

The result of the overlay is the combination of each map's information, coded as already explained. For the present investigation purposes, the 44th CLC class -Sea and Oceans- was, of course, neglected.

The result of the two maps' combination is therefore a new raster, with potentially 43*6=258 different values. 253 independent values were obtained, as some combination did not occur (as expectable, for the class accounting for glaciers and perpetual snow, as they are clearly placed predominantly upstream). In addition to this, several combinations were scarcely relevant, occurring only on a small number of "pixels" across Europe, for example, 15 combinations below 150 ha, 27 below 300 ha. Nevertheless, the number of values, even when limited to artificial surfaces alone (66), was quite high for analysis purposes.

The different administrative levels, from NUTS0 to NUTS3, were then used to integrate the data, thus generating a number of tables according to the CLC/Hazard/Time distribution in each unit, along with selected calculations accounting for the relative importance of the area in hazard with respect to the Land Cover distribution, as well as differences in time of the territorial conditions.

The output table produced from the process sketched in figure 3.6, carries the overall amount of land of a given CLC class, lying in a given hazard class, for a given NUTS3 region, and follow a simple nomenclature, so that -for example- the field named LCH_111_4 represents the amount of "continuous urban fabric" (class 111) lying in "moderate hazard". The one in the lower part of the figure, is carrying the "relative" value of the land cover in hazard, in terms of the ratio between the amount of land lying in a given hazard class to the total amount

of that class in that region. Some peculiar values (-9) can be found, to highlight when a division-by-zero error occurs, that is, when that land cover class is totally absent in the region (as happens for class 111 in several NUTS3 of Austria, such as AT111, AT113, AT125 etc., in the table 3.3 below).

The time dimension is analysed by different calculations: basically the absolute and relative change of both the above defined values. The readout of the evolution of the territory with respect to the flood hazard can thus be performed seeing how the extension and the relative importance of the land under threat have changed. This should also be compared to the way the land cover itself, independently of the hazard, has correspondingly changed.

Given the high number of tables brought about by the above described combinations, the database was therefore designed and customized in order to allow selection queries to gather the information required for the analysis. In figure 3.7 a screenshot of the query interface and resulting selection is given.

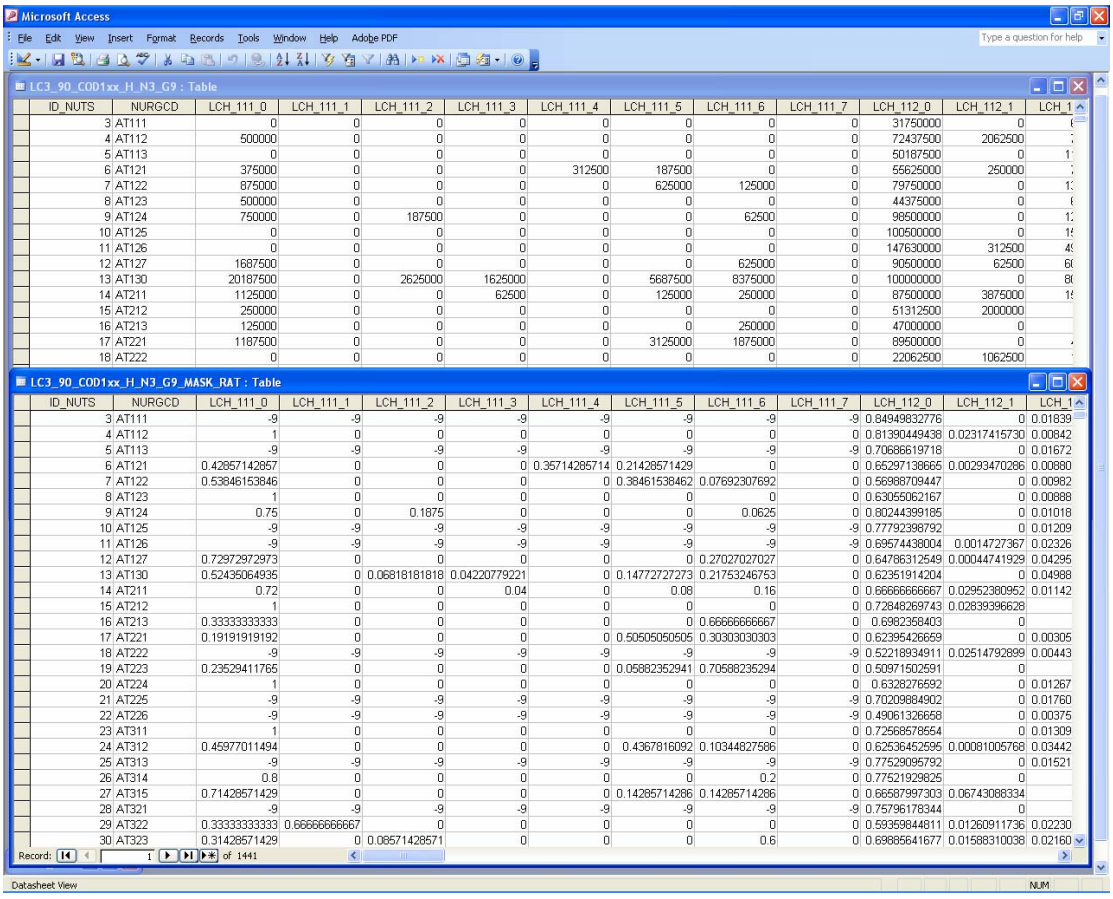

***Table 3.3**: Table of land use exposure to floods for Austria, represented at NUTS-3*

Notwithstanding the possibility of custom queries, the number of fields carrying information is quite high. We therefore performed a reclassification of the hazard values into two classes and it was decided to group the three higher hazard values into one hazard class, leaving only the two lower ones in the other, namely:

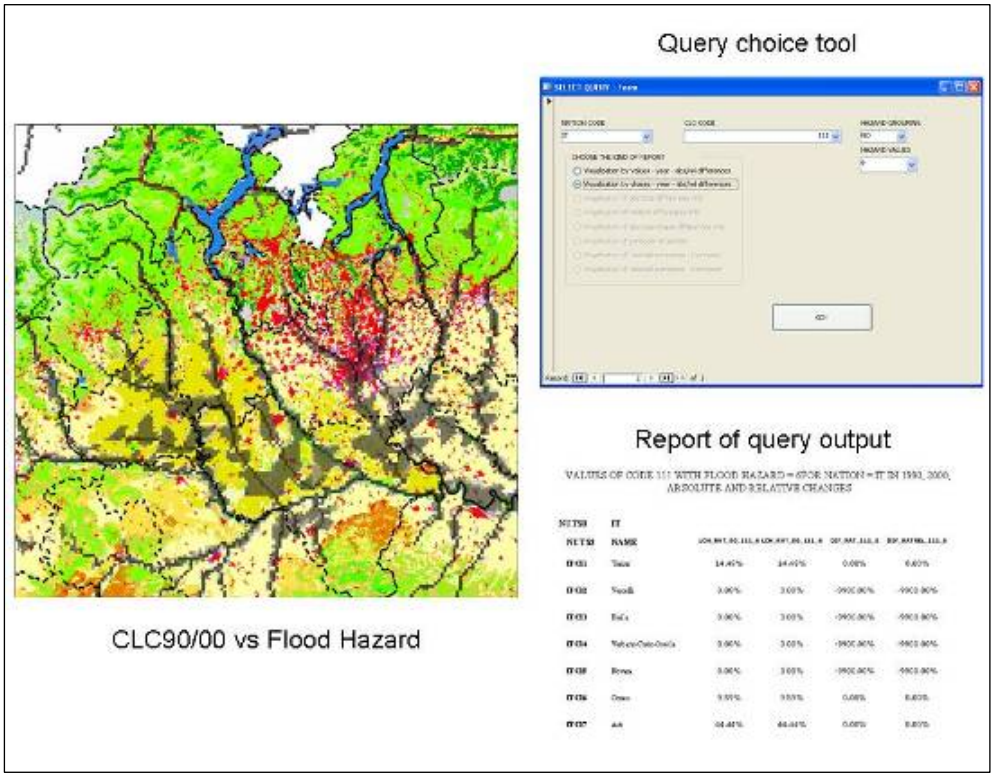

***Figure 3.7**: Screen-shot of the temporal evolution of land use exposure to floods, measured by means of CLC 1990 and 2000.*

Value 2 (very low) and 3 (low) grouped into hazard class "LOW";
Value 4 (moderate), 5 (high) and 6 (very high) grouped into hazard class "HIGH".

An analysis performed on national (NUTS0) level follows. This is limited to the land cover classes belonging to the "Artificial Surfaces" 1st level group (first digit of the CLC legend =1). Land cover data for 1990 and 2000 have been used. Therefore the analysis is restricted to those Countries which were mapped in both surveys.

The total hazard area considered in the analysis is more than 350.000 km^2 across, of which about nearly 30.000 km^2 are artificial surfaces.

The chart in figure 3.8 shows the increase of artificial surfaces development in Europe in flood prone areas (Lavalle et al., 2005). The first class we analysed is residential, which includes continuous and discontinuous urban fabric.

Between 1990 and 2000 the "continuous urban fabric" land use in Europe rose by 27 km^2 and the "discontinuous urban fabric" by 552 km^2, equivalent to an increase of 3%. Also "sport and leisure facilities" class increased by 84 km^2. This confirms the initial statement on the increasing exposure to floods due to new artificial development.

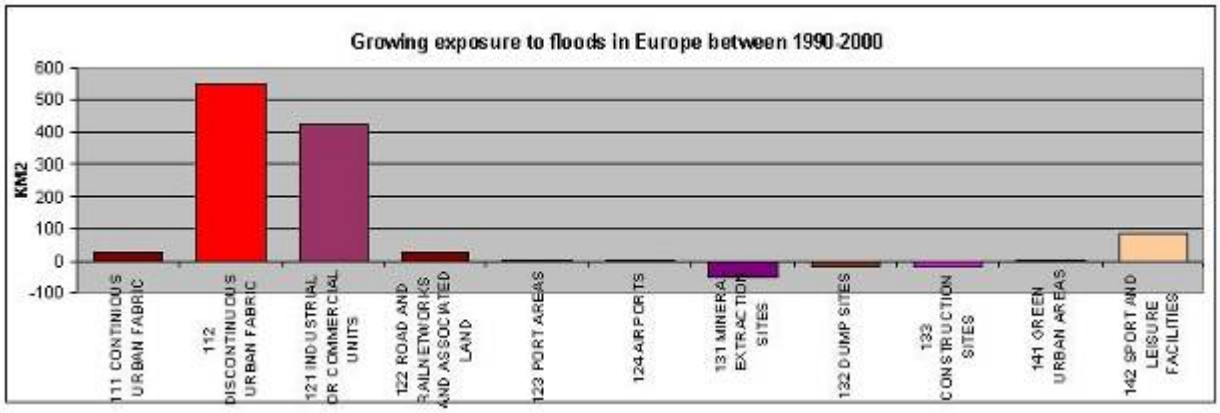

***Figure 3.8**: Artificial areas in Europe between 1990 and 2000.*

The same trend is found for the "industrial and commercial units" class: this class rose by 11%, to a further 424 km^2 of industrial areas placed in flood hazard areas. Therefore, main developments occurred in areas potentially affected by flood are in these two classes and higher damage can be expected in such areas.

Otherwise, extraction, dump and construction sites were decreasing between 1990 and 2000. It's interesting to pay attention to the decrease of mineral extraction sites equal to 50 km^2 in 2000 (corresponding to -5% compared to 1990). These sites were replaced by urban, industrial or commercial areas, exactly where it would have been expedient to contain the growth of new urban areas because of the flood hazard.

A further analysis has been carried out to evaluate land use exposure to floods for the year 2000 only.

The national accounts for artificial surfaces have been tabulated, along with their thematic distribution within each hierarchical CORINE legend level. Average values were also calculated in three different groups of nations: "EU 27" collects values on all EU member states, plus Bulgaria and Romania; "EU15" groups the so-called "old member states"; "ST13" represents the group of nations that can receive support from Structural Funds under the Convergence objective: Spain, Greece, Portugal, Hungary, Poland, Slovenia, Czech Republic, Slovakia, Estonia, Latvia, Lithuania, Romania and Bulgaria. Cyprus and Malta, which would belong to this group, were removed from the analysis of the combined CLC-hazard data, because of the lack of hazard data (Cyprus is not covered by the hazard map, while Malta only shows coastal hazard). These countries were, instead, included in the basic analysis of general Land Cover national accounts. The results are shown in Tab. 3.4.

The first observation is on the "weight" of artificial areas on each nation's surface. This is usually small, well below a two-digit percent value, with the exception of Belgium (20.4%) and The Netherlands (12.1%); Malta shows, indeed, the highest share (28.9%), but, for its small extension (100 times smaller than BE or NL), it should be treated separately.

The average value is very similar in EU27 and EU15, 4.13% and 4%, respectively. It's a little bit smaller in the ST13, with a value of 3.43%. The minimum share of artificial surfaces is found, not unexpectedly, in Sweden (1.29%). Among the newly accessed countries, apart from the small island of Cyprus (7.47%), the highest share is shown by the Czech Republic (6.09%) which is slightly surpassed by Romania (6.25%) if we include the two newest Eastern countries. Latvia (1.32%) has the least artificial surface cover of all the countries here

studied. The low shares of Spain (1.56%), Greece (2.09%) and Portugal (2.65%), the only "EU 15 countries" included in the "Structural funds" group, should also be noted.

Spain also shows a peculiar behaviour when looking at the distribution of continuous vs. discontinuous urban fabric within the country (codes 111 and 112, which constitute the higher level code 11 "Urban Fabric"). Urban fabric is very important within artificial surfaces, as it usually accounts for the largest part (EU27 average is 75.5%). The balance of continuous and discontinuous fabric is usually by far in favour of the latter (EU27 avg. 95.8% vs 4.2%). Only in Spain, this balance is almost even, with 48.2% of continuous vs. 51.8% of discontinuous urban fabric, which, in turn, represent 31.8% and 34.1% of all artificial surfaces, respectively. The latter figures should be compared to the EU27 average of 3.2% and 72.3%. Conversely, from the CLC 2000 survey, no continuous urban fabric exists in Finland and the Netherlands, where the only urban land cover is the discontinuous one.

Among all other nations, only Italy shows a two-digit value for the share of continuous urban fabric on artificial surfaces (10.1%), while the distribution of such share in the countries considered here is rather flat, especially for the newly accessed and candidate countries (below 1%), while Greece and Portugal are close to 6% and Malta around 3%.

Discontinuous fabric is always above 60% in the 15 studied countries, with the only exceptions being Estonia (55.2%) and Romania, with the top value of 86.4%.

The second "best performance" in artificial land cover types is almost always represented by code 121, Industrial or Commercial Units (EU27 avg. 11%), with the only exceptions being Denmark, Ireland and the UK with two-digit artificial surface shares for the code 142, Sports and Leisure facilities. All this, makes the first three land cover types (111, 112 and 121) account for more than 85% of EU territory. Only Latvia shows a peculiarly high share in code 141, Green Urban Areas, with 9.5%, far above each group's averages, placed around 1.5%.

NUTS0	LC_111	LC_112	LC_121	LC_122	LC_123	LC_124	LC_131	LC_132	LC_133	LC_141	LC_142
BG	0.19%	75.57%	14.10%	0.77%	0.08%	0.66%	5.53%	0.79%	0.06%	0.82%	1.42%
BE	0.77%	81.78%	8.05%	1.75%	0.96%	0.93%	1.37%	0.23%	0.25%	0.70%	3.22%
CZ	0.30%	75.51%	11.33%	1.08%	0.03%	1.18%	3.57%	2.89%	0.18%	1.34%	2.60%
DK	1.98%	63.78%	8.35%	0.29%	0.54%	2.22%	1.77%	0.07%	0.10%	3.60%	17.28%
DE	0.79%	76.74%	10.60%	0.60%	0.36%	1.63%	3.60%	0.62%	0.26%	1.47%	3.32%
EE	0.47%	55.20%	21.12%	3.86%	0.30%	2.80%	8.10%	4.23%	0.12%	2.44%	1.37%
IE	3.83%	64.81%	4.54%	1.59%	0.39%	1.74%	6.29%	0.25%	2.07%	2.88%	11.62%
GR	5.94%	57.12%	12.85%	3.60%	0.21%	3.35%	9.94%	0.19%	4.17%	0.35%	2.28%
ES	31.77%	34.09%	15.03%	0.93%	0.38%	1.80%	8.16%	0.89%	3.73%	0.74%	2.48%
FR	1.76%	74.46%	11.84%	1.39%	0.30%	1.66%	3.24%	0.28%	0.55%	0.74%	3.77%
IT	10.11%	65.53%	15.52%	0.95%	0.42%	1.47%	3.38%	0.14%	0.53%	0.71%	1.23%
LV	0.87%	61.19%	17.72%	2.56%	0.69%	2.09%	4.12%	0.31%	0.05%	9.52%	0.88%
LT	0.11%	69.01%	17.65%	2.82%	0.20%	1.36%	2.95%	0.41%	0.84%	3.51%	1.15%
LU	3.24%	77.68%	9.00%	1.58%	0.11%	1.61%	1.22%	2.91%	0.14%	1.14%	1.38%
HU	0.60%	78.39%	9.34%	0.92%	0.07%	1.16%	1.31%	0.98%	0.22%	1.06%	5.95%
NL	0.00%	66.04%	13.69%	1.19%	2.63%	1.36%	0.55%	0.15%	2.86%	2.48%	9.05%
AT	2.05%	88.04%	3.20%	0.75%	0.04%	0.99%	2.18%	0.09%	0.07%	0.69%	1.89%
PL	0.80%	74.95%	9.74%	1.13%	0.25%	2.08%	3.56%	1.21%	0.53%	2.60%	3.16%
PT	5.79%	67.65%	12.03%	1.02%	0.57%	1.64%	5.47%	0.19%	1.78%	0.61%	3.25%
RO	0.71%	86.39%	9.18%	0.47%	0.12%	0.19%	1.55%	0.47%	0.09%	0.44%	0.39%
SI	0.30%	76.58%	11.85%	3.49%	0.29%	1.27%	2.31%	0.62%	0.47%	0.47%	2.34%
SK	0.36%	81.71%	10.19%	0.66%	0.09%	0.84%	1.23%	0.54%	0.33%	0.40%	3.64%
FI	0.00%	76.97%	10.98%	0.38%	0.30%	1.70%	4.48%	0.48%	0.18%	1.47%	3.09%
SE	0.76%	66.92%	10.13%	3.88%	0.22%	2.45%	1.75%	1.19%	0.07%	5.61%	7.03%
UK	1.56%	67.68%	7.66%	0.44%	0.52%	2.50%	3.06%	0.38%	0.27%	3.23%	12.69%
EU 27	3.21%	72.29%	10.99%	1.07%	0.39%	1.59%	3.35%	0.59%	0.63%	1.57%	4.33%
EU 15	4.21%	70.00%	10.98%	1.09%	0.47%	1.78%	3.55%	0.42%	0.76%	1.62%	5.12%
ST 13	4.95%	71.41%	11.63%	1.10%	0.20%	1.30%	3.93%	0.94%	0.95%	1.28%	2.32%

***Table 3.4**: Land use exposure to floods in EU 27.*

The readout of the shares of artificial surfaces among European nations presented above, was also leading the following analysis, per nation and per land cover type, of the distribution of the artificial surfaces of different kinds within the areas under river flood hazard.

The national details are displayed for all European nations, along with European averages as a reference. The table is split into two parts, to report the areas in each “macro-category” of flood hazard, namely, “high” (with suffix “_H”) and “low” (with suffix “_L”).

The results are reported in Tabs. 3.5 and 3.6, respectively, while an example of graphical display representing class 111, is shown in Fig. 3.9.

Detailed comments can be found in (Lugeri et al., 2006); we herby only report the description of the general findings.

At continental level, we find that 77.9% of the territory is not exposed to flood hazard; the remaining part (about 4Mha out of 17.6Mha of artificial surfaces) is subdivided as 18.7% into High and 3.4% into Low hazard class.

The pattern does not change much if we look at the smaller groups already defined: “old EU15” has 17.9% in High hazard areas and 3.3% in low, the newly accessed countries show 20.7 vs. 3.8 and the countries in this study 18.8 vs. 3.3.

The above mentioned decision to include three out of the five original flood hazard classes into the “high” group is not the only factor to explain the huge inbalance between high and low hazard exposure of artificial surfaces in Europe. In fact, the class named “moderate flood hazard”, if passed from High to Low class would only account for a minimum shift in this inbalance. Rather, this is the confirmation that, in the past, human settlements were very often built up in floodplains, which are of course more likely to be exposed to flood events.

Moving forward in the analysis of the overall artificial surfaces vs. hazard distributions, we should notice that the “best performances” are obtained by nations either not very rich in artificial surfaces or where the main settlements are placed along the coast (so influenced by the neglect of coastal hazard), like Denmark, the Netherlands, United Kingdom, and, more interestingly in this study, Portugal, Greece and Spain.

NUTS0	111_H	112_H	121_H	122_H	123_H	124_H	131_H	132_H	133_H	141_H	142_H
BG	6.1%	12.2%	18.1%	28.1%	7.2%	14.1%	9.6%	11.4%	74.5%	16.7%	9.4%
BE	31.6%	15.1%	20.9%	16.1%	4.4%	2.3%	17.6%	14.2%	0.0%	12.8%	12.0%
CZ	51.3%	16.3%	26.4%	33.3%	80.0%	8.6%	17.8%	17.2%	11.8%	25.4%	18.5%
DK	12.2%	4.5%	3.8%	3.0%	8.8%	0.0%	0.0%	0.0%	0.0%	9.5%	1.3%
DE	45.5%	22.2%	30.6%	33.9%	59.1%	14.2%	22.1%	19.0%	20.9%	39.4%	24.7%
EE	9.4%	13.2%	13.6%	11.3%	17.5%	10.0%	15.7%	34.2%	0.0%	13.9%	13.0%
IE	35.6%	14.4%	10.5%	6.1%	5.0%	0.0%	9.7%	23.5%	16.0%	26.4%	7.3%
GR	8.3%	11.3%	13.2%	13.6%	0.0%	16.2%	10.8%	0.0%	6.7%	2.6%	4.5%
ES	15.9%	8.9%	19.6%	14.8%	11.3%	18.3%	8.5%	17.1%	13.7%	23.6%	9.5%
FR	31.8%	19.7%	26.5%	22.2%	21.5%	10.3%	31.4%	21.7%	10.3%	26.0%	19.5%
IT	10.3%	18.8%	24.3%	23.1%	2.8%	16.2%	13.2%	30.2%	19.2%	23.1%	18.7%
LV	5.9%	21.9%	24.7%	24.4%	8.5%	4.9%	20.7%	0.0%	0.0%	18.0%	35.0%
LT	23.7%	18.9%	18.0%	18.0%	0.0%	14.2%	27.5%	9.4%	20.4%	26.9%	24.2%
LU	82.9%	30.8%	31.4%	22.8%	100.0%	0.0%	56.8%	21.9%	0.0%	80.5%	0.0%
HU	39.3%	23.8%	26.3%	20.7%	91.4%	9.9%	11.7%	25.4%	15.7%	27.1%	19.3%
NL	0.0%	16.3%	19.2%	11.9%	1.9%	1.5%	15.2%	4.6%	10.4%	8.4%	9.7%
AT	44.1%	30.2%	40.0%	36.7%	100.0%	19.4%	22.7%	17.3%	23.8%	46.3%	26.4%
PL	28.9%	17.6%	20.1%	16.4%	16.7%	11.8%	14.7%	13.6%	14.3%	20.7%	25.1%
PT	6.0%	6.1%	4.7%	1.3%	0.0%	3.1%	5.7%	1.4%	3.4%	0.0%	1.5%
RO	28.8%	23.5%	30.3%	28.2%	56.3%	4.4%	23.0%	29.3%	33.3%	33.7%	28.4%
SI	73.1%	31.1%	40.3%	14.8%	0.0%	5.4%	21.4%	48.1%	2.4%	58.5%	31.9%
SK	43.0%	26.0%	43.0%	45.4%	51.2%	35.9%	12.8%	33.6%	15.0%	50.0%	14.4%
FI	0.0%	21.3%	19.0%	12.0%	0.9%	10.0%	6.1%	10.1%	3.0%	10.5%	11.4%
SE	24.7%	19.5%	24.3%	19.2%	12.1%	19.6%	4.3%	6.7%	2.9%	20.3%	15.2%
UK	12.5%	8.5%	12.7%	8.3%	2.2%	3.1%	12.3%	9.0%	3.8%	10.2%	8.5%
EU 27	**17.85%**	**18.42%**	**23.51%**	**20.70%**	**17.14%**	**10.78%**	**16.74%**	**17.76%**	**12.25%**	**21.35%**	**13.94%**
EU 15	**17.26%**	**17.73%**	**23.17%**	**20.09%**	**15.68%**	**10.70%**	**17.07%**	**15.76%**	**11.67%**	**20.80%**	**12.95%**
ST 13	**16.30%**	**18.55%**	**22.28%**	**19.64%**	**20.37%**	**12.58%**	**12.70%**	**19.31%**	**12.22%**	**22.36%**	**16.85%**

Table 3.5*: Exposure to "high" flood hazards for artificial surfaces in EU 27.*

NUTS0	111_L	112_L	121_L	122_L	123_L	124_L	131_L	132_L	133_L	141_L	142_L
BG	12.8%	1.4%	2.5%	2.1%	4.3%	4.2%	1.1%	1.0%	3.6%	4.2%	0.1%
BE	9.5%	4.8%	6.0%	8.0%	12.2%	0.9%	1.5%	0.9%	3.2%	7.7%	3.6%
CZ	0.0%	1.9%	3.3%	3.9%	20.0%	3.3%	1.6%	0.9%	7.4%	1.5%	2.3%
DK	0.1%	1.6%	2.0%	0.0%	1.6%	0.0%	1.1%	0.0%	0.0%	0.9%	0.3%
DE	5.1%	5.1%	7.1%	8.4%	6.8%	8.1%	3.9%	4.8%	4.1%	6.7%	6.1%
EE	14.1%	4.4%	4.2%	6.7%	0.0%	12.9%	8.5%	1.9%	0.0%	4.8%	1.6%
IE	6.9%	3.2%	2.1%	2.7%	0.0%	0.0%	4.1%	0.0%	2.4%	1.7%	2.1%
GR	0.8%	2.5%	1.6%	1.3%	0.0%	2.1%	0.4%	0.0%	0.8%	0.7%	0.0%
ES	2.3%	1.0%	1.7%	2.4%	0.0%	1.7%	0.8%	2.4%	1.1%	1.2%	1.1%
FR	3.9%	2.9%	4.1%	4.5%	1.3%	2.5%	3.7%	6.3%	1.3%	3.2%	1.9%
IT	1.6%	2.6%	3.7%	4.9%	0.0%	2.5%	0.9%	3.9%	2.0%	3.6%	1.3%
LV	1.7%	6.5%	7.5%	10.0%	0.0%	0.4%	7.5%	14.3%	0.0%	5.1%	10.0%
LT	0.0%	3.8%	5.0%	4.3%	0.0%	11.4%	8.2%	6.5%	5.2%	2.6%	5.6%
LU	0.0%	1.1%	0.3%	1.8%	0.0%	0.0%	0.0%	0.0%	0.0%	0.0%	0.0%
HU	2.8%	7.4%	6.9%	7.8%	0.0%	8.8%	6.0%	8.7%	2.7%	8.2%	3.6%
NL	0.0%	4.6%	4.9%	2.3%	0.0%	2.1%	8.8%	0.0%	0.9%	2.6%	4.5%
AT	7.4%	3.0%	8.1%	7.1%	0.0%	11.3%	2.6%	1.9%	0.0%	5.9%	6.2%
PL	5.3%	4.3%	4.9%	5.8%	6.6%	3.0%	5.2%	1.9%	5.6%	5.4%	4.0%
PT	0.3%	0.7%	0.8%	0.3%	0.0%	0.0%	0.4%	0.0%	0.0%	0.0%	0.0%
RO	4.7%	3.0%	4.3%	3.8%	3.1%	0.4%	1.3%	5.1%	2.3%	6.3%	2.2%
SI	0.0%	3.9%	5.3%	7.2%	0.0%	0.0%	2.0%	0.0%	4.9%	0.0%	2.5%
SK	0.0%	4.1%	5.3%	6.9%	29.3%	1.6%	0.6%	2.9%	6.1%	9.1%	1.5%
FI	0.0%	3.6%	2.4%	0.0%	2.3%	2.8%	0.7%	0.0%	0.0%	0.7%	0.4%
SE	0.4%	2.7%	3.0%	4.4%	3.4%	3.4%	1.1%	3.4%	0.0%	3.3%	2.4%
UK	3.2%	2.1%	3.3%	0.6%	0.0%	3.6%	2.3%	1.9%	2.6%	2.6%	1.4%
EU 27	**2.56%**	**3.41%**	**4.30%**	**4.72%**	**2.91%**	**3.89%**	**2.59%**	**3.24%**	**1.80%**	**3.88%**	**2.47%**
EU 15	**2.46%**	**3.34%**	**4.26%**	**4.52%**	**2.69%**	**3.83%**	**2.36%**	**3.56%**	**1.44%**	**3.54%**	**2.20%**
ST 13	**2.32%**	**3.27%**	**3.67%**	**4.25%**	**2.87%**	**3.31%**	**2.20%**	**2.78%**	**1.73%**	**4.47%**	**2.42%**

Table 3.6*: Exposure to "low" flood hazards for artificial surfaces in EU 27.*

In general, the highest share of artificial surfaces under threat from flood hazard is in Slovenia (35.3%) and the lowest in Denmark (5.3%) then in Portugal (6.1%). If we focus on High hazard areas, Slovenia is slightly surpassed by Luxembourg (31.3% vs. 32.2%, respectively), while the same positions are kept by the above mentioned "best performers": Denmark with 4% and Portugal with 5.5%.

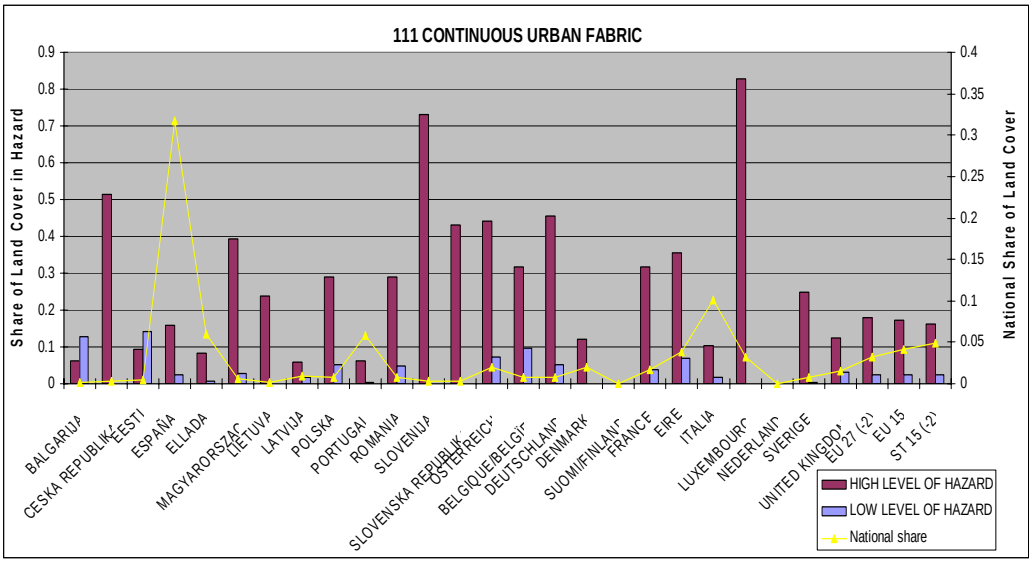

***Figure 3.9**: Overall representation of exposure to flood for the land use class 111 – continuous urban fabric.*

3.3.2 Exposure of population

In this application, population exposure to inland river floods has been estimated, by overlaying the Flood Hazard Map and a dataset which we may call "Gridded population density of Europe", hereafter described.

This dataset is based on CLC, processed in order to provide an average value of the population density for the group of neighbouring pixels derived by the CLC 2000 raster dataset, according to the work of Gallego and Peedell (Gallego 2001).

A statistical analysis of the population distribution in the EU territory has been performed, in order to understand how people are settled as a function of the landcover patterns (coded according to the CORINE legend) or, in other words, to investigate the existing correlation between type of land cover and type of dwelling. Population density has therefore been "territorialized", i.e., a local function (at municipal level) has been applied to each landcover patch, so that the population density for that kind of landcover is assigned to each pixel belonging to that class. Accuracy and limitations of the dataset are described in the above cited publication.

The dataset is released and maintained by the EEA, in the version with pixel size of 100m (EEA dataservice website). Resampling to the coarser version of the raster CLC that has been used in the other applications described in this report was not feasible, due to the statistical methods behind the original dataset. We have therefore overlaid the two raster layers,

notwithstanding the huge resolution difference, provided a reasonably good matching of the layers after the necessary reprojection procedure was guaranteed.

Given the definition of the dataset, a straightforward conversion from population density to "true" population number was performed. With 100m being the raster resolution, and because the value of the pixel is expressed in people/Km^2, the estimated (average) number of people in each pixel is given by this value divided by 100.

The overlay procedure involved selecting those pixels of the gridded population dataset lying in each given flood hazard class. Each pixel of the dataset was therefore given the corresponding value from the hazard map,

The sum of this pixel-based population distribution was then performed over the NUTS3 level (version 9) administrative boundaries. Such sums were made for each of the significant hazard values (from 2 to 6). In addition to this, following the approach described above, two grouped calculations were performed, summing hazard values 2 and 3 into "LOW HAZARD" and 4, 5 and 6 into "HIGH HAZARD".

The values of the exposed population, as tabulated for the administrative units, were calculated both in absolute and relative terms (divided by the total population of the NUTS unit). The total population was also calculated by the gridded population density data, in order to maintain a consistent approach.

In fact, both statistical and raster dataset resolution/accuracy effects affect the data and so, the whole procedure. In order to reduce geographical coverage and geometric mismatching effects, we have decided to "mask" the population density raster dataset with the hazard map one, thereby considering only the superimposing part of the datasets calculations and comparison. This also affects the absolute population figures. Table 3.7 below synthesizes the differences, at national level, of the population figures obtained by the raster population density data (with and without mask) from the Eurostat data on average population in Europe for the year 2000.

Field description is as follows:

POP2000 = Population from Eurostat
POP_GRD = Population derived from the gridded population density
Delta = POP2000 - POP_GRD
Delta_rel = (POP2000 - POP_GRD)/ POP2000
POP_HM = Population derived from the gridded population density, with the hazard map as a "mask"
Delta_HM = POP2000 - POP_HM
Delta_rel_HM = (POP2000 - POP_HM)/ POP2000

NUTS0	POP2000	POP_GRD	Delta	Delta_rel	POP_HM	Delta_HM	Delta_rel_HM
AT	8011566	8032408	-20842	-0.26%	8032408	-20842	-0.26%
BE	10251250	10296979	-45729	-0.45%	10293175	-41925	-0.41%
BG	8059889	8017500	42389	0.53%	7989532	70357	0.87%
CZ	10272322	10230199	42123	0.41%	10230199	42123	0.41%
DE	82211508	82224949	-13441	-0.02%	82125160	86348	0.11%
DK	5339616	5343481	-3865	-0.07%	5145976	193640	3.63%
EE	1369515	1371249	-1734	-0.13%	1229262	140253	10.24%
ES	40263216	39137362	1125854	2.80%	38334444	1928772	4.79%
FI	5176209	5192041	-15832	-0.31%	5078610	97599	1.89%
FR	59012502	58518653	493849	0.84%	58208771	803731	1.36%
GR	10917482	10812635	104847	0.96%	10495292	422190	3.87%
HR	4502499	4435843	66656	1.48%	4293698	208801	4.64%
HU	10210971	10196901	14070	0.14%	10196901	14070	0.14%
IE	3805368	3735514	69854	1.84%	3653973	151395	3.98%
IT	56948606	56763669	184937	0.32%	55519644	1428962	2.51%
LT	3499536	3484068	15468	0.44%	3482515	17021	0.49%
LU	436300	439503	-3203	-0.73%	439503	-3203	-0.73%
LV	2372985	2377782	-4797	-0.20%	2376167	-3182	-0.13%
MT	385808	394485	-8677	-2.25%	386176	-368	-0.10%
NL	15925513	15985639	-60126	-0.38%	15959642	-34129	-0.21%
PL	38453757	38220542	233215	0.61%	38203981	249776	0.65%
PT	10225836	9868740	357096	3.49%	9747714	478122	4.68%
RO	21892131	22188245	-296114	-1.35%	22144591	-252460	-1.15%
SE	8872109	8870667	1442	0.02%	8683803	188306	2.12%
SI	1988925	1964316	24609	1.24%	1959698	29228	1.47%
SK	5388720	5403051	-14331	-0.27%	5403051	-14331	-0.27%
UK	58892514	58729959	162555	0.28%	57903527	988987	1.68%

Table 3.7*: Exposure of Population to Flood Hazards in EU 27*

Rather than reviewing differences between the calculated population figures and the “official” figures, it’s important in our analysis to check that no dramatic variations occur when limiting the study to the only superimposing territory between the two datasets. Big changes appear only in countries having vast coastal extension, where the 1Km pixel effect may cause some coastal residential areas to be missed. Nevertheless, this is not a big issue in our study, as we are focused on inland river floods and coastal flood hazard is neglected.

A main table containing the values of people exposed to the different degrees of flood hazard per NUTS3 administrative area has been built. The field names in the table reflect the above described data in a simple structure:

POP_SFX1_SFX2

With SFX1 (suffix1) = ABS or REL, stands for absolute or relative population values;

SFX2 (suffix2) = 0,2,3,4,5,6,HI or LO, stands for the different classes (or groups of classes) of the hazard map.

For example the field POP_ABS_0 carries the values of population not affected by flood hazard in a given NUTS3 region. POP_REL_LO represents the share of population exposed to the hazard map classes coded as 2 = Very low flood hazard or 3 =Low flood hazard;

NURGCD is the field containing the NUTS3 code; POP_HM is defined in tab. 3.7, above.

An excerpt of this dataset is reported in Tab. 3.8:

NURGCD	POP_ABS_LO	POP_REL_LO	POP_ABS_HI	POP_REL_HI	POP_ABS_6	POP_REL_6	POP_HM
AT111	426	1.12%	3858	10.12%	1496	3.92%	38136
AT112	3826	2.72%	17945	12.73%	6345	4.50%	140930
AT113	2636	2.68%	24108	24.49%	11504	11.69%	98437
AT121	3373	1.42%	55427	23.35%	30187	12.72%	237406
AT122	5075	2.06%	84739	34.42%	32479	13.19%	246216
AT123	1878	1.32%	42438	29.81%	12687	8.91%	142382
AT124	5872	2.62%	34191	15.24%	21616	9.64%	224317
AT125	3734	3.02%	20182	16.30%	8989	7.26%	123821
AT126	17182	6.18%	71880	25.84%	20626	7.41%	278204
AT127	15261	5.20%	76111	25.95%	36880	12.58%	293283
AT130	153560	9.91%	504007	32.51%	194705	12.56%	1550140
AT211	10409	3.87%	74608	27.76%	38427	14.30%	268726
AT212	936	0.71%	29802	22.63%	25799	19.59%	131682

Table 3.8*: Potential exposure of population to flood hazard in Austria.*

Four maps, showing the distribution of exposed population for the highest hazard class per-se (class 6 - “very high”) and the grouped one named “High” are given as an example of mapping the overall tabular data. Class breaks was slightly adjusted from the built-in “natural breaks” classification scheme in ArcMap. Such a scheme is based on an analysis of the data distribution and identifies break points by picking the class breaks that best group similar values and maximize the differences between classes. The features are divided into classes whose boundaries are set where there are relatively big jumps in the data values, according to Jenks optimization (ESRI ArcMap documentation).

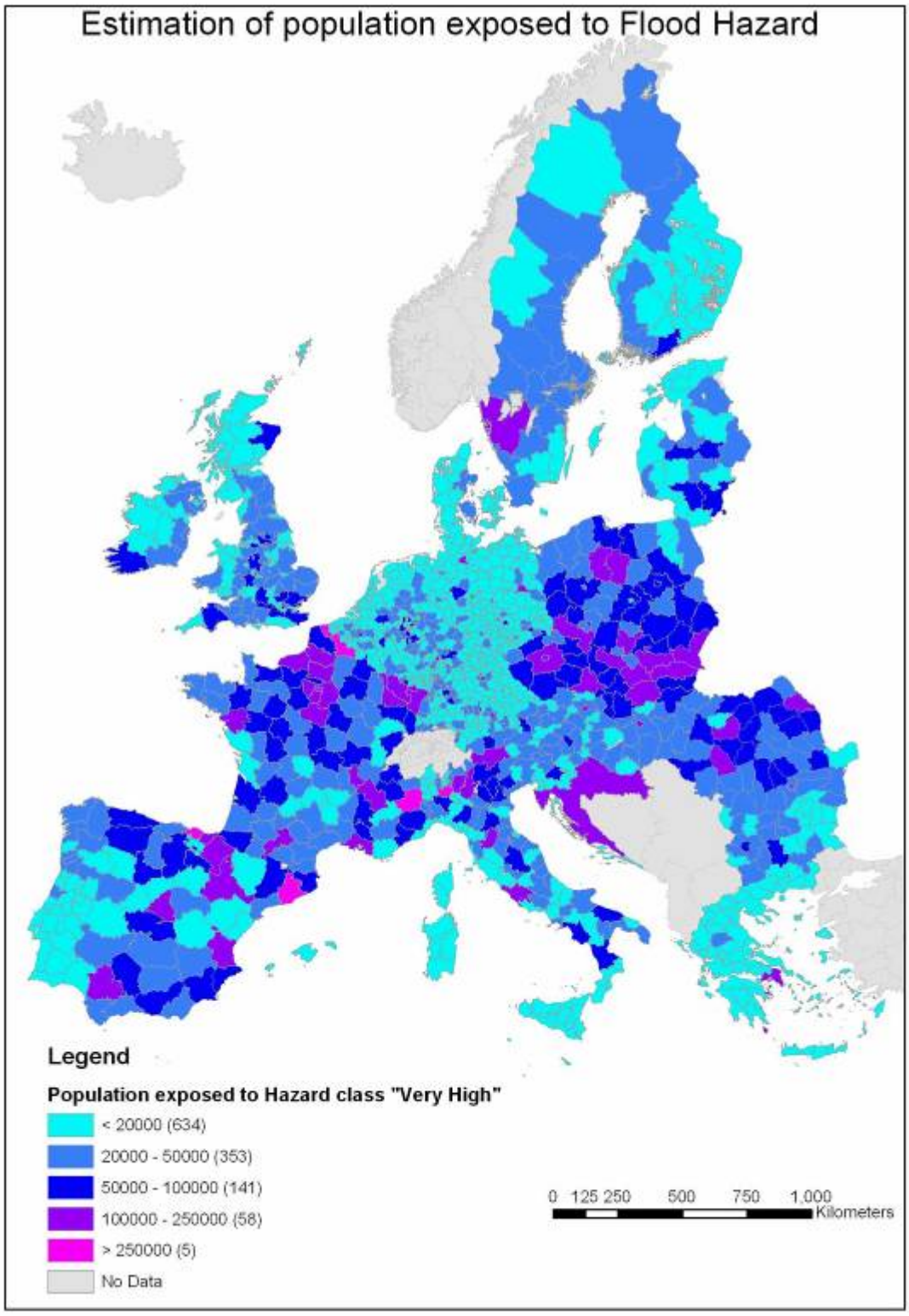

***Figure 3.10 (a)**: Exposure of population to floods for hazard class "Very high".*

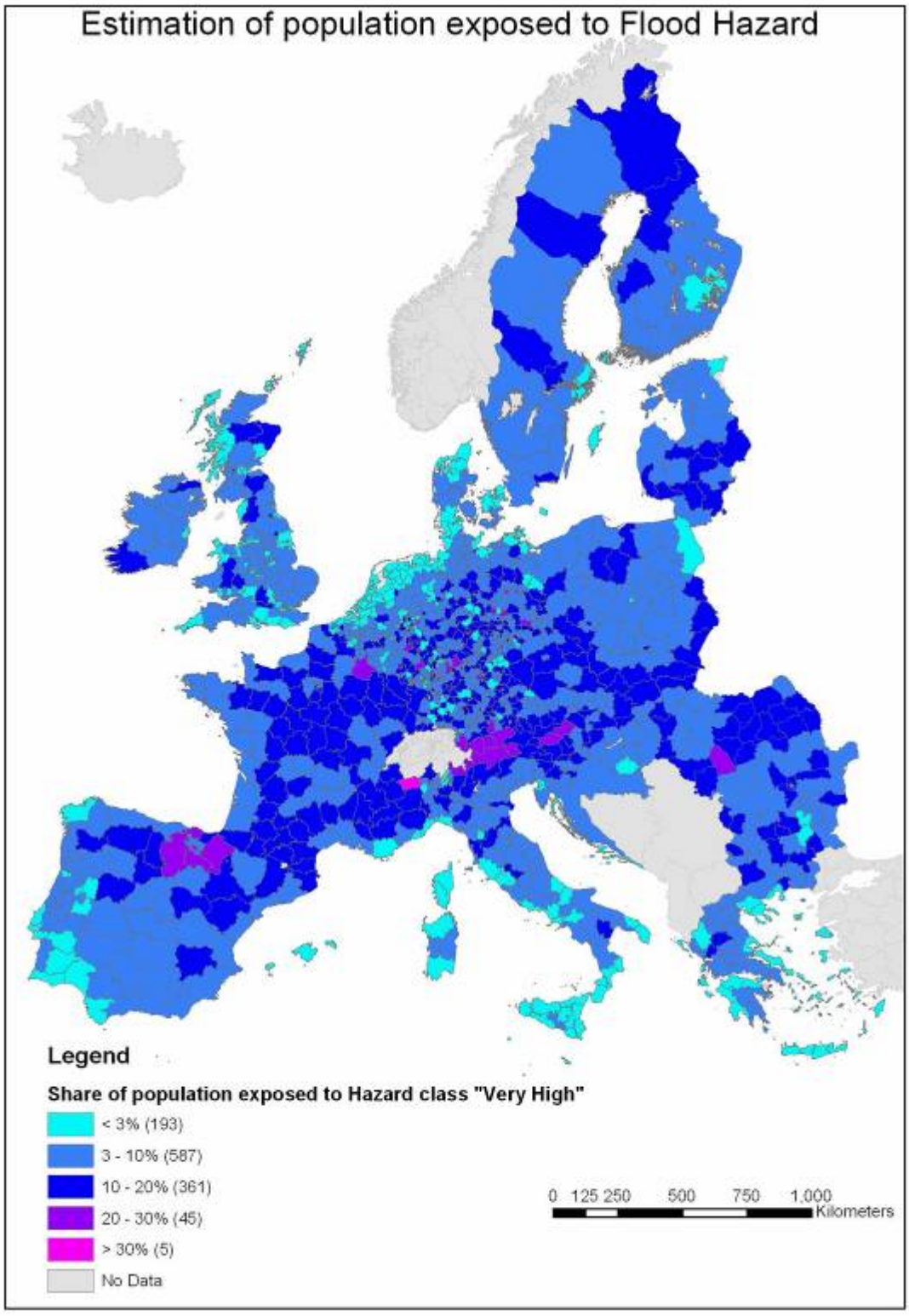

***Figure 3.11 (b)**: Share of exposure of population to floods for hazard class "Very high"*

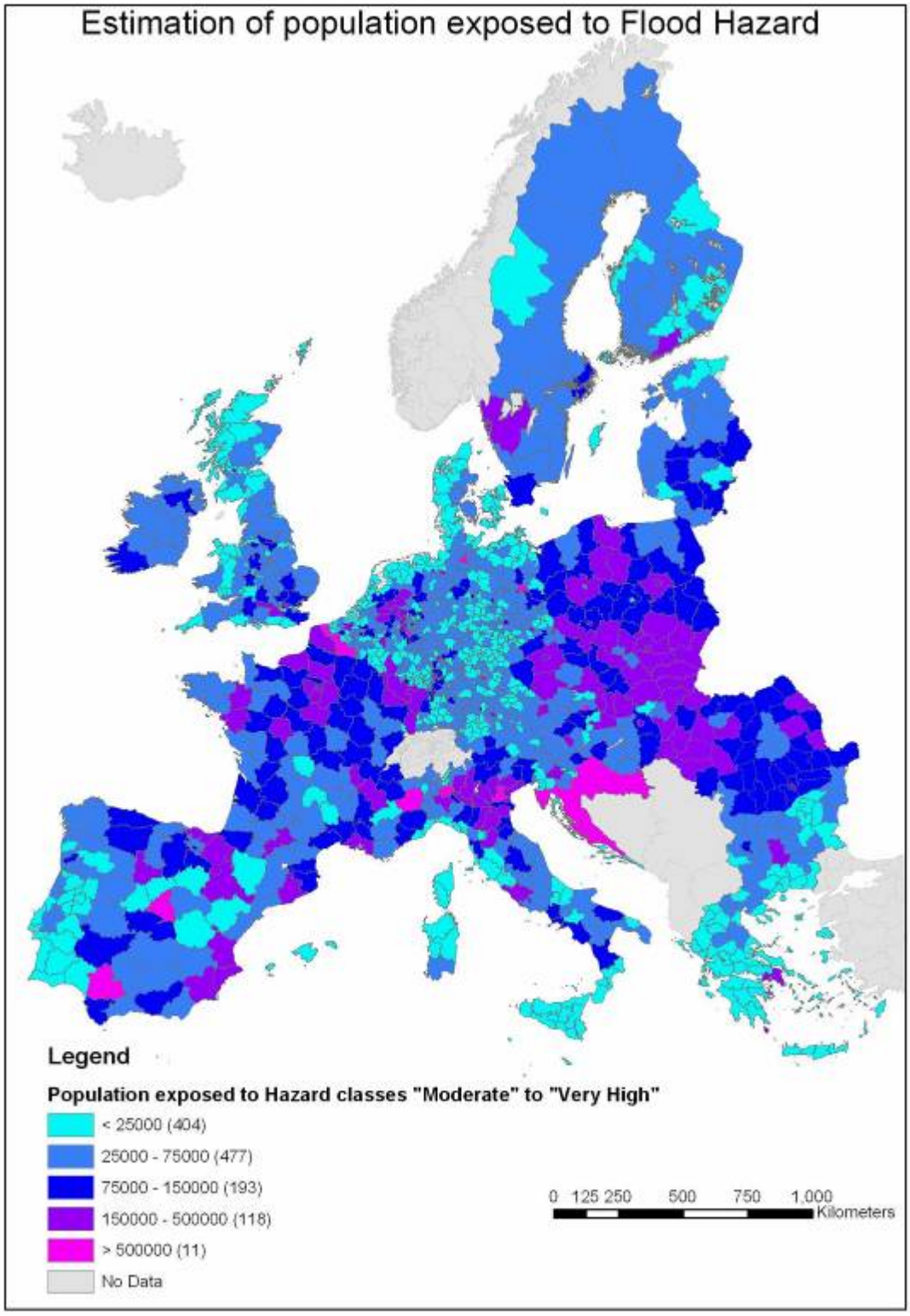

***Figure 3.12 (a)**: Exposure of population to floods for hazard classes "Moderate" and "Very high"*

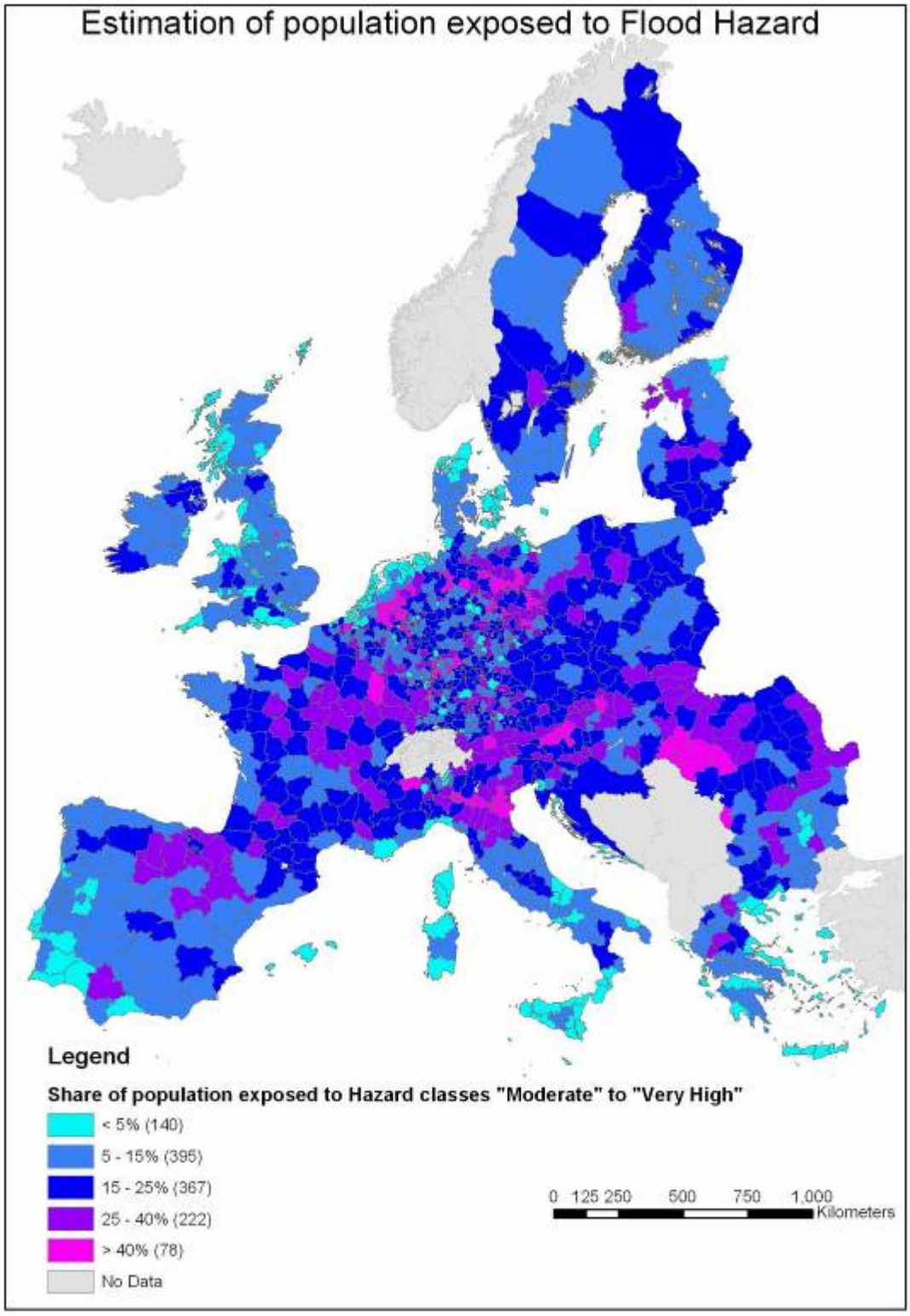

***Figure 3.13 (b)**: Share of exposure of population to floods for hazard class "Moderate" to"Very high"*

3.4 Vulnerability to floods: damage functions for land use types

The third component of the risk assessment procedure is usually dedicated to describing how the exposed people, goods, infrastructures and services are sensitive to damage from a given extreme phenomenon. It is therefore a function of the event and of its particular features. For example, during a flood event, a bridge can bear being completely covered by the rising waters, provided flood velocity is not high enough to cause a damaging stress to its structure.

Another very important parameter driving vulnerability is for example the run-up time to a flood event and the time between the first warning and the actual flood. A short run-up time is a key reason why flash floods are a considerable threat to lives and property (Kron, 2003; ICPR, 2002).

The most important parameters influencing flood impact are:

- Water depth
- Duration of flooding
- Flow velocity,
- Sediment concentration
- Sediment size
- Wave or wind action
- Pollution load of flood water
- Rate of water rise during flood onset (Van Der Sande, 2001).

Generally, flood depth and extent are most important for direct losses, duration for indirect losses and warning time for intangible losses (Green et al., 1994). Therefore, although the flood intensity parameters mentioned above include many different flood effects, in our present focus on direct losses, only water depth has been taken into account.

In the most widely used approaches, vulnerability is usually represented by depth-damage curves which describe the fraction of the value of properties exposed that could be lost if the event should occur. (ICPR, 2002).

A study recently finalized for JRC featured a survey and analysis of actual and expected damages as a function of main land categories and flood depth (HKV, 2007). Land use was described both according to the CORINE and MOLAND[2] legends. For each Country, flood damage functions are produced for any of the 44 land use/cover classes of the CLC (see table in Annex 1). The study was based on a thorough literature review, questionnaires to authors of specific studies and to experts of the field, and on adaptation of the collected data both to present time and to those countries for which no actual data could be found.

The functions represent the potential monetary loss (direct damage) occurred for given water depth. The resulting database relates water depth and monetary damage for the assessment of direct damage as consequence of floods. The flood damage functions are specific for each land use type (e.g. residential, industrial, etc.) per unit (e.g. hectare or squared-meter) and for each of the 27 Member States of the European Union. What is provided by this “flood

[2] See http://moland.jrc.it

damage database", is therefore the combination of the Exposure and Vulnerability as defined in the "risk triangle" approach.

In order to maintain the risk triangle structure, monetary land values were "attached" to the land cover layer representing the exposure, while the territorial-specific damage fraction (percent of damage as a function of flood depth) was built as an information layer to represent vulnerability.

Figure 3.14 shows the damage function (fraction) for the land use class 111 (continuous urban fabric) for Belgium. The degree of damage is expressed as a percentage of the full value as function of water depth.

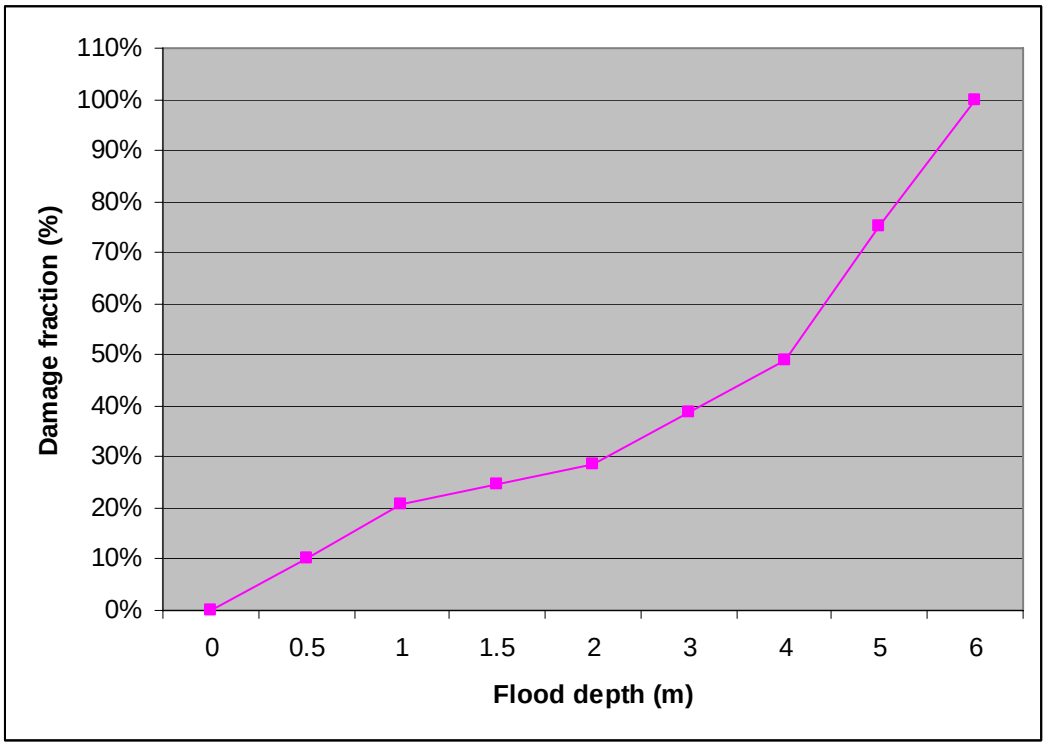

***Figure 3.14**: Damage function for continuous urban fabric (CLC class 111) for Belgium.*

Monetary figures in the database are updated to current prices and standardized for the EU Countries according to their Purchasing Power Parities. They represent asset values according to the "full replacement" scheme (FloodSITE 2006).

This approach represents a remarkable improvement with what was originally planned for A2.1, when the use of a single generalized damage function was envisaged for the whole of Europe. The new flood damage functions have been reconstructed in a dedicated study carried out by the JRC, outside the financing scheme of ADAM.

As an example, the derivation of damage functions and consequent damage assessment for the city of Prague following flooding in 2002 is given in Annex 2.

3.5 Monetary Damage Assessment

The final output of the methodology so far described is a digital map at European scale of flood related monetary risk. The risk gives the integrated monetary damage that could occur at a given location with an associated return period (or occurrence frequency).

As already mentioned the method has been developed and applied in the ESRI ArcGis environment, through raster-based map calculations and overlay operations. According to ESRI data formats and terminology, raster datasets were formatted as “Grids”, and stored with a naming convention recalling the different inputs, namely, the return period and the flood depth. The geometrical/geographical properties of the data have been presented in Section 3.1, i.e. CLC grid size 250m, Hazard map resolution 1km, while the territorial attributes are given by the Land Cover nomenclature, as translated into damage values.

Therefore, a set of Grids was prepared, to select and group portions of territory from the CLC2000 map according to their flood hazard level described by table 3.2. Accordingly, a set of “flooded” CLC grids, one per flood depth as defined in the damage functions, was prepared. Therein, each pixel of the CLC map is assigned its own damage value per square meter (total damage will be given by a multiplication by $250*250=62500m^2$), according to the corresponding damage function. Damage values are also weighted by the regional (NUTS2) GDP.

Each final grid results from the crossing of water depth levels (finally 11 levels were set) and the four return periods defined from the 5 classes of the FHM, as defined above. These 44 Grids represent the geographical database for flood damage assessment, to be performed on the territorial basis defined by the required application or study, such as a basin, local community area, administrative boundary (NUTS2 or 3), or abstract grids of given width (provided it’s broader than the dataset spatial information detail, which is 1km).

Two key assumptions had to be made in order to operationally use the flood hazard map in the damage calculations:

1. The different (possibly grouped) hazard classes define the flood extent expected with the corresponding probability, and each return period’s territorial extension includes the previous one.
2. The topography around the riverbed is assumed not to be complex, i.e., pixels with lower elevation are flooded before those with higher elevation with respect to the river level (no “dike-effect”).

In addition, we have to recall that a range of water depths (or extreme water levels) correspond to one return period, therefore more than one damage value must be used for each hazard class.

Given the above assumptions and the characteristics of the hazard flood map, the production of the final damage maps has required the development of a computing scheme for the proper application of the damage functions. It is important to note that the scheme allows obtaining the maximum and minimum values of expected damage, for each return period.

Table 3.9 illustrates the computational scheme.

The final distribution of water levels vs. return periods is therefore resulting from the final overlay of zones belonging to the various flood hazard classes. Therefore the water depth for a given return period is contained within a range of values which in turn provides a direct indication of the variability of the results. This variability could, after successive analyses, be related to the quantification of the uncertainties.

Return Period of Damage Value	MIN Damage Value	MAX Damage Value
20 years	0	All zones classified as FHC 6 below 0.5 m
50 years	All zones classified as FHC 6 below 1 m + all zones in FHCs 5 and 4 below 0.5 m	All zones classified as FHC 6 below 2 m + all zones in FHCs 5 and 4 below 1.5 m
100 years	All zones classified as FHC 6 below 3.5 m + all zones in FHCs 5 and 4 below 2 m + all zones in FHC 3 below 0.5 m	All zones classified as FHC 6 below 6 m + all zones in FHCs 5 and 4 below 4.5 m + all zones in FHC 3 below 1.5 m
500 years	All zones classified as FHC 6 below 6m + all zones in FHCs 5 and 4 below 5 m + all zones in FHC 3 below 2 m + all zones in FHC 3 below 0.5 m	All floodable zones above 6 m

Table 3.9: *Computational scheme used for the definition of the zones to be considered for the calculation of the flood damage value at each return period. The ultimate return period of each damage map corresponds to the value indicated in the first column of the table. FHC = Flood Hazard Class as defined in table 3.2,*

For each return period, we have computed two values (minimum and maximum) of potential monetary loss. The products are represented in two territorial units:

- Accumulated values over cell (grid) of 50 x 50 Km size and
- Accumulated values over administrative aggregation level (NUTS-2, sub national)

The monetary damage is computed assuming that for a given return period, the flood event is occurring **simultaneously** in the whole territorial unit.

The corresponding maps are given in Annex 3.

3.6 Annual Average Damage

In the terms defined above, the "spatial integration" of the expected damage means that, once a portion of territory and a recurrence period (hence, a range of flood depths) are chosen, the overall damage is the sum of each "elementary territorial damage unit", which is nothing but the pixel (250*250 m^2) encoded with its depth-dependent damage, as described above. The damage is therefore the "accumulation" of the contributions coming from the exposed portions of land. In fact, in a probabilistic approach as adopted here, where the recurrence (or return) period is the inverse of the yearly probability of exceedance of a given hydrological event, the total losses that one may expect from different events in given span time is the sum of any single local events that have the same return period. This analysis should then be performed for different return periods, in order to build up a Damage-Probability curve (**Figure 3.15** A) which, with the area subtended by the curve itself, defines one of the most widely used quantities in flood damage assessment: the Annual Average Damage (AAD) (FLOODsite, 2006).

This data can then be expressed in absolute, as well as GDP-relative terms, and mapped according to the integration level used, to display how differently the European territories behave.

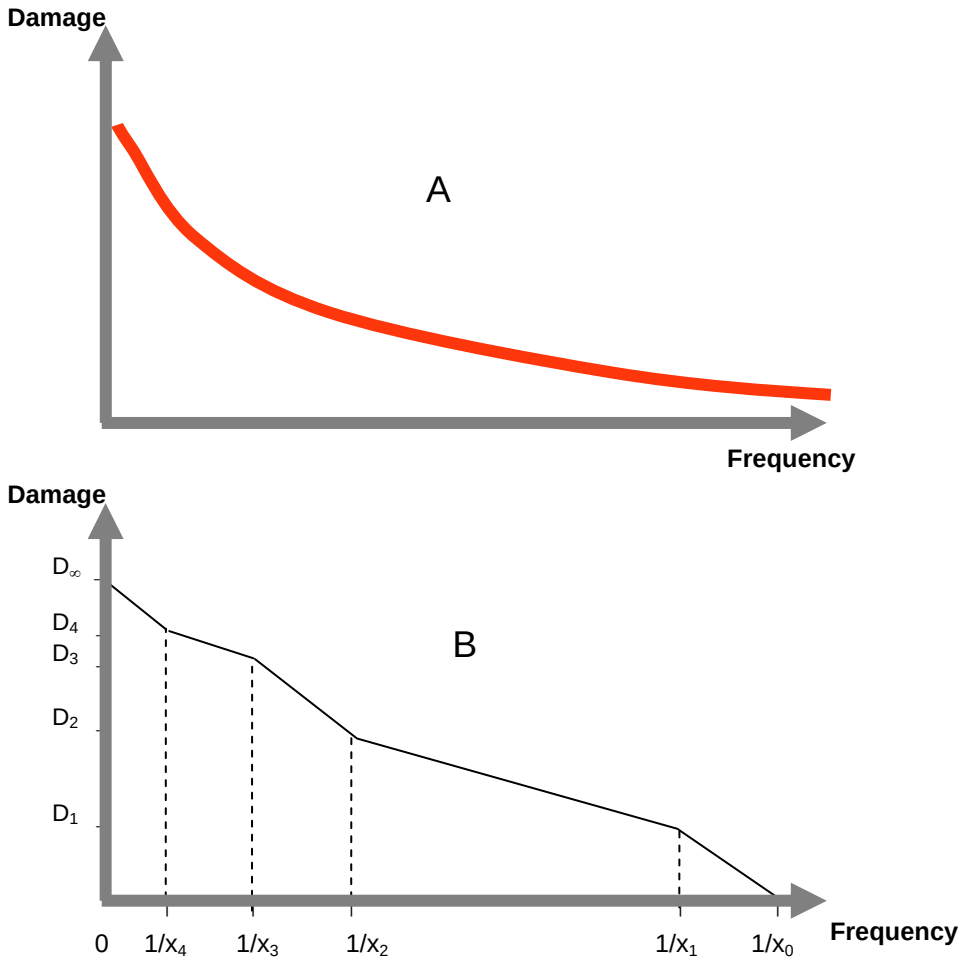

***Figure 3.15**: A: Damage-Probability curve. B: Damage-Probability curve as estimated for a discrete series of frequency-points.*

In practical terms, the Damage-Probability curve is approximated by the damage values recorded or estimated for various return periods, plotted in **Figure 3.15**-B, and accordingly calculated as the sum of the trapezoids drawn by the corresponding damage-frequency pairs. It's worth emphasising the definition of two particular entries in the graph, namely x_0 and D_∞ which represent, respectively, the maximum return period (hence, the frequency $1/ x_0$) at which no damage occurs, and the maximum possible damage for a catastrophic flood for which return period tends to infinity (hence, frequency tends to 0).

The calculation can therefore be expressed as follows:

$$AAD = \frac{1}{2} \cdot \sum_{n=0}^{N} \left(D_n + D_{n+1}\right) \cdot \left(P_n - P_{n+1}\right)$$

where $D_0 = 0$, $D_N = D_\infty$ and $P_N = 0$.

According to the approach defined above and described in Tab. 5.6, the AAD for the whole of Europe was calculated pixel-wise, in two versions, according to the "maximum" and

"minimum" defined in the columns of Tab 5.6, namely AAD_{min} and AAD_{MAX}. For both calculations, what we have defined as 500 years maximum damage, which in turn represent the entire exposed land (above the flood depth of 6m, all of the damage functions return the multiplying factor 1), was taken as D_{∞}.

As of x_0, in the calculation of AAD_{min}, according to Tab 5.6, it was set to 20 years, while for AAD_{MAX}, an arbitrary, although reasonable, value of 5 years was chosen. The above values do not affect the overall calculations dramatically, nevertheless, they also play a non negligible role and will be investigated in the method calibration phase.

A first check of the result was however performed, through the comparison of the AAD values, as calculated with the present method, with those published for England and Wales in 2001 by the UK Department for Environment, Food and Rural Affairs (DEFRA, 2001) with a consortium of scientists. The choice of UK and Wales was practically univocal, as there are very little published works on Flood damage assessment with comparable scale ("macro" scale, as defined in (FLOODsite, 2006)) and synthetic results (AAD, rather that single event analysis). As a further reference for the same area, another two recent works by Hall et. al (Hall, 2003 and 2005) were taken into account, also for an estimation of the uncertainty. The comparison was performed with DEFRA results because they report the capital value of assets at risk (the exposure) and the expected AAD, in a scenario where no defences exist, thus similar to what is described by our flood hazard map.

Although the study also includes a regional breakdown, the comparison was made only on England and Wales, because the regional borders in that report do not follow the NUTS standard, and regional data is described as less reliable in the DEFRA report. Values were standardised to 2007 Euros according to the yearly inflation rates for UK and average Pound/Euro exchange ratios from EUROSTAT . In addition to this, the damage figures originating from our method were downscaled by a factor of 2 in order to account for the difference between capitalised economic damage values like those in the DEFRA report and full replacement ones, as of our database.

the results of the comparison are shown in tab. 5.5, where the last column represents the mean value between AAD_{min} and AAD_{MAX}, with corresponding semi-dispersion.

	Exp. assets (Bln. €) DEFRA	Exp. assets (Bln. €) JRC	AAD (Bln. €/year) DEFRA	AAD (Bln. €/year) JRC
England	**152.3**	**197.5**	**3.0**	**7.4 ± 2.9**
Wales	**8.5**	**10**	**0.2**	**0.5 ± 0.2**
Total	**160.8**	**207.5**	**3.2**	**7.9 ± 3.1**

Table 3.10: *comparison with DEFRA 2001 Flood damage assessment in England and Wales*

At this stage of refinement of the technique, such comparison is quite satisfactory and in line with what could be expected with the level of detail imposed by the input data in our method. In fact, although it can be classified as a "macro scale" study, carried out at a national level, the resolution of the basic data in the DEFRA survey is much higher than that in our approach. The exposed assets are overestimated by around 30%. It is not possible now to distinguish whether the overestimation is attributable only to the extent of exposed surfaces as defined by the flood hazard map or to the monetary values per unit area given to the land

cover classes, or both. As a partial comparison we could see that DEFRA estimates that the agricultural areas under threat from fluvial floods are as wide as 10,000 km^2, while according to the CLC classes describing agricultural land covered by the river flood hazard classes, this figure is 40% smaller. Nevertheless, agricultural land values are largely smaller than the residential, commercial or infrastructure values, in both studies.

In the AAD_{MAX} case the results from our calculations are more than three times higher than those from the DEFRA survey, while the overestimation gets back to around 50% (that is, slightly more than the contribution from the exposure alone) when assessed on the basis of the AAD_{min} figure. No estimation of uncertainty is given in the DEFRA study. However, when assessing the AAD with flood defences in 2002, Hall estimates the overall figure for river and coastal flood at 1 billion pounds, with an uncertainty range from 0.6 to 2.1 billion. If we prudently interpret this range as the maximum dispersion around a center value of 1.35 instead of 1, we can accordingly apply to the values in Tab. 5.7 an uncertainty factor of

$$\frac{(2.1-0.6)}{(2.1+0.6)}$$

resulting in 0.56. We therefore obtain a maximum value for the AAD of England and Wales from the DEFRA assessment of about 3.2 *1.56 = 5.0 bln €. This figure gets even closer to our result if we apply the straight 2.1 factor arising from the upper uncertainty of Hall's study (3.2 * 2.1 = 6.7 bln €). In both cases, the values fall within the respective uncertainty ranges.

With such uncertainty values, we can definitely say that the two methods yield comparable results. The analysis of the uncertainties and the improvement of the return periods calibration will be further addressed in the next phase of the work.

The maps resulting from the application of the whole methodology, and representing the cumulated annual average expected damage cumulated across administrative units (NUTS2), are presented in the following figures.

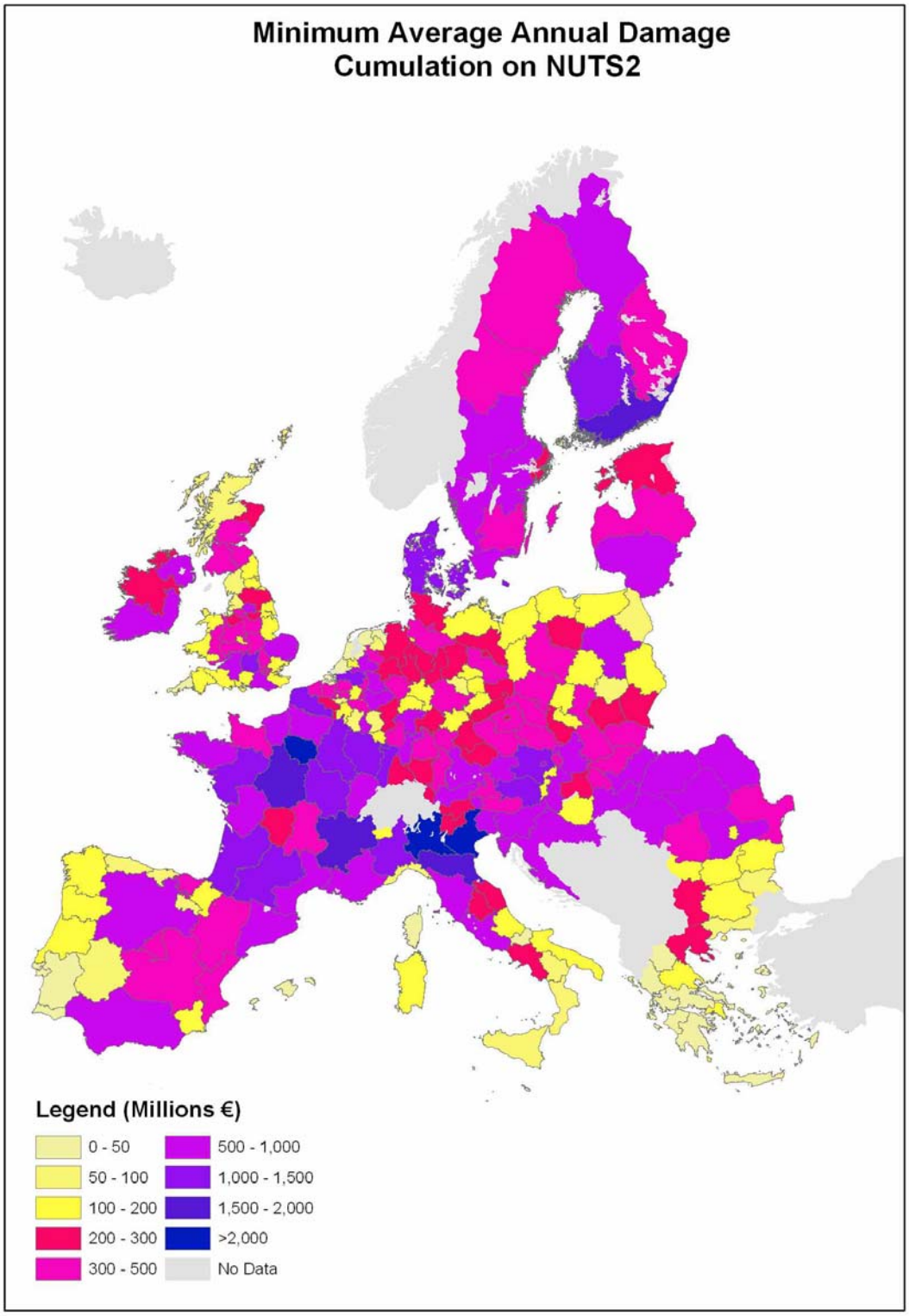

***Figure 3.16**: Minimum Average Annual Damage.*

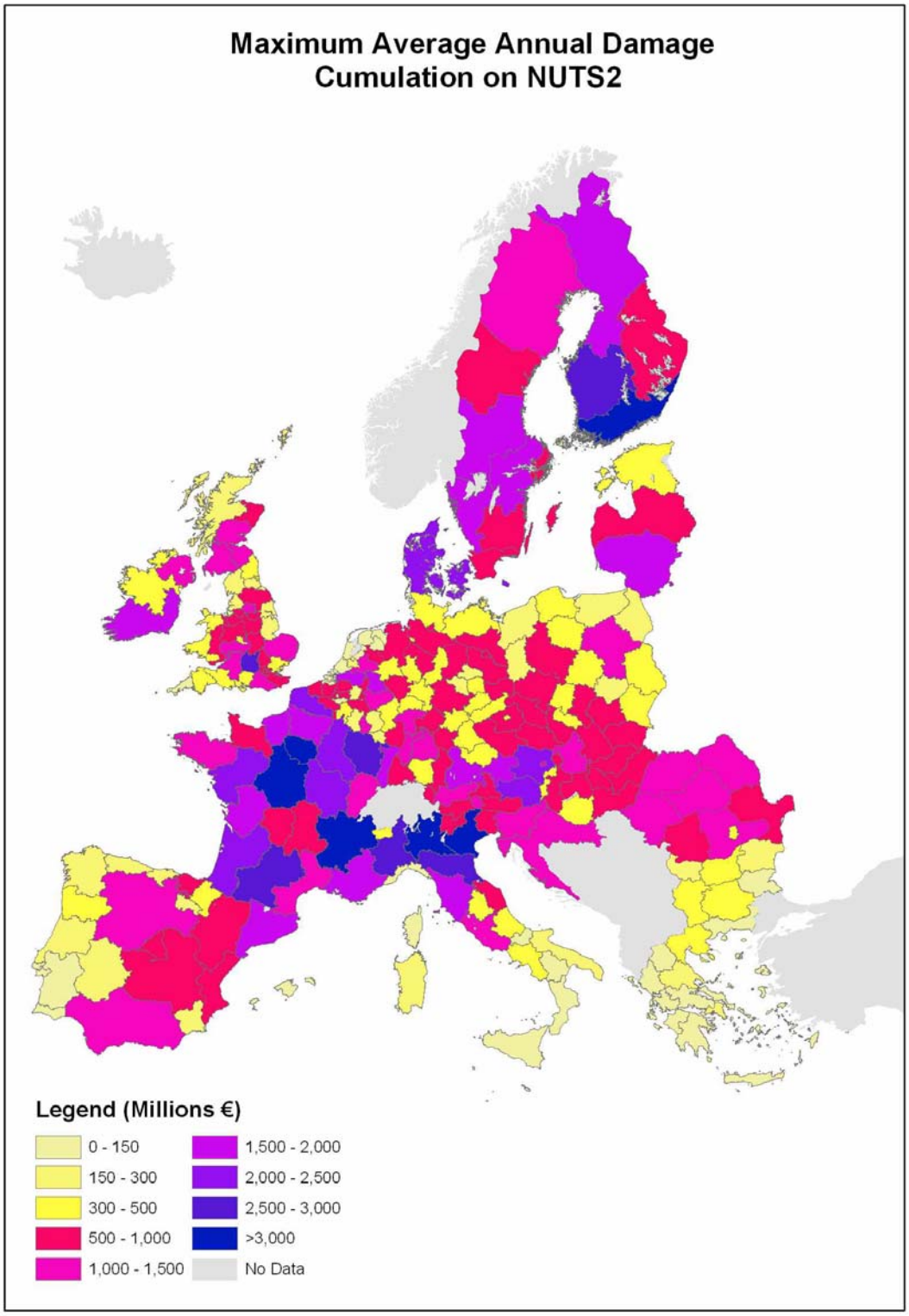

***Figure 3.17**: Maximum Average Annual Damage.*

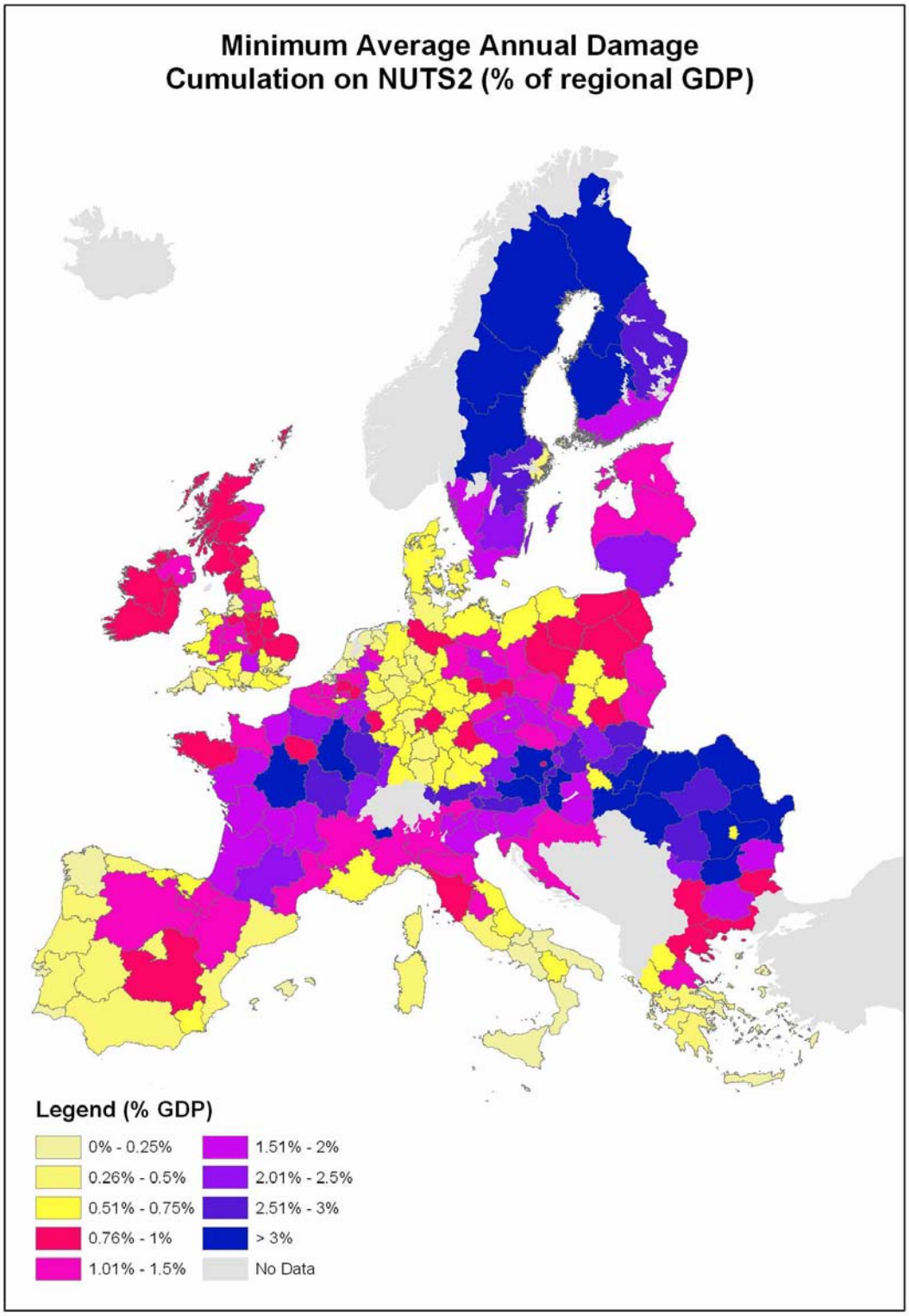

***Figure 3.18**: Minimum Average Annual Damage: fraction of regional GDP*

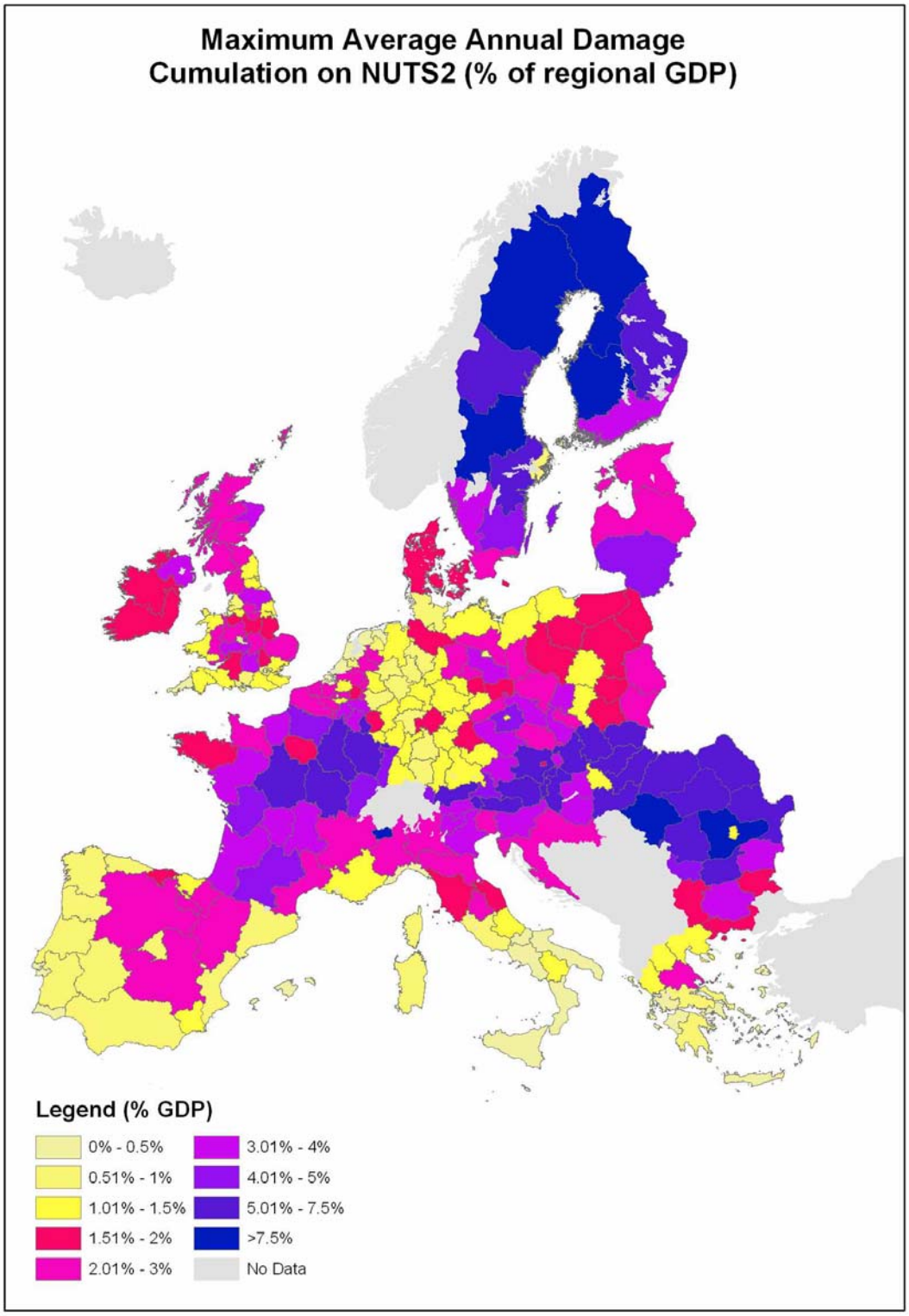

***Figure 3.19**: Maximum Average Annual Damage: fraction of regional GDP.*

4 Drought and heat stress risk assessment in agriculture.

The assessment of climatic stress impact in agriculture is not a simple task. This evaluation implies the knowledge of interactions between factors associated with stresses and factors associated with crops. While severity, duration, number of exposures and presence of other stresses are important from a stress perspective, plant response to stress depends on the physiological processes affected, sensitivity of the tissue or organ, developmental stage of the crop and type and/or variety of crop subjected to the stress. In general, flowering is the most sensitive stage and any stress during that period can reduce yield significantly. Similarly, a moderate stress may slow down photosynthesis but may continue to fill the sink (seed) by a re-translocation stored photosynthates.

To assess the interaction between climatic stresses and plant growth several methodologies have been employed such as crop experiments, bioclimatic indexes, etc. Of these, crop growth models seem to be the most suitable. Such a tool, in fact, allows the implementation of the experience gained from crop experiments for a quantitative assessment of yield loss. Finally, these tools may be used for a reliable simulation of climate change impact on final yield by coupling climate conditions (as simulated by General Circulation Models, GCMs) with data for CO2 effects on photosynthesis, which were experimentally obtained (e.g. FACE).

4.1 Application of the risk triangle to crop yield

The implementation of the risk-triangle methodology defined above applies to the damage assessment in agriculture, according to the scheme of Fig. 4.1a, with the following specifications:

Hazard is the probability of occurrence, which is related to the climate of an extreme event which, in turn, causes an impact on the growing plants. The investigation of extreme events and their parameterisation in terms of probability of occurrence (or return periods) was performed through the analysis of observed events having impact on agriculture.

The Cropsyst model has been used to assess crop yield on the basis of the Regional Circulation Model at low (50x50Km) or high (12x12Km) resolution over Europe and Guadiana respectively for SRES scenarios A2 and B2[3]. As concerning crop growth, extreme events having higher impact on final yield will be taken into account in this work, namely heat waves and water stress at anthesis stage.

[3] The A2 storyline and scenario family describes a very heterogeneous world. The underlying theme is self-reliance and preservation of local identities. Fertility patterns across regions converge very slowly, which results in continuously increasing global population. Economic development is primarily regionally orientated while per capita economic growth and technological change are more fragmented and slower than in other storylines.
The B2 storyline and scenario family describes a world in which the emphasis is on local solutions to economic, social, and environmental sustainability. It is a world with continuously increasing global population at a rate lower than A2 and intermediate levels of economic development. While the scenario is also orientated towards environmental protection and social equity, it focuses on local and regional levels.

Exposure is interpreted as the areas where cultivation is present and its actual economic value. In other words, it depends on land use (type of crop) and the monetary value of that crop. This could be measured as the product of the simulated average yield of each crop by the price that is actually paid per ton. Maps of yield of different crops including maize, wheat, sorghum and barley were produced for the present period (1960-1990) and the monetary value of each crop was assessed on the basis of average yield for 30 years and the average producer price. CLC and EUROSTAT/FAOSTAT crop statistics has been used in this context.

Vulnerability here measures the extent to which the subject matter could be affected by the hazard. In other terms, it describes the degree of coupling (impact) between exposed crops and extreme events (heat waves and water stress) occurring during the growing season. Since crop sensitivity to extreme events is phenological-stage dependent, only extreme events occurring at more sensible phenological stages will be considered. In particular, heat stress or drought, occurring at anthesis stage were indicated as the most detrimental for crop yield. Vulnerability is expressed as the fraction of yield loss for the different return period (potential-actual yield)

Figure 4.1.b shows the basic flow diagram of the implementation of the "risk triangle" methodology.

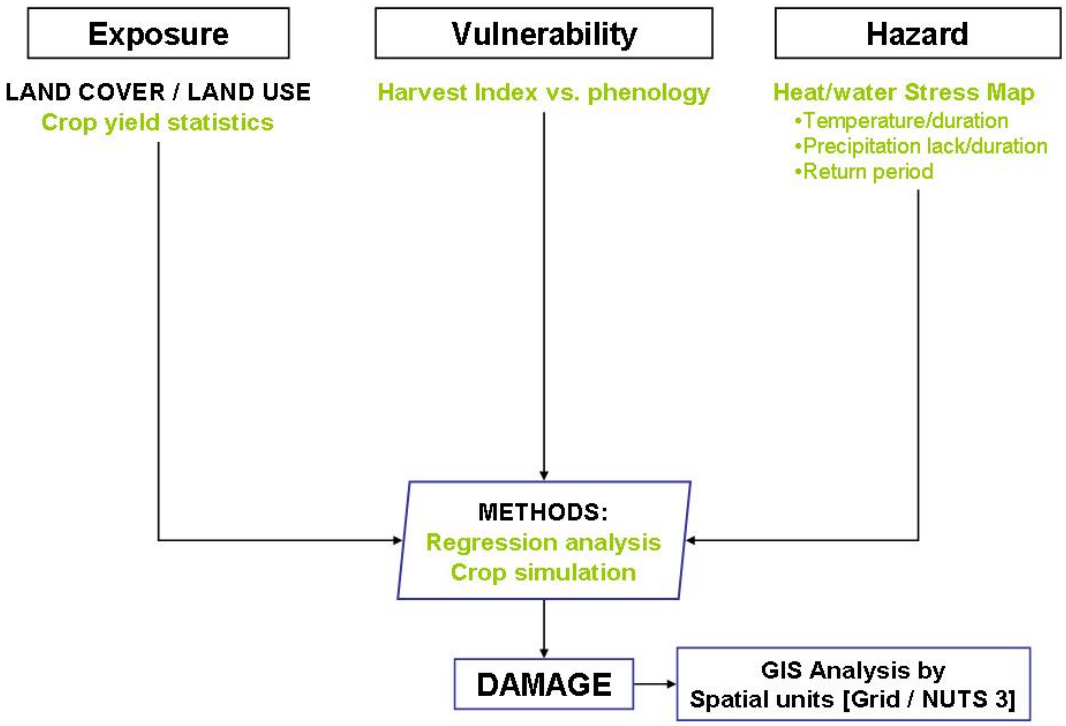

***Figure 4.1a**: Application of the risk triangle to crop yield.*

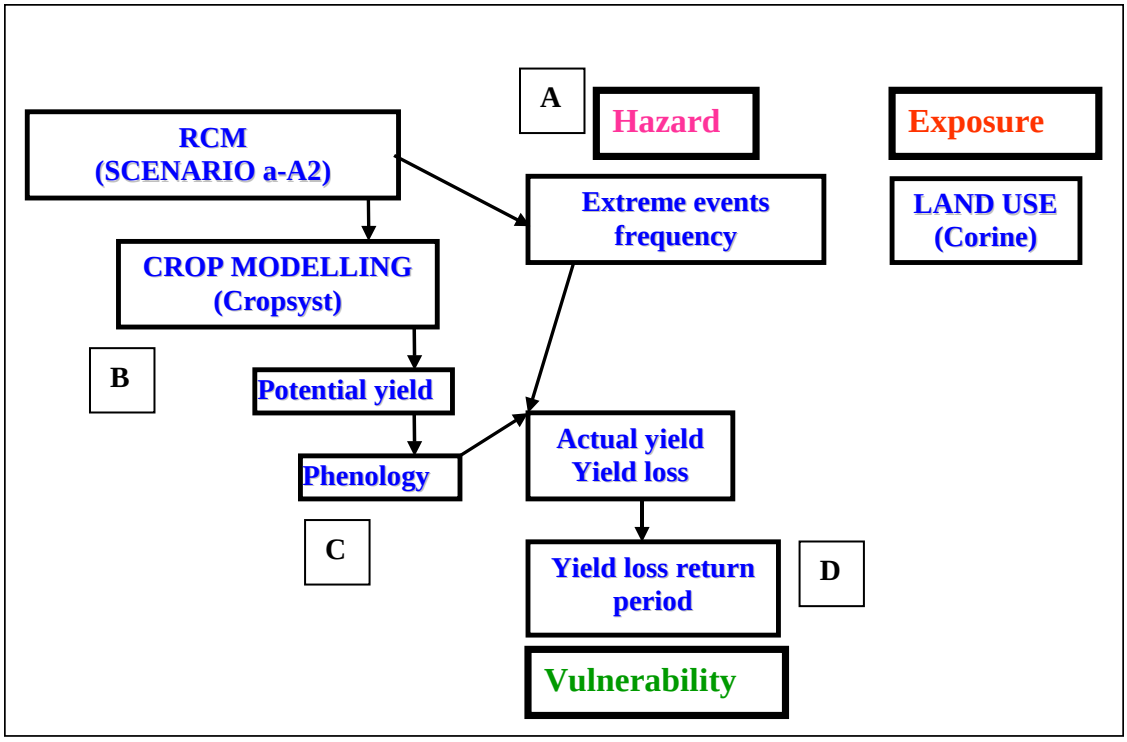

***Figure 4.1b**: Flow diagram of risk triangle implementation for climate change impact assessment on agriculture. First stage: use of climate data for extreme events frequency calculation (A). Second stage: use of climate data as crop growth simulation model to simulate potential yield (not including extreme events impact) and phenological stages (B). Intersection of extreme events frequency information to phenological stages dates to assess number and intensity of extreme events occurring at anthesis stage (C). Assessment of yield loss and its return period over 30 years (D) and overlay to the exposure map.*

4.2 Crop modelling

Cropsyst (Cropping Systems Simulation Model) was the crop simulation model selected for this work. This is a multi-year, multi-crop, daily time step crop growth simulation model, developed with emphasis on a user-friendly interface (Stockle et al, 2003). The model simulates the soil water budget, the soil-plant nitrogen budget, crop canopy and root growth, crop phenology, dry matter production, yield, residue production and decomposition, and erosion. The model allows the user to specify management parameters such as sowing date, cultivar genetic coefficients (photoperiodic sensitivity, duration of grain filling, maximum LAI, etc.), soil profile properties (soil texture, thickness, water and nitrogen initial content), fertilizer and irrigation management, tillage, atmospheric CO_2 concentration etc. The core of crop growth simulation is the determination of unstressed (potential) biomass growth based on crop potential transpiration and on crop intercepted photosynthetically active radiation. This potential growth is then corrected by water and nitrogen limitations, if any, to determine actual daily biomass gain. The simulated yield is then obtained as the ratio between actual total biomass accumulated at physiological maturity and the harvest index[4] (HI=harvestable yield/aboveground biomass).

$$final\_yield = HI \times TOTAL\_BIOMASS$$

[4] The HI is determined using as a base an unstressed harvest index modified according to stress intensity (water and nitrogen) and crop sensitivity to stress during flowering and grain filling.

The simulation of crop phenology is mainly based on the thermal time required to reach specific development stages. Thermal time is calculated as growing degree days (GDD, °C day^{-1}) accumulated throughout the growing season (from planting until harvest). Average air temperature above a base temperature and below a cutoff temperature is considered for GDD calculation. Moreover, the simulation of crop development considers other environmental aspects such as day-length, low temperature requirements, *i.e.* "vernalisation[5]", and soil water content.

In the current work, Cropsyst was applied both for simulating plant phenology and for estimating total biomass and final yield.

We will use Cropsyst model for climate change impact assessment on crop yield for a number of crops including winter wheat, barley, sunflower, sorghum and maize at a resolution of 50x50Km (European domain) and 12*12 km (regional domain=Guadiana).

In order to provide a good statistical sample, crop yield will be simulated on a 30 year period at the required spatial resolution.

4.2.1 Impact of water stress events on final yield

As concerns the effect of extreme events on final yield, at the moment the Cropsyst model includes only the effect of water stress, in general during the growing season (affecting total biomass accumulation), and in particular at anthesis and post-anthesis stage (affecting floret fertility and grain set). The model simulates the water budget, on a daily time step, depending on daily rainfall, Actual Evapo-transpiration (AET) and the soil type (which determines the amount of maximum water retention). According to the amount of soil water content, crop potential growth is corrected by water stress, if any, to calculate actual daily biomass gain.

When drought events occur during sensible growth stages, in particular anthesis and post-anthesis stages, the model simulated a direct effect on final yield between 10 and 15% of the harvest index depending on the crop susceptibility to this event. Accordingly, a potential (unstressed) final HI is decreased according to water stress intensity and crop sensitivity to stress during flowering and grain filling.

$$HI\_water\_stress = HI \times stress\_factor$$

where stress factor ranges from 0 (highest stress) to 1 (no stress)

4.2.2 Impact of heat stress events on final yield

The effect of heat stress on final yield was not directly simulated by Cropsyst and was then introduced into the model taking into account that final HI can be expressed as a function of the grain filling duration (GF) and the daily increse of HI.

This approach lies on the observation that HI increases linearly over much of the seed development period and that the rate of increase of HI (dHI/dt) is almost constant for most crops whatever the treatment (water stress, sowing date, fertilisation, etc..) (Bindi et al., 1999, Moriondo et al. 2005) (Fig. 4.2). These characteristics make this index particularly reliable for

[5] Vernalization is a process required for certain plant species to enter the reproductive stage through an exposure to low, nonfreezing temperatures. Thermal time accumulation is limited until vernalization requirements are met

modelling purposes and it was adopted in many crop growth models such as, wheat, maize, etc.. In particular the use of dHI/dt avoid the simulation of different aspects of seed growth such as the predictions of seed number and size since, assuming a constant dHI/dt, seed growth is simply calculated by multiplying total plant biomass by daily value of harvest index.

Accordingly,

$$HI = dHI / dt \times GF$$

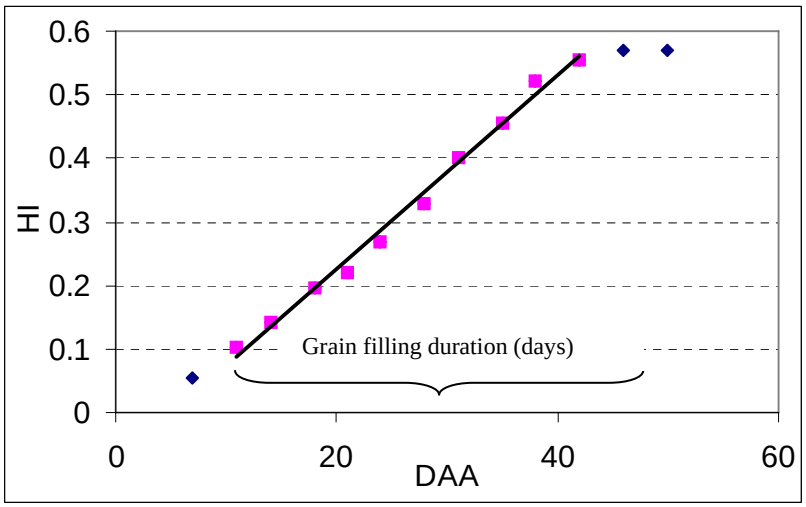

***Figure 4.2**: Increase of Harvest index as function of days after anthesis (DAA). The linear phase of its increase is shown. The slope of the regression line measures dHI/dt.*

Heat stresses occurring during anthesis have been demostrated to be a reducing factor for dHI/dt (Wollenweber et al. 2003; Challinor et al. 2005) by decreasing the number of fertile florets or grain fertility (Wheeler et al., 1996; Chimenti and Hall, 2001) thus affecting final yield.

Subsequently, the approach proposed by Challinor et al (2005) was used to calculate the impact of heat stress events on dHI/dt during anthesis for winter and summer crops: such episodes were identified by comparing the mean 8 am–2 pm[6] temperature (Tam) to a critical value (Tcr) as in Porter and Gawit, 1999, above which grain-set starts to be reduced up to the minimum level corresponding to a severe heat shock (Tlim, the temperature at 0% grain-set).

For this experiment durum wheat and sunflower were chosen as typical winter and summer crops respectively. For both crops, a period between –5 days from the start to +8 days from full anthesis was assumed as sensible to the effects of heat stress (Tashiro and Wardlaw, 1990) with Tcr=31°C and Tlim=40°C (Narciso et al., 1992; Connor and Hall, 1997; Porter and Gawit, 1999; Chimenti and Hall, 2001).

Any high temperature episode happening during the 'sensible' period was identified and valued according to its duration and the centered time at which it occurred. Each of these episodes was assumed to have a different potential impact depending on timing relative to each of the days in the flowering stage. As a consequence, the number of possible discrete

[6] Hourly temperature was simulated by applying a sinusoidal function to daily Tmin and Tmax

events impacting the grain-set was calculated as the number of episodes multiplied by the number of days in the flowering stage. For each discrete event (for Tlim>Tam>Tcr) the impact on grain was calculated as:

$$P = 1 - \frac{Tam - Tcr}{T\,\mathrm{lim} - Tcr}$$

where P decreases proportionally from 1 (no stress) to 0 (highest stress) according to the intensity of heat stress Tam-Tcr.

For each high temperature episode, the reduction in the total grain-set was calculated as the sum of the daily impact of that episode during the flowering developmental stage. Hence, for each episode the fractional grain-set was given by the product:

$$Ptot = \sum_{i=1}^{Nf} P(i) \times Fd(i)$$

where the flowering distribution Fd indicates the fraction of total flowers opening on day i.

This results in a value of Ptot for each identified high temperature episode. The lowest of these values was then used as coefficient to calculate HI variation according to:

$$\frac{dHIa}{dt} = \frac{dHIu}{dt} \times \left[1 - \frac{(Pcr - Ptot)}{Pcr}\right] \qquad \text{for Ptot<Pcr}$$

where Pcr is the critical fractional grain-set below which dHI/dt begins to be reduced from its non-stressed value (dHIu/dt) to the actual value dHIa/dt. (Fig. 4.3)

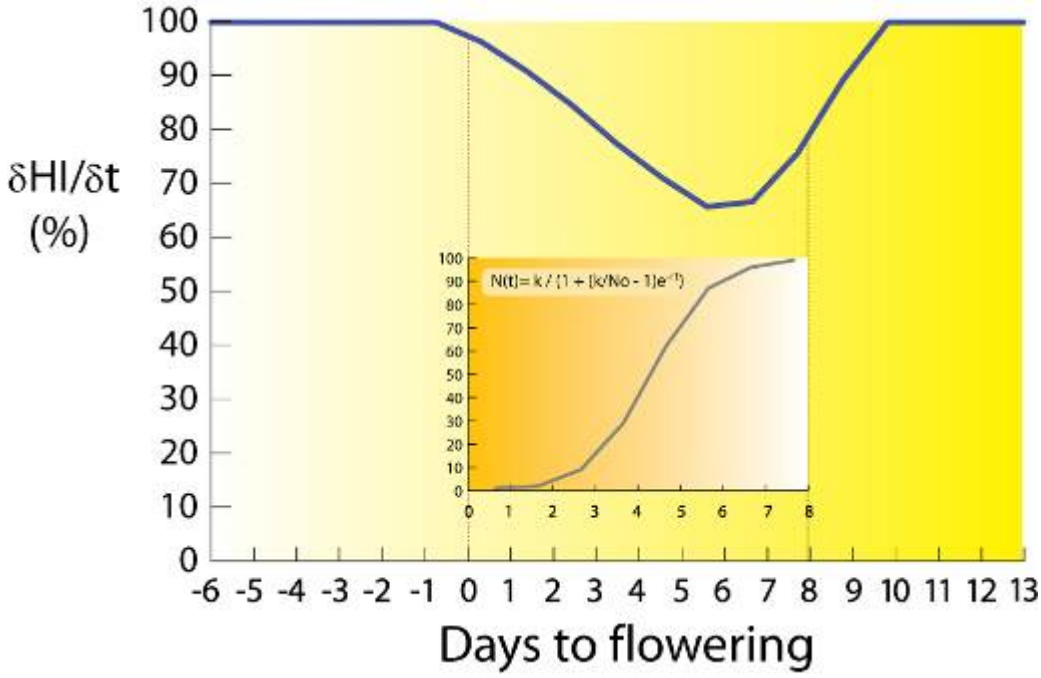

Figure 4.3*: Pattern describing the impact of heat stress during days around anthesis on daily increase of harvest index (dHI/dt). The pattern simulated the effect of 3 consecutive heat stress days (Tmin=20, Tmax=40) occurring in a period between –6 and +8 days respecively to the beginning of anthesis. The subfigure shows a logistic curve describing the cumulative distribution of total flowers opening.*

Final HI was then calculated as the product of the obtained dHIa/dt and GF (fig. 4.4) and yield was recalculated as the product of HI and total cumulated biomass as simulated by Cropsyst.

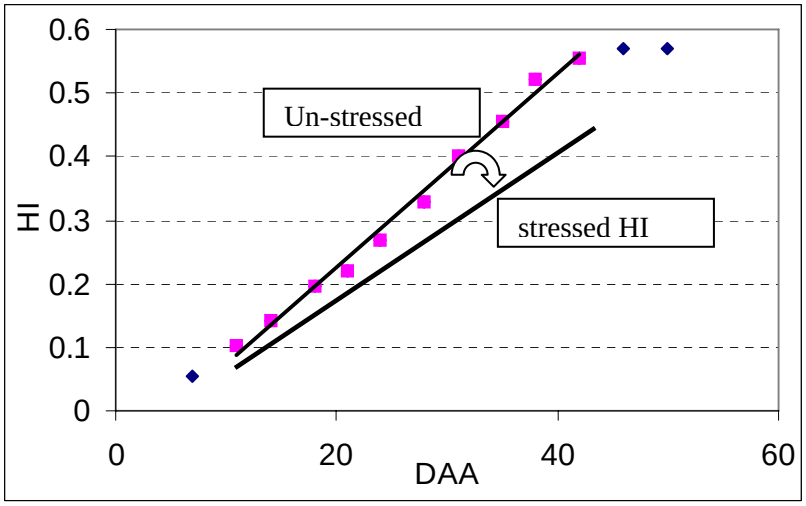

***Figure 4.4**: Effect of heat stress events on dHI/dt*

4.2.3 Final yield and yield loss calculation

On the premises exposed in the previous section, the effects of water stress and heat stress on final yield were assessed.
The actual final yield can be expressed as follows

$$Actual\_final\_yield = total\_biomass \times (dHI/dt_{heat\_stress}) \times water\_stress\_factor \times GF$$

where actual final yield is affected both by a water stress factor (during anthesis and post-anthesis stages) and heat stress (at anthesis stage).
Accordingly this function can be divided into 2 components each describing the impact of a single stress:

$$Actual\_final\_yield\_WS = total\_biomass \times (dHI/dt_{no\_stress}) \times water\_stress\_factor \times GF$$

$$Actual\_final\_yield\_HS = total\_biomass \times (dHI/dt_{heat\_stress}) \times GF$$

where actual final yield WS and actual final yield HS represent final yield as affected by water stress and heat stress respectively.
On this basis, the yield loss due to water stress and heat waves can be assessed separately as the difference between the potential yield (where no extreme events occurred) and yield affected respectively by heat waves and water stress.
In turn, yield loss was converted into economical damage taking into account the average price paid to the farmer per ton of yield (Producer price, refers to the prices paid to farmers

per ton at the time the commodity leaves the farm) derived from FAOSTAT, (http://www.faostat.fao.org) for the main European countries and averaged for the last 10 years.
On the basis of the economic loss distribution over a period of 30 years, the frequency and return period of economic loss can be assessed on the basis of a Gumbel distribution.

4.3 Crop Model set-up

Criteria to establish sowing dates: A climatic criterion was adopted to establish sowing date of winter (barley, wheat) and summer crops (sunflower, maize, sorghum, soybean).
Winter crops require cold temperatures in early development stages to meet vernalization requirements. In our simulations the sowing dates were matched when, starting from September 1st, the mean temperature of 5 consecutive days was 11 °C or lower.

In summer crops, which require high radiation for good yield level, sowing time has to intercept the maximum radiation during the growing season. According to Narciso et al. (1992) and Harrison and Butterfield (1996), this time was matched after March 15th, when the mean temperature was 10 °C or higher for 5 consecutive days.

Environmental input: Daily minimum and maximum temperature, rainfall and global radiation of HadRM3P-HIRAM-RCMs for the present climate scenario (1961-1990) were used as input variables for CropSyst model running over the European window.
Soil properties (thickness and texture) for each grid point of the window were extracted from the European soil database Eusoils (ESDBv2 Raster Archive - A set of rasters derived from the European Soil Database distribution version 2, http://eusoils.jrc.it/) (10 Km x 10 Km). The soil class with higher frequency within each RCM grid point was chosen.

Crop management options and yield thresholds: Optimal nitrogen fertilization and no irrigation were assumed for both crops. Tillage (primary disc plow at 20 cm depth) was set in late summer before sowing for winter wheat and 10 days before sowing date for sunflower.

Crop model outputs: Total biomass and final yield (per hectare) were collected on an annual basis. The dates of the main phenological phases (sowing, emergence, anthesis, grain filling, maturation), actual and potential evapo-transpiration and soil water content during the season were also collected for a better characterization of the growing season

4.4 Crop model validation

The present approach has been applied, for a rough validation at national level for the present period, using the RCM HADRM3P model as meteorological inputs and the results were compared to the average yield provided by FAOSTAT. At this stage durum wheat and sunflower yield simulation were tested.

In general, CropSyst appropriately predicted the mean yields and the yield variability of both crops across the European-Mediterranean countries (Fig. 4.5), with the exception of Portugal where the simulated yield was substantially higher than those observed. However, taking into account the uncertainties included in the statistical data and comparing these results with those obtained in other works (e.g. Harrison and Butterfield, 1996), the model reproduced well wheat and sunflower yields with average differences ranging from 25% to 15%. This

result may be considered very useful in performing climate change impacts on crop development and yield.

4.5 Losses at regional and European scale

The proposed approach has been firstly tested over the Guadiana basin, which has been identified as a possible hotspot of global climate change issues. For this basin located in southern Spain (fig. 4.6), a detailed spatial database was available. A meteorological data-set for this region, including minimum and maximum temperature rainfall and solar radiation at daily time step, was obtained for HIRAM RCM running at high spatial resolution (12.5*12.5 Km) for the period 1961-1990. CORINE land cover was used to identify which areas can be potentially used for cropping (fig. 4.6). Eurostat database was used to obtain the average price per ton of both wheat and sunflower.

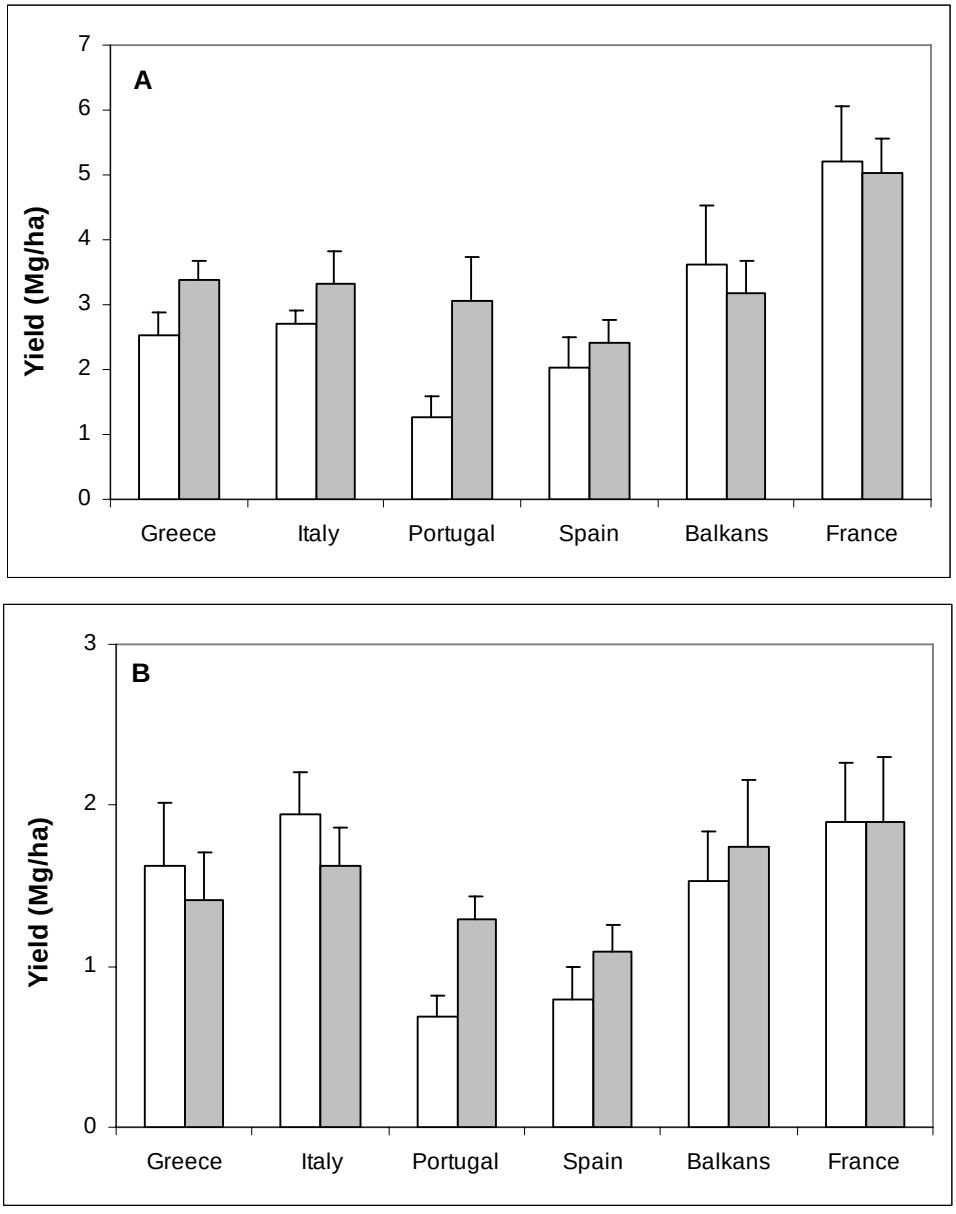

Figure 4.5*: Simulated (grey) and observed (white) yield of wheat (A) and sunflower (B) for the period 1975-1990. Bars represent standard deviation.*

This approach has now been extended to the European countries of the Mediterranean basin using an RCM (HadRM3P) running at lower resolution (50*50 Km) for the same time period. The limitation to the south of Europe was due to the fact that the crop yield data at hand for the regression analysis on Hazard was focused on durum wheat only, so that the distribution area of this cereal was used. Extension to the whole of Europe and to other crops is in progress, with preliminary results shown in Annex 4.

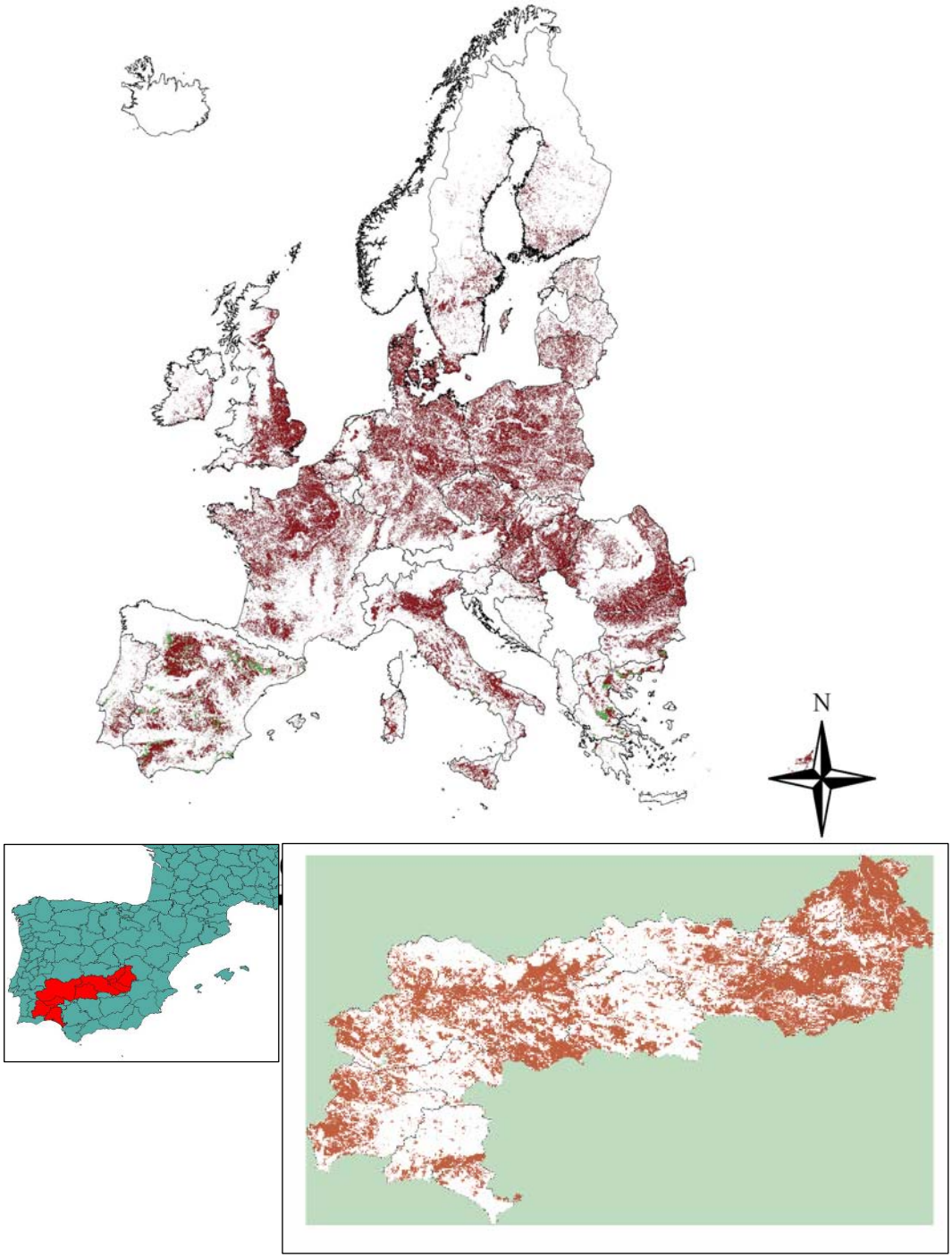

Figure 4.6*: Above: areas potentially exposed to damage (arable lands) in Europe, as derived from CLC 2000. Lower-right: Zoom in to the Guadiana basin, drawn in red over NUTS3 administrative level in the lower-left box.*

The combined analysis of the temperature and water stress events provided a distribution of effects which can be synthesised in terms of the expected economic loss as shown in the following figures. In figure 4.7 we report a picture showing the computed hazard from heat waves in the Guadiana basin. The legend indicates the number of expected events with Tmax>31°C during flowering period for two return periods, namely 10 and 20 years.

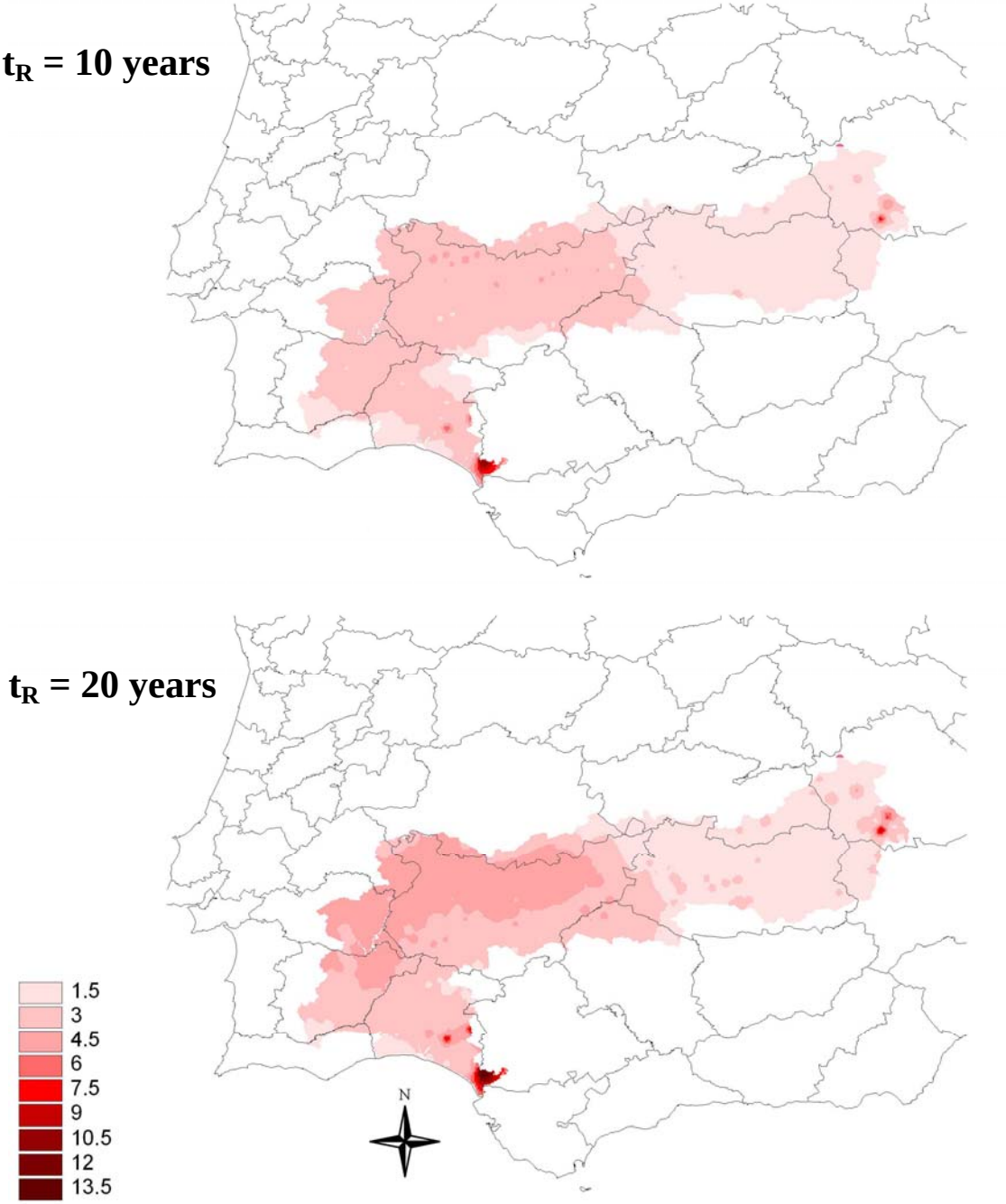

***Figure 4.7**: Heat stress Hazard Map for Guadiana Basin: the map shows the number of expected events with Tmax>31°C during flowering period for the return periods of 10 and 20 years, respectively*

Accordingly, figure 4.8 shows the corresponding result for water stress (droughts) events in the same area. In this case, the drought event is not measured quantitatively, rather it represents the fraction of the total flowering period undergoing water stress. The legend is therefore expressed in percentage values. In this respect, these maps are not expressing "pure" hazard information, as they have been calculated with a focus on a specific crop. For both maps, interpolation to 1km grid size was performed using the inverse distance method.

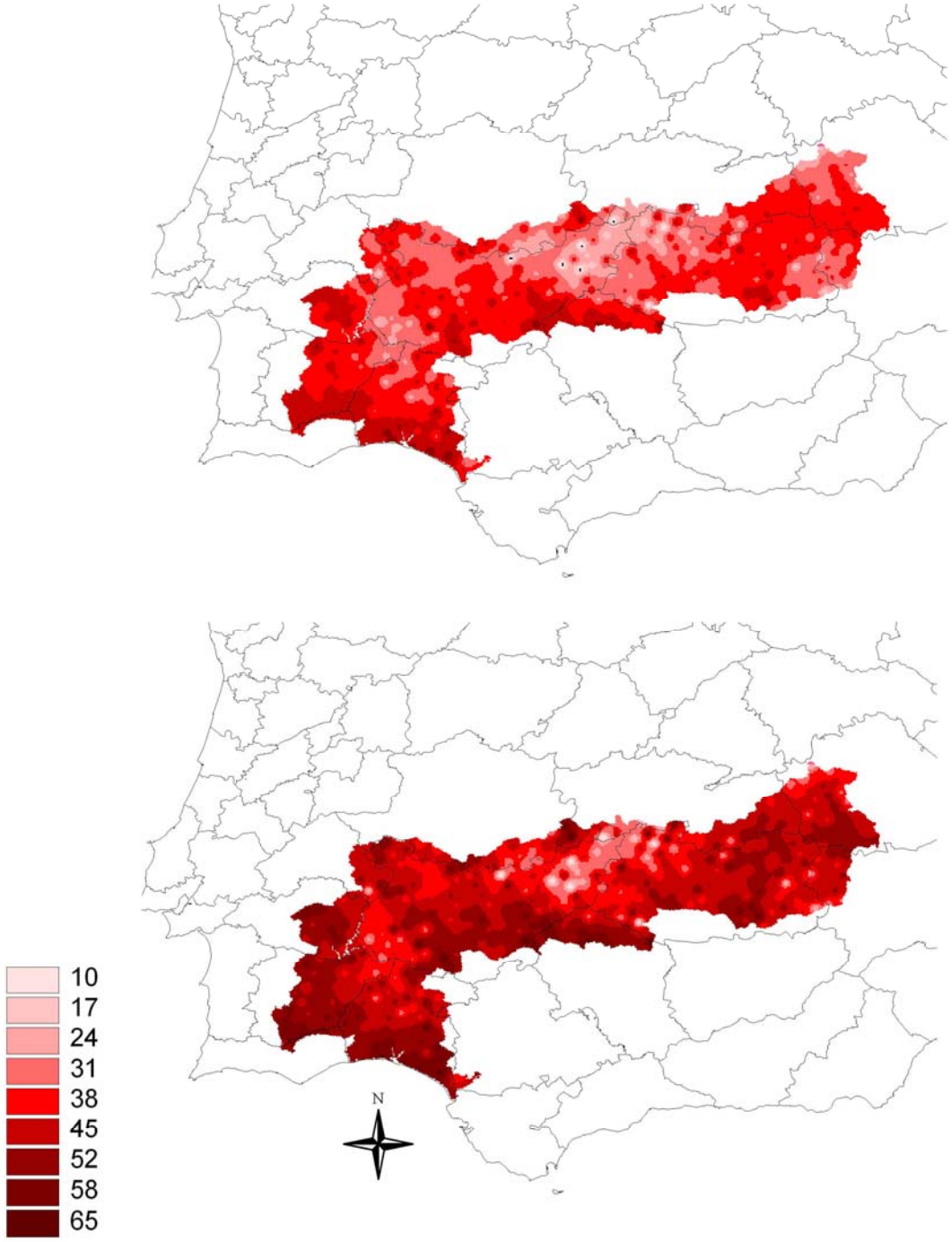

***Figure 4.8**: Water stress Hazard Map for Guadiana Basin: the map shows the fraction (in %) of the flowering period with drought conditions, for the return periods of 10 and 20 years, respectively*

According to the methodological scheme, the economic loss deriving from the combined impact of water and heat stress was calculated for each grid point, for a return period of 10 years. The calculation was performed using ARC-View GIS.

As in the previous figures, the return periods of 10 and 20 years (fig. 4.9 and 4.10, respectively) are displayed for the overall expected damage for the territories identified by the CLC class describing arable land (see figure 4.6).

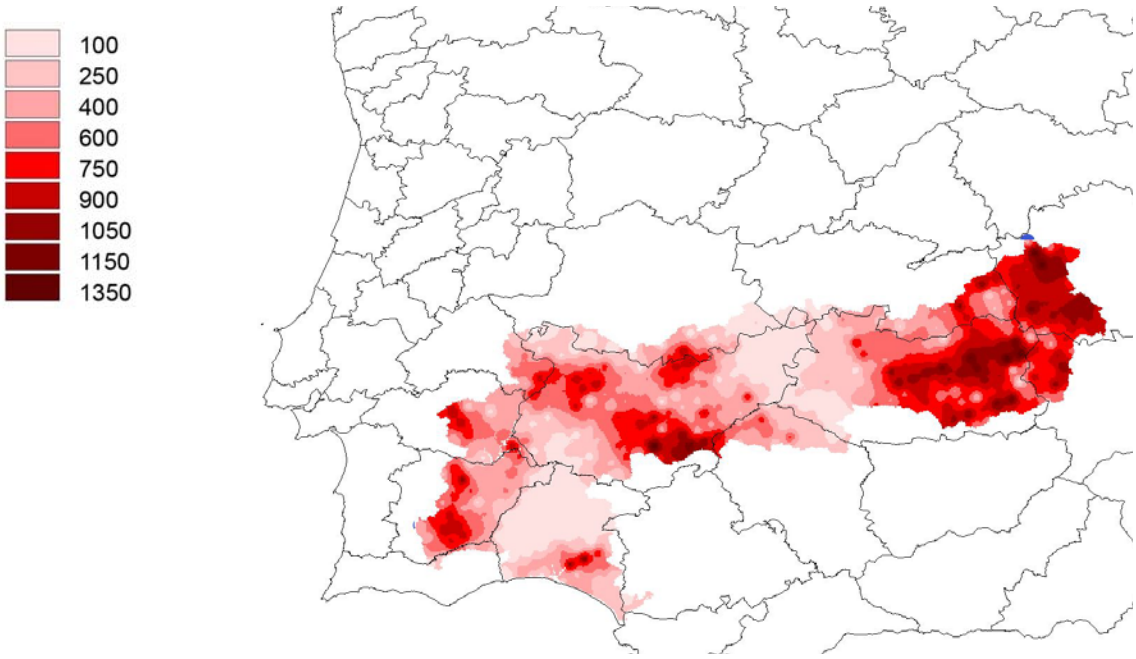

***Figure 4.9**: Economic loss (€/Km^2) due to heat and water stress, calculated for durum wheat for a return period of 10 years*

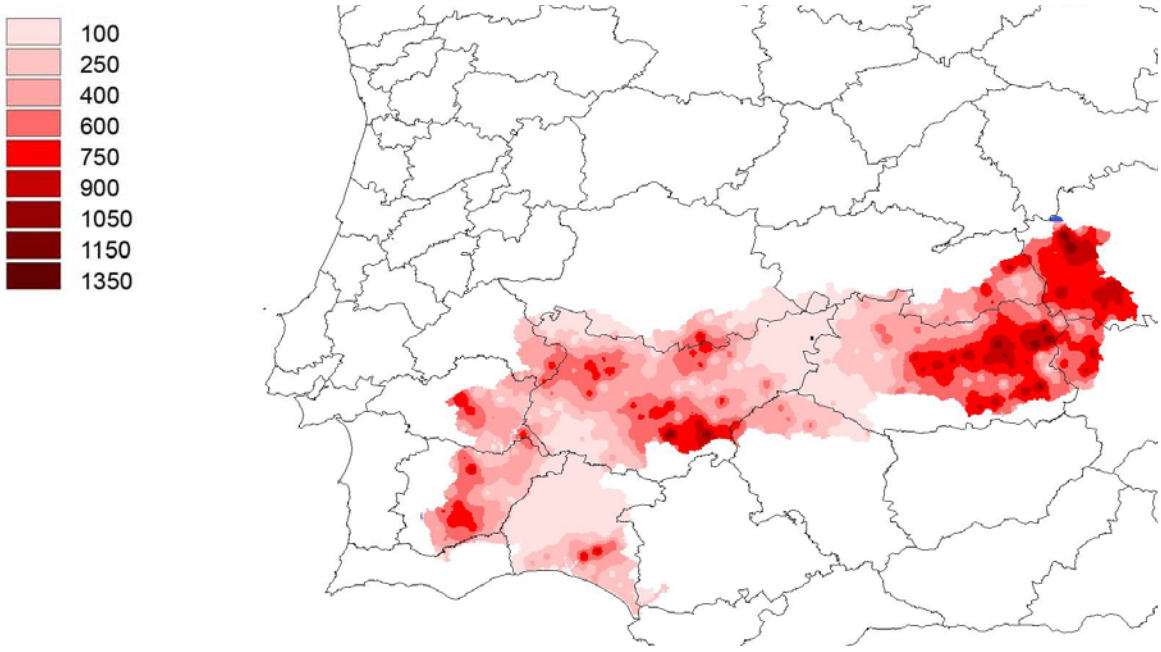

***Figure 4.10**: Economic loss (€/Km^2) due to heat and water stress, calculated for durum wheat for a return period of 20 years*

Damages are expressed in €/ Km^2 in the previously described grid-based scheme (after interpolation on 1km grid spacing).

Finally, a synthesis of the process is given through the loss-frequency distribution for the present period (due to both water stress and heat waves) fitted using the Gumbel distribution, calculated for a single grid cell in Guadiana, as shown in fig. 4.11.

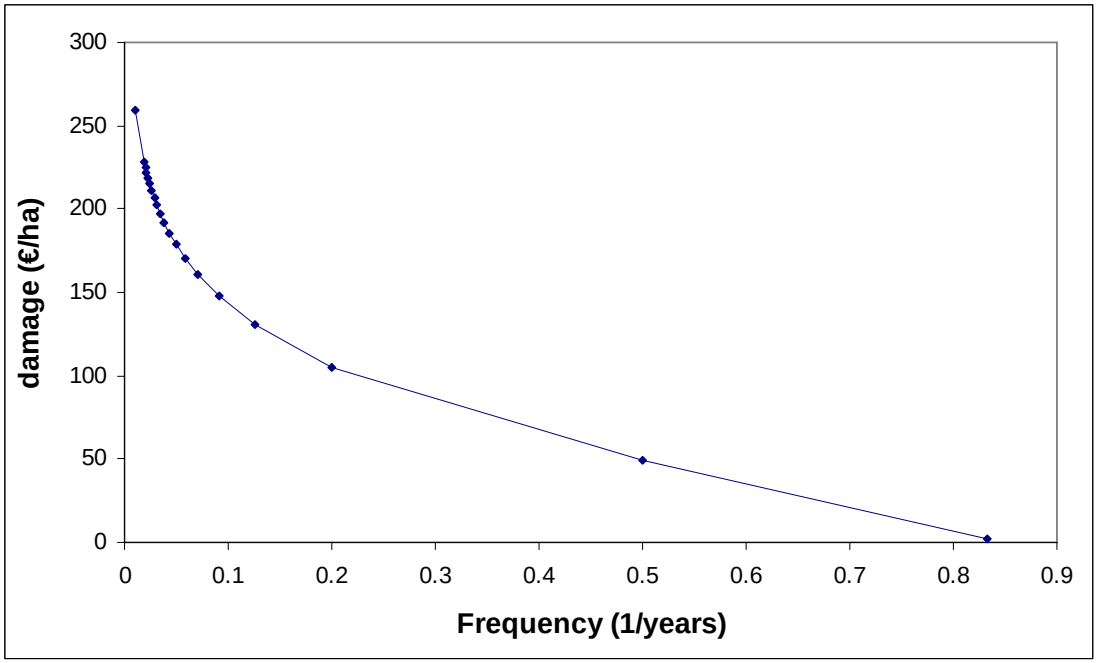

***Figure 4.11**: Damage-Probability curve fitted according to the Gumbel distribution of the observed losses, due to heat and water stress for a sample grid cell*

The same approach has then been extended to the Mediterranean basin, in the areas suitable for wheat. The conceptual scheme previously applied for the Guadiana Basin is again followed by the sequence of the figures, with the exception of the overall damage result, as explained below. Grid spacing is now 20km, as a result of the interpolation of meteorological data with inverse distance weighting.

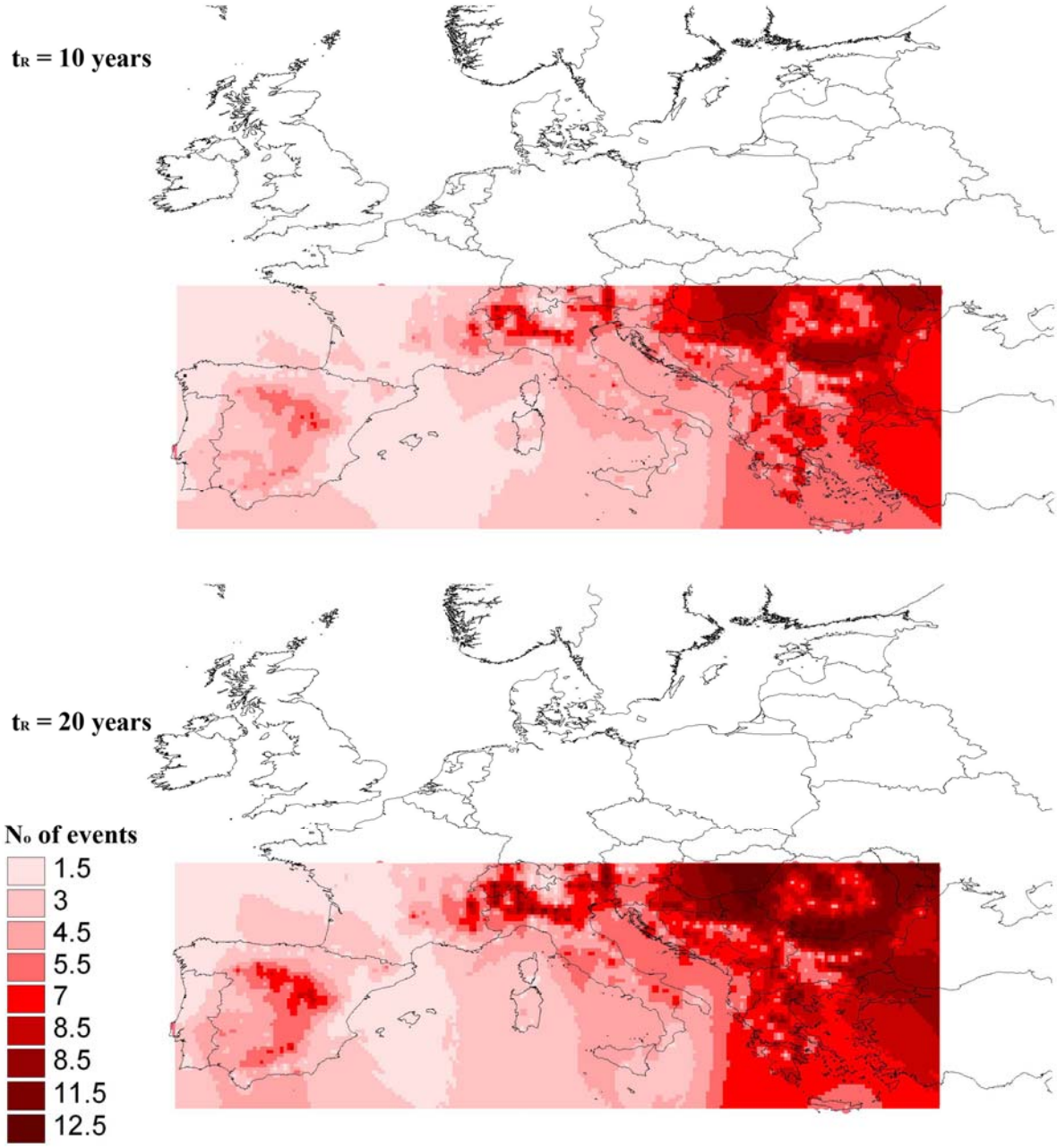

***Figure 4.12**: Heat stress Hazard Map for Mediterranean Basin: the map shows the number of expected events with Tmax>31°C during flowering period for the return periods of 10 and 20 years, respectively*

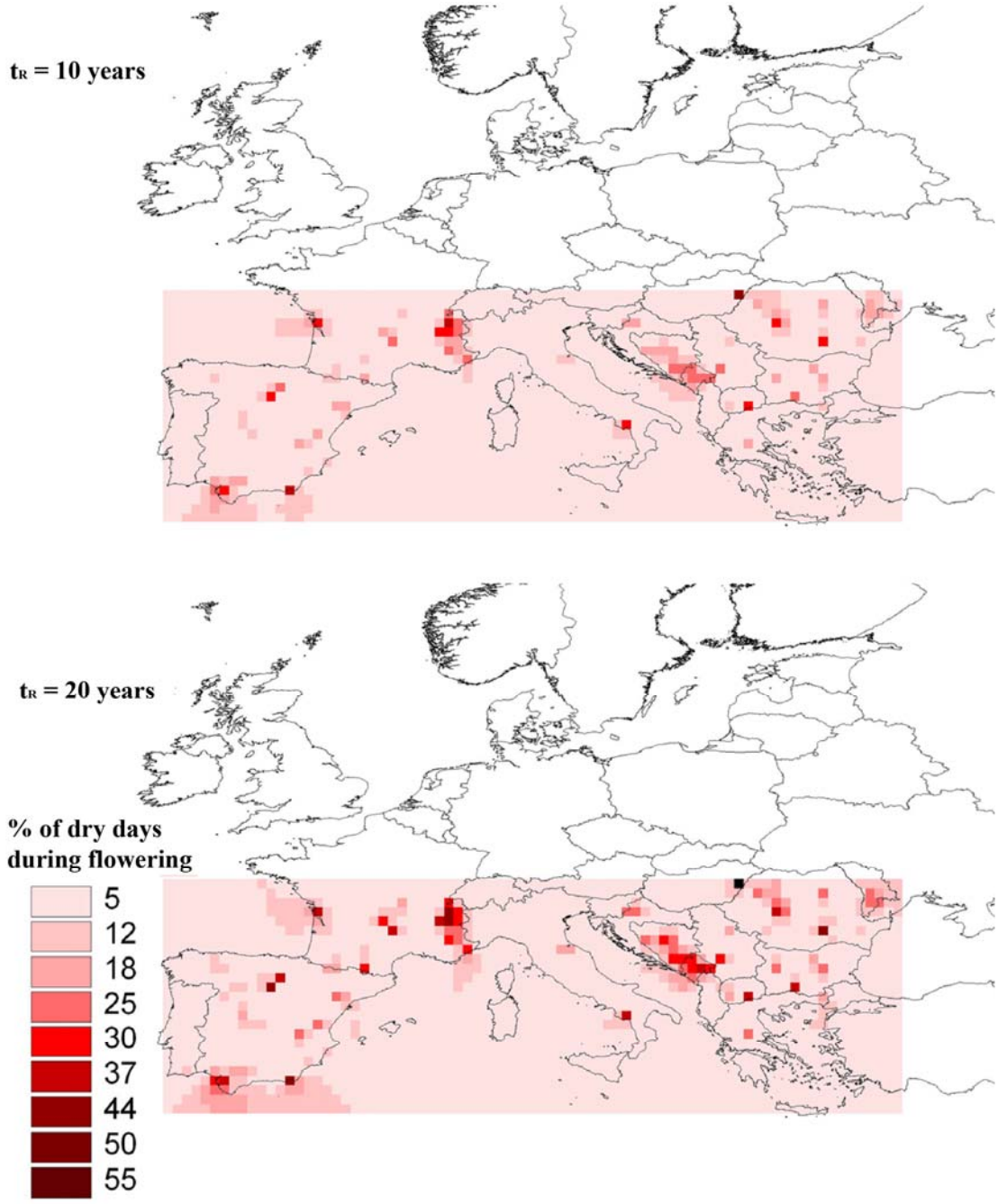

***Figure 4.13**: Water stress Hazard Map for the Mediterranean Basin: the map shows the fraction (in %) of the flowering period with drought conditions, for the return periods of 10 and 20 years, respectively*

The following figures show the potential damage in the same area which would be expected independently of the actual distribution of the crops in the territory. In terms of the risk triangle, this would represent a uniform exposure across all the land. CLC data was not inserted here as it was made in the Guadiana case study, because of the extremely different resolution of the datasets. We are presently assessing the validity of estimating a cumulative figure over Europe with arable land information from CLC data or from NUTS-3 level averages, as well as investigating a calibration procedure to validate the results. The first results are reported in Annex 4.

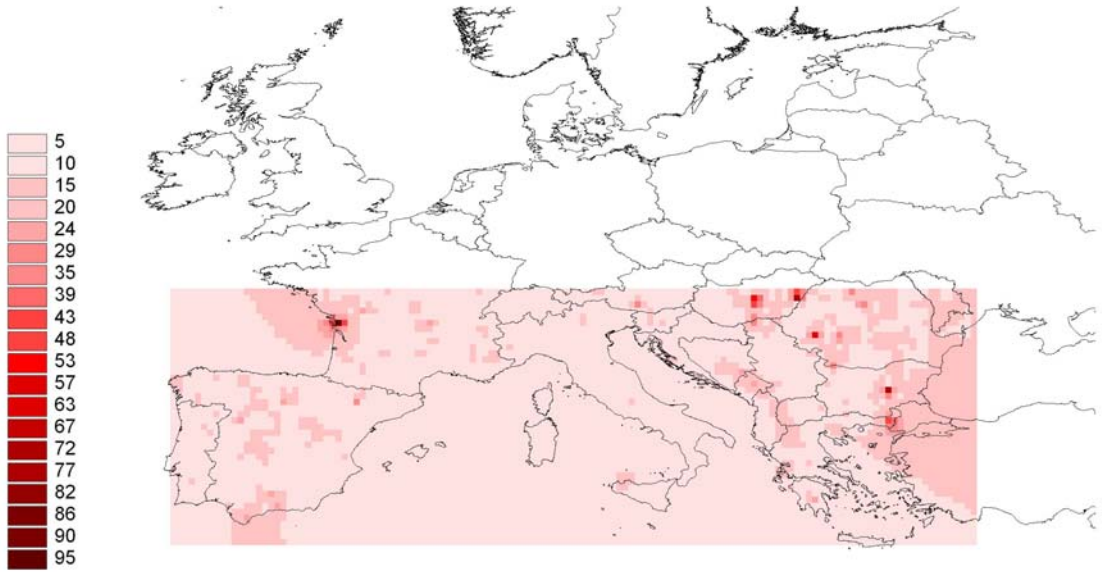

***Figure 4.14**: Potential economic damage (euros/hectare) due to heat and water stress, calculated for durum wheat for a return period of 10 years.*

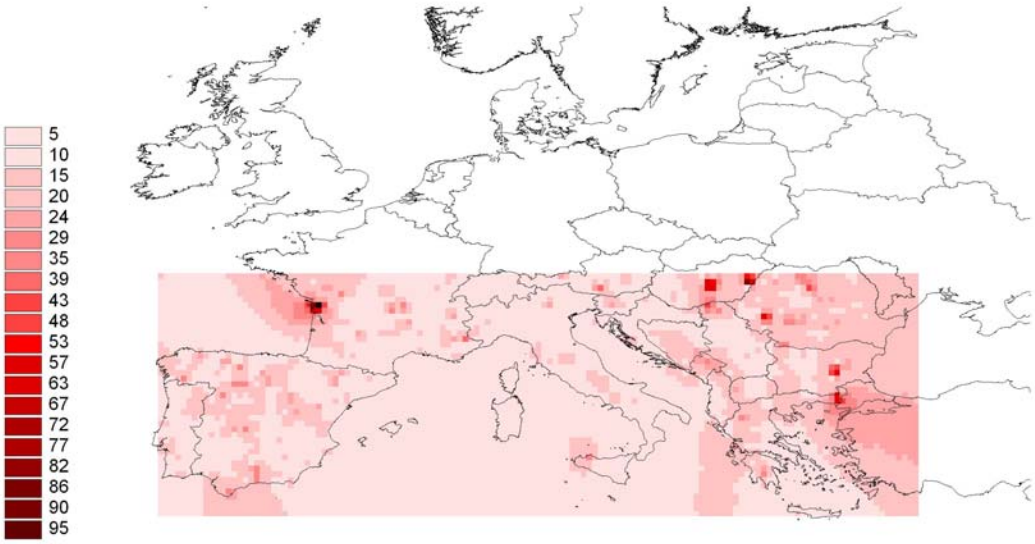

***Figure 4.15**: Potential economic damage (euros/hectare) due to heat and water stress, calculated for durum wheat for a return period of 20 years.*

Figure 4.16 below, again shows the damage-probability curve for a grid cell of the wide-area study. No straightforward comparison can be made, at this stage, with the analogous result for the Guadiana case.

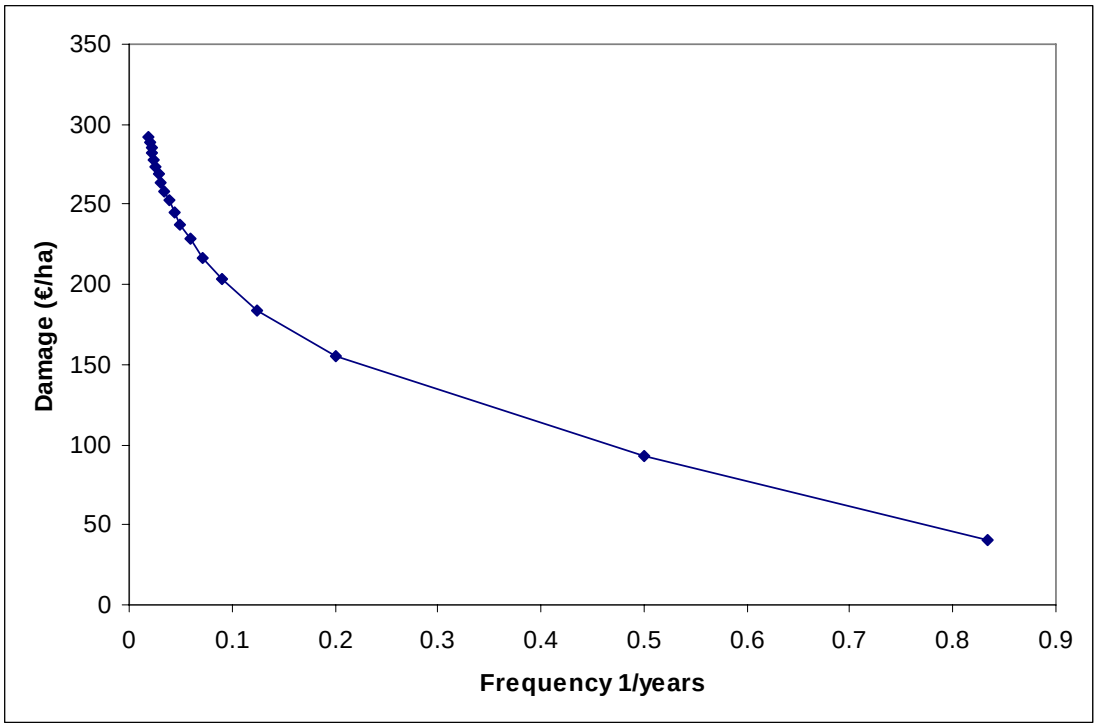

***Figure 4.16**: Damage-Probability curve fitted according to the Gumbel distribution of the observed losses, due to heat and water stress for a sample grid cell*

5 Advantages, Limitations and Future Work

The approaches described in this report for the evaluation of the risk deriving from extreme weather events (focus on flood, drought and heat-waves) allow the quantitative computation of direct losses for the overall European territory. The methodology is strongly based on a spatial (land-use) approach which in turn presents a number of advantages with respect to other methodology based, for example, on statistical extrapolations and or on meta-analysis or econometrics.

The resulting maps have the very specific feature of being territorially differentiated, and therefore allow combining the computed parameters with other data and information characteristics of the location under investigation.

5.1 Flood risk analysis

The method implied for the computation of the flood hazard map presents some limitations due to the discrepancy in scale between the various layers of data used in the analysis (e.g. flood hazard grid: 1 km, land use: 250 metres). This induces putting into the same hazard level parts of dwelled territory which can or cannot be affected as a function of water levels.

The hazard map is based purely on physical (geomorphological) features. It does not take into account protection measures, river bank height and so on. It's an indication of the possibility of being affected by a flood. Therefore the probabilities of flood occurrence (or return periods) are inferred by calibrating the maps with output from other modelling studies and from trial and error on selected river catchment. The uncertainties relating to the computation of return periods have been for the moment tackled by computing a range of values within which the monetary damage lies for a given return period.

A further assumption made, concerns the evaluation of the damage function. Although well justified in literature, neglecting various flood characteristics (such as flow speed and time of exposure to water) may give rise to some degree of inaccuracy.

While keeping in mind the above considerations, the first comparisons with similar exercises based on flood damage analysis for Wales and England, provide quite satisfactory results, indicating a difference of values within the respective ranges of uncertainty.

Additionally, it is worth stressing that the produced flood risk maps are unique because of their geographical extension and characteristics, and the range of return periods covered. These are the first maps of flood risk computed at European scale for four return periods.

In conclusion, the figures presented in this report are well suited to be ingested into statistical econometric models. The probability-based computations are indeed appropriate to perform studies on medium and long-term future scenario.

5.2 Crop yield analysis

The main limitations of this approach lie in the impossibility of a proper calibration and validation of the proposed methodology at regional scale. At the moment this methodology was only calibrated for peanuts whereas for the other crops, including maize, sunflower, wheat, etc., this operation has not yet been performed. In other words, the temperature

thresholds at anthesis causing yield loss should be determined for each crop, as well as the beginning and the end of the period, around this stage, where the crop is subjected to extreme temperatures.

However, the difficulty of such a calibration could be partially overcome and the impact of climate extremes assessed with a good approximation on the basis of the literature findings.

Many papers and reviews describing crop developmental thresholds were produced (e.g. Narciso et. Al, 1992, Porter and Gawith, 1999, Wheeler et al., 2000) indicating the temperatures above which (and below which) plants are damaged. In a review, Narciso et al. (1992) describes this threshold for a number of crops, including wheat, sunflower, sorghum, rice, sugar beet, soya bean, potato and barley. A more in depth analysis for wheat and sunflower was performed by Porter and Gawith, (1999) and Chimenti and Hall (2001) respectively.

Accordingly, the results that are presented, at the moment for the Guadiana basin and later for Europe, should be retained based on the present knowledge of which are the extreme temperatures causing yield loss for each crop and what is the frequency of extreme events as simulated by the RCM. The uncertainties are then produced by the actual yield loss determined by extreme events and by the ability of RCM in simulating the actual frequency of extreme events.

5.3 Future work

The remaining work to be carried out in months 19-24 will be largely dedicated to the refinement of the products described in this report. In particular the following aspects of work will be dealt with:

- Improvements to data format following requirements from other tasks in A2. This aspect is essential to ensure that the data can be used as input into the micro and macro-economic models to be adopted in A2.3, However, it is already envisaged that no further data processing will be feasible.

- Quantification of inaccuracies and uncertainties. The proposed approach allows the quantification of direct impacts of extremes at continental scale but, due to the nature of the different datasets implied in the study, it does contains limitations mainly coming from the processes of geographical scale-conversion. The aim is to quantify such inaccuracies.

- The analysis performed for drought and heat-waves for Guadiana and the Mediterranean basin will be extended to the whole EU for the assessment of climate change impact in agriculture at continental level. The analysis will include the more important crops and the economic losses derived from this analysis, will be weighted on the basis of relative importance of each crop

- Further pursue the calibration of the return period for flood related events. Although it is considered that possible errors in the values of the return periods do contribute on the final figure to a lesser extent than the scale-conversion processes, it is envisaged to perform the calibration of a selected test site (e.g. Tisza catchment and possible other hot-spots) also making use of records of direct monetary losses for known flood events.

- Definition of hot-spot following criteria, not yet fixed at the current stage of the project, in coordination with other tasks in A2. Study areas already identified in ADAM (e.g. Tisza and Guadiana catchments) will be analysed in further detail. Other areas of potential interest are: the Upper Danube, Austria and possibly some Mediterranean regions.

5.4 Integration and Complementarities with other ADAM packages

The main aim of Tasks A2.1 is to quantify the impacts of extreme events in such a way to allow further modeling and evaluation. A2.1 can therefore be considered as a provider of information to other packages in ADAM.

The first receptors are the other two packages dealing with extreme events' impacts in Work-Package A2. In details:

- A2.2 deals with the impact assessment of projected events for 2025 and 2100 and, although based on a different methodology, will reference to A2.1 to establish trends.
- A2.3 is about financial and economic vulnerability to extreme events. A2.1 furnishes the direct and essential input data to micro/macro economic models.
- A2.4 dealing with costs and benefits of adaptation options will use the monetary evaluation of A2.1 as reference figures.

Work Package A1's digital atlas of Europe's vulnerability to climate change will benefit from the digital maps produced in A2.1 for what concerns extreme events.

A further, and possibly more ambitious, integration could occur with Work Package S – Scenarios to evaluate the feasibility to include extreme events impacts in the formulation of new framing scenarios – although this aspect deserves a more profound discussion.

The linkages with the case studies in Tisza and Guadiana are part of the direct continuation of A2.1

Acknowledgements

Dr. R. Dankers and Dr. L. Feyen are greatly acknowledged for providing their expert judgment and scientific support in the carrying out of this study.

So are Ms. Catherine Hale and Mr. Ceri Whitmore for careful review of the language.

6 References

Andjelkovic I. (2001), International Hydrological Programme, *Guidelines on non-structural measures in urban flood management*, IHP-V, Technical Documents in Hydrology, No.50 UNESCO, Paris. Available at: http://www.floods.org/PDF/Intl_BestPractices_EU_2004.pdf).

Barredo J.I., Lavalle C., Sagris V., Kasanko M. (2004), "Climate change impacts on floods in Europe. Toward a set of risk indicators for adaptation", DG-JRC, Ispra, EUR 21472 EN.

Barredo J. I., Lavalle C., De Roo A. (2005), "European flood risk mapping", EC DG JRC, 2005 S.P.I.05.151.EN.

Bates P., De Roo, A.P.J. (2000), A Simple Raster-Based Model For Flood Inundation Simulation. Journal of Hydrology, Vol.236, 54-77.

Bergstrom S.,1995 The HBV model. In *Computer Models of Watershed Hydrology* Singh VP (ed.) Water Resources Publications: Highlands Ranch, CO 137-159

Berz G., Kron W., Loster T., Rauch E., Schimetschek J., Schmieder J., Siebert A., Smolka A., & Wirtz A. (2001). World Map of Natural Hazards - A Global View of the Distribution and Intensity of Significant Exposures. Natural Hazards, 23(2-3), 443-465.

Beven K.J., Kirkby M.J., 1979 A physically based, variable contributing area model of basin hydrology. Hydrological Sciences Bulletin 24 (1) 43-69

Bindi M., Sinclair T.R., Harrison J. 1999. Analysis of seed growth by linear increase in Harvest index. Crop Science 39, 486-493.

Büchele B., Kreibich H., Kron A., Thieken A., Ihringer J., Oberle P., Merz B., andNestmann F. (2006), Flood-risk mapping: contributions towards an enhanced assessment of extreme events and associated risks, Nat. Hazards Earth Syst. Sci., 6, 485–503.

Challinor A.J., Wheeler T.R., Craufurd P.Q., Slingo J.M. (2005). Simulation of the impact of high temperature stress on annual crop yields. Agricultural and Forest Meteorology, 135, 180-189.

Chimenti C.A., Hall A.J. (2001) Grain number responses to temperature during floret differentiation in sunflower. Field Crop Res 72: 177-184.

Crichton, D. (1999) "The Risk Triangle", pp. 102-103 in Ingleton, J. (ed.), Natural Disaster Management, Tudor Rose, London.

Christensen J.H., Christensen O.B., Lopez P., Van Meijgaard E. & Botzet M. (1996), *The HIRHAM4 regional atmospheric climate model*, DMI Scientific Report 96-4, Copenhagen, Denmark.

Christensen J.H. & Christensen O.B. (2007), 'A summary of the PRUDENCE model projections of changes in European climate by the end of this century', *Climatic Change*, vol. 81, pp. 7–30, DOI 10.1007/s10584-006-9210-7.

Colombo A.G., Vetere Arellano A.L. (eds.) (2002), "Lessons learned from flood disasters", NEDIES Project, European Commission, Joint Research Centre, Ispra. Available at: http://nedies.jrc.it.

Compton K. (2004), "Report on the use of Murbandy data for flood risk assessment", final report, International Institute for Applied System Analysis, Austria, European Commission, Joint Research Centre, Ispra, Contract No 19591-2002-06 S0SC ISP AT.

Connor D.J., Hall A.J. (1997) Sunflower physiology. In Schneiter AA, ed. Sunflower technology and production, Monograph No. 35. Madison, WI: ASA, CSSA, SSSA, pp. 113–182.

Dankers R., Feyen L., Christensen O.B., de Roo A. (2007): Future changes in flood hazard in Europe. Proceedings, Third International Conference on Climate and Water, Helsinki, Finland, 3-6 September 2007, in press.

De Roo, A.P.J. (1998) Modelling runoff and sediment transport in catchments using GIS. In: GIS Applications in Hydrology. Hydrological Processes,Vol.12, 905-922

De Roo A.P.J. (1999), "LISFLOOD: a rainfall-runoff model for large river basins to assess the influence of land use Modelling, Management and Flood Mitigation", Concerted action, European Commission, EUR 18287 EN, pp. 349–357.

De Roo A.P.J., Wesseling, C.G., Van Deurzen, W.P.A. (2000), Physically-based river basin modelling within a GIS: the LISFLOOD model. Hydrological Processes, 14, 1981-1992.

De Roo A.P.J., Barredo J.I., Lavalle C., Bodis K., Bonk R. (2007). Potential flood hazard and risk mapping at pan-European scale. In Peckham, R. and Jordan, G. (editors). Digital Terrain Modelling. Development and Applications in a Policy Support Environment. Series: Lecture Notes in Geoinformation and Cartography. Springer-Verlag Berlin.

DEFRA Department for Environment, Food and Rural Affairs (2001), "National Appraisal of Assets at Risk from Flooding and Coastal Erosion", Final Report. http://www.defra.gov.uk/environ/fcd/policy/NAAR1101.pdf

EEA (1995), CORINE Land Cover -.http://reports.eea.europa.eu/COR0-landcover/en

EEA (2000), CORINE land cover technical guide - Addendum, Tech. rep. 40. http://reports.eea.europa.eu/tech40add/en/tech40add.pdf

EEA (2002), Environmental Signals 2002, "Environmental assessment report 9". European Environment Agency (EEA), Office for Official Publications of the European Communities, Luxembourg.

EEA (2004), "Impacts of Europe's changing climate: an indicator-based assessment", European Environment Agency (EEA), Report 2/2004, Office for Official Publications of the European Communities, Luxembourg.

EEA (2006), The Thematic accuracy of CORINE Land Cover 2000, Assessment using LUCAS (land use/cover area frame statistical survey), EEA Technical report n.7/2006 Office for Official Publications of the European Communities, Luxembourg.

Ferris R., Ellis R.H., Wheeler T.R., Hadley P., 1998. Effect of high temperature stress at anthesis on grain yield and biomass of field-grown crops of wheat. Ann. of Bot., 82, 631-639.

Feyen L. et al. "PESETA – Flood risk in Europe in a changing climate" European Commission, 2006 EUR 22313 EN

FLOODsite 6th FP Integrated Project (www.floodsite.net) Report Number T9-06-01 2006: Guidelines for Socio-economic Flood Damage Evaluation.

Gallego J., Peedell S., 2001, Using CORINE Land Cover to map population density. Towards Agri-environmental indicators, Topic report 6/2001 European Environment Agency, Copenhagen, pp. 92-103.

Genovese E. (2006), "A methodological approach to land use-based flood damage assessment in urban areas: Prague case study" European Commission, 2006 EUR 22497 EN

Gouldby B., Samuels P. (2005), "Integrated Flood Risk Analysis and Management Methodologies, Floodsite, Language of Risk, Project Definitions", Report: T32-04-01.

Green C. et al. (1994), "Vulnerability refined: analysing full flood impacts" (Chapter 3). In: Penning-Rowsell, E., Fordham, M. (eds.), *Floods across Europe (EUROflood): hazard assessment, modelling and management*, London, pp. 32-68.

Gurnell A., Montgomery D. (1999), Hydrological Applications of GIS. John Wiley & Sons, pp 176.

Harrison P.A., Butterfield R.E. (1996) Effect of climate change on Europe-wide winter wheat and sunflower productivity. Clim Res 7: 225-241.

Hewitt K. and Burton I. (1971) "The Hazardousness of a Place: A Regional Ecology of Damaging Events", Department of Geography, University of Toronto, Toronto (1971).

Hewitt K. (1983), Interpretations of calamity from the viewpoint of human ecology, Boston, Allen and Unwin.

Hewitt K. (1997), Regions of risk: a geographical introduction to disasters, Harlow, UK, Longman.

HKV Consultants "Flood damage functions for EU member states" – Final Report for Contract n. 382441 – F1SC for the European Commission, Joint Research Centre, 2007 – **not for disclosure**

Hiederer R., De Roo A. (2003) "A European flow network and catchment data set" Report of the European Commission, Joint Research Centre, EUR 20703 EN,

ICPR (2002), International commission for the protection of the Rhine, "Non-structural flood plain management: Measures and their effectiveness", Koblenz. Available at: http://www.iksr.org/GB/bilder/pdf/rz_iksr_engl.pdf

IPCC (2001a), "Climate Change 2001: The Scientific Basis", Contribution of Working Group I to the Third Assessment Report of the Intergovernmental Panel on Climate Change, Published for the Intergovernmental Panel on Climate Change, Cambridge University Press, University Press, New York. Available at: http://www.grida.no/climate/ipcc_tar/wg1/index.htm

IPCC (2001b), "Climate Change 2001: Impacts, adaptation and vulnerability", Contribution of Working Group II to the Third Assessment Report of the Intergovernmental Panel on Climate Change (IPCC), Cambridge University Press.

Jones D.A., Kay A.L., (2007) "Uncertainty analysis for estimating flood frequencies for ungauged catchments using rainfall-runoff models" Advances in Water Resources 30, 1190-1204

Kok M. (2001) "Damage functions for the Meuse River floodplain" HKV internal memorandum

Konrad C.P. (2003), "Effects of Urban Development on Flood", U.S. Department of the Interior, U.S. Geological Survey, USGS Fact Sheet FS-076-03.

Kostopoulou E., Jones P.D., 2005. Assessment of climate extremes in the Eastern Mediterranean. Meteorol. Atmos. Phys. 89, 69–85.

Kron W. (2002), "Flood risk = hazard x exposure x vulnerability". In: Wu M. et al., (ed.), *Flood Defence*, Science Press, New York, 82-97.

Kron W. (2003), "High water and floods: resist them or accept them?", Schadenspiegel 2003 (3), pp. 26-35. Also available at: http://www.munichre.com/publications/302-03751_en.pdf.

Lavalle C., De Roo A., Barredo J., Niemeyer S., San-Miguel-Ayanz J., Hiederer R., Genovese E. (2005), "Towards an European integrated map of risk from weather driven events: a

contribution to the evaluation of territorial cohesion in Europe", Technical EUR Reports, EUR 22116 EN.

Lindstrom G., Johansson B., Persson M., Gardelin M., Bergstrom S. (1997), Development and test of the distributed HBV-96 hydrological model. Journal of Hydrology 201:272-288

Lugeri N., Genovese E., Lavalle C., De Roo A. (2006) Flood risk in Europe: analysis of exposure in 13 Countries. JRC IES EUR 22525 EN

Montz B.E. (2000), "The generation of flood hazards and disasters by urban development of floodplains", in Parker D.J., *Floods*, Volume I, Routledge, London & New York, pp.116-127.

Maracchi G., Sirotenko O., Bindi M. 2004: Impacts of present and future climate variability on agriculture and forestry in the temperate regions: Europe. Climate Change.

Moriondo M., Bindi M., Sinclair T.R. (2005) Analysis of Solanaceae spp. harvest-organs growth by linear increase in harvest index and harvest-organ growth. J. Amer. Soc. Hort. Sci 130: 799-805

Moriondo M., Good P., Durao R., Bindi M., Giannakopoulos C., Corte-real J., 2006. Potential impact of climate change on fire risk in the Mediterranean area. Clim. Res. 31, 85-95.

Morris D.G., Flavin, R.W. (1996) "Flood risk mao for England and Wales", Report n. 130, Institute of Hydrology, Wallingford, Oxfordshire, UK, ISBN 0 948540 75 3

Munich Re (1997), "Überschwemmung und Versicherung" (Flooding and insurance), Munich. (Available at: http://www.munichre.com/publications/302-00688_de.pdf).

Narciso G., Ragni P., Venturi A. (1992). Agrometeorological aspects of crops in Italy, Spain and Greece. Joint Research Centre, Commission of the European Communities, Brussels, Luxembourg.

Olesen J.E., Bindi M., (2002) Consequences of climate change for European agricultural productivity, land use and policy. Eur. J. Agron. 16, 239-262.

Parker D.J. (2000), *Floods*, Volume I&II, Routledge, London & New York.

Parker D.J. (2000a), "Introduction to floods and flood management". In: Parker, D.J. (ed.): *Floods*, Volume I, London & New York, pp. 3-39.

Parry M.L. (2000), Assessment of the Potential Effects and Adaptations for Climate Change in Europe: The Europe ACACIA Project. Jackson Environment Institute, University of East Anglia, Norwich, UK, 320 pp.

Petry B. (2002), "Coping with floods: complementarity of structural and non-structural measure". In: Wu B. et al., *Flood Defence 2002*, ed. Science Press, New York Ltd., ISBN 1-880132-54-0.

Pielke R.A. (2000), "Flood impact on society". In Parker D.J. (2000), *Floods*, Volume I, Routledge, London & New York, pp.131-155.

Porter J.R., Gawith M., 1999. Temperatures and the growth and development of wheat: a review, Eur. J. Agron. 10, 23–36.

Risk Management Solution (2003), "Central Europe Flooding, August 2002, Event Report". Available at: http://www.rms.com.

Schelhaas M.J., Nabuurs G.J., Schuck A. (2003) "Natural disturbances in the European forests in the 19th and 20th centuries". Global Change Biol 9:1620–1633

Stockle C.O., Donatelli M., Nelson R., 2003. CropSyst, a cropping systems simulation model. Eur. J. Agron. 18, 289-307.

Tashiro T., Wardlaw I.F., 1990, “The response to high temperature shock and humidity changes prior to and during the early stages of grain development in wheat”, Aust. J. Plant Physiol. 17, 551– 561.

Van der Sande C.J. (2001), “River flood damage assessment using Ikonos imagery, Natural Hazards Project-Floods”, DG-JRC, S.P.I. 01.147, Ispra, August 2001.

Van der Sande C.J., de Jong S.M., de Roo A.P.J. (2003), “A segmentation and classification approach of IKONOS-2 imagery for land cover mapping to assist flood risk and flood damage assessment”, International Journal of Applied Earth Observation and Geoinformation, pp. 217–229.

Water Directors (2003), “Core group on flood protection of the water directors (Europe): Best practices on flood prevention, protection and mitigation”, European initiative on flood prevention, 25/9/2003

Wheeler T.R., Hong T.D., Ellis R.H., Batts G.R., Morison J.I.L., Hadley P., 1996. The duration and rate of grain growth, and harvest index, of wheat (Triticum aestivum L.) in response to temperature and CO2. J. Exp. Bot. 47, 623–630.

Wheeler T.R., Craufurd P.Q., Ellis R.H., Porter J.R., Vara Prasad P.V., 2000. Temperature variability and the yield of annual crops. Agric. Eco. Environ. 82, 159–167.

White G.F. (1945), “Human Adjustments to Floods: A Geographical approach to the Flood Problem in the United States”, Doctoral Dissertation and Research paper no. 29. Department of Geography, University of Chicago.

White G.F. (1964). *Choice of adjustment to floods.* University of Chicago, Department of Geography, Research Paper No. 93, University of Chicago Press.

Wilson M.D. (2004), Evaluating the effect of data and data uncertainty on predictions of flood inundation. PhD thesis, University of Southampton.

Wilson M.D., Atkinson P.M. (2003), Prediction uncertainty in elevation and its effect on flood inundation modeling. Proceedings of the 7th International Conference on GeoComputation, University of Southampton, United Kingdom, 8 - 10 September 2003, http://www.geocomputation.org/2003/

Wollenweber B,. Porter J.R., Schellberg J. (2003) Lack of Interaction between Extreme High-Temperature Events at Vegetative and Reproductive Growth Stages in Wheat J. Agronomy & Crop Science 189, 142—150.

7 ANNEX 1 CORINE Land Cover Nomenclature

1 Artificial surfaces	1.1 Urban fabric	1.1.1 Residential continuous urban fabric
		1.1.2 Residential discontinuous urban fabric
	1.2 Industrial, commercial and transport units	1.2.1 Industrial, commercial, public and private units
		1.2.2 Road and rail networks and associated land
		1.2.3 Port areas
		1.2.4 Airports
	1.3 Mine, dump and construction sites	1.3.1 Mineral extraction sites
		1.3.2 Dump sites
		1.3.3 Construction sites
		1.3.4 Abandoned land
	1.4 Artificial non-agricultural vegetated areas	1.4.1 Green urban areas
		1.4.2 Sport and leisure facilities
2 Agricultural areas	2.1 Arable land	2.1.1 Non-irrigated arable land
		2.1.2 Permanently irrigated land
		2.1.3 Rice fields
	2.2 Permanent crops	2.2.1 Vineyards
		2.2.2 Fruit trees and berry plantations
		2.2.3 Olive groves
	2.3 Pastures	2.3.1 Pastures
	2.4 Heterogeneous agricultural areas	2.4.1 Annual crops associated with permanent crops
		2.4.2 Complex cultivation patterns
		2.4.3 Land principally occupied by agriculture, with significant areas of natural vegetation
		2.4.4 Agro-forestry areas
3 Forests and semi-natural areas	3.1 Forests	3.1.1 Broad-leaved forests
		3.1.2 Coniferous forests
		3.1.3 Mixed forests

	3.2 Shrub and/or herbaceous vegetation associations	3.2.1 Natural grassland
		3.2.2 Moors and heath land
		3.2.3 Sclerophyllous vegetation
		3.2.4 Transitional woodland/shrub
	3.3 Open spaces with little or no vegetation	3.3.1 Beaches, dunes, sands
		3.3.2 Bare rock
		3.3.3 Sparsely vegetated areas
		3.3.4 Burnt areas
		3.3.5 Glaciers and perpetual snow
4. Wetlands	4.1 Inland wetlands	4.1.1 Inland marshes
		4.1.2 Peat bog
	4.2 Coastal wetlands	4.2.1 Salt marshes
		4.2.2 Salines
		4.2.3 Intertidal flats
5. Water bodies	5.1 Inland waters	5.1.1 Water courses
		5.1.2 Water bodies
		5.2.1 Coastal lagoons
	5.2 Marine waters	5.2.2 Estuaries
		5.2.3 Sea and oceans

8 ANNEX 2: Flood Damage Assessment: Prague case study

This specific application describes methodology for the assessment of direct monetary potential flood damage. Combined with existing information on land use and flood depth, maps of the flooded areas provide information that can be used for flood damage assessment, urban and rural planning and validation of flood simulation models (De Roo et al., 1999).

The applied damage function, compared to the one previously described, contains important differences in the chosen data: the average price per m^2 for a house or an apartment used for Prague are specific for that urban areas and are collected in the web-database named Urban Audit (available on-line at www.urbanaudit.org) (therefore not from the HKV study described in Section 3 of this report).

Moreover, the flood depths here considered are established on a detailed local DEM and not on the pan-European hazard map.

The flooding throughout Europe in 2002 constituted one of the most severe flood events in at least a century. Total economic losses reached more than EUR 15 billions (Risk Management Solution, 2003). During this event, the Vltava river exceeded the water level of the major 1890 floods in Prague.

***Figure 8.1**: Prague 2002: overview of flooded city (ANSA, 2002; in www.corriere.it)*

Total damage in Prague is estimated at nearly 1 billion Euro. The districts of Lesser Town (Malá Strana), Old Town, the Jewish Quarter (Josefov), and Karlin suffered particularly heavy losses, where very old and unmapped tunnels aggravated the problem in this historic city.

Some 200.000 Czech residents were evacuated during the flooding. Insured losses in the Czech Republic amounted to € 1.2 billion compared with an economic loss of € 2.3 billion.

The concept of damage function is used when calculating flood damage.
This basic methodology was outlined already in 1945 by White and is referred to as stage-damage curve representing the relation between inundation depth and damage cost for a land use class. In the case of built-up areas, the land use class is either expressed per number of buildings or per unit area. The economic value of the land use class has to be known in order to calculate the damage. This value is based on the principle of replacement value: how much money it would cost to obtain the 'identical' object. The damage function has values included between 0 and 1, with the value 0 if there is no damage and the value 1 if there is maximum damage (Van der Sande, 2001; Kok, 2001).

Stage-damage curves can be developed from actual flood events and then can be used for damage estimation of potential flood events, also if this approach should present problems like extrapolation difficulties from place to place due to differences in warning time and in building type and content.

White (1964) introduced a new methodology by constructing 'synthetic' stage-damage curves and these are based on hypothetical analysis. The US Federal Insurance Agency (FIA) administered the first main application of standardised stage-damage curves. Residential buildings were divided in insurance classes, each with their own stage damage curve based on dimension, type of building and contents (Van der Sande, 2001).

Penning-Rowsell and Fordham (1994) coordinated the Euroflood project that was designed to improve the understanding of causes and impacts to flood hazards in the European Countries. It gives, among other subjects, an overview of flood damage assessment models developed in several countries.

This analysis has the purpose to give an assessment of the damage of urban flood by using the damage functions which are available in the literature. The following sources are used:

- Kok M. (2001), Damage functions for the Meuse River floodplain, Internal report, JRC (Ispra).
- Van der Sande C.J., de Jong S.M., de Roo A.P.J. (2003), A segmentation and classification approach of IKONOS-2 imagery for land cover mapping to assist flood risk and flood damage assessment, International Journal of Applied Earth Observation and Geoinformation, pp. 217–229.
- Van der Sande C. (2001), River flood damage assessment using Ikonos imagery, Natural Hazards Project-Floods, Joint Research Centre of the European Commission, S.P.I. 01.147, Ispra, August 2001.

As suggested by Van der Sande (2001, 2003), the assumptions listed below had to be made to do the flood damage assessment:

- The damage function is a function only of inundation depth, although flood damage is determined by more factors. In the literature, there is not much information available with respect to factors other than inundation depth;
- The damage functions must be increasing functions, which means that as the inundation depth grows, also damage rises.

During a flood event, some damage can be avoided by appropriate action from the people who live in the floodplain. Examples are the caravans on a camping ground, which can be removed during the winter period, when there is a higher risk of flooding and the cars, because there is enough time to remove them from the area that is going to be flooded. Therefore caravans and cars are not taken into account of the damage assessment.

***Figure 8.2**: IRS satellite image of Prague central area (1998, source: MOLAND database); the blue area represent the portion of urban territory flooded in 2002 (source: Prague City Council).*

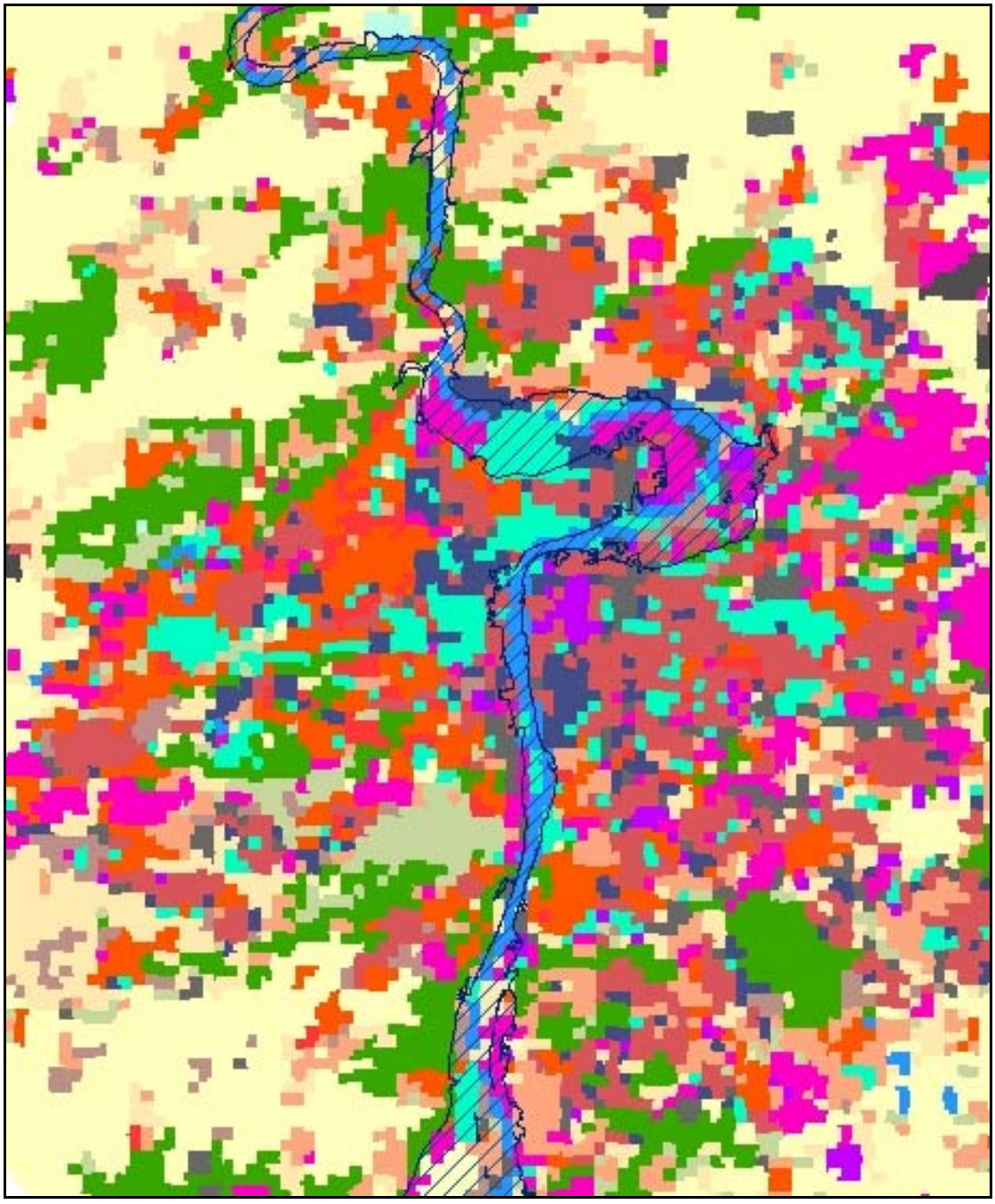

***Figure 8.3**: MOLAND Land Use (1998) for Prague and flooded area of 2002 (source: Prague City Council). Red pixels represent continuous and discontinuous urban fabrics; violet pixels are industrial and commercial areas. The box outlines the study area considered for the damage assessment.*

An important question in damage calculation is which assumption has to be made with respect to the behaviour of the people. This is caused by the fact that damage is a function of many physical and behavioural factors, like for example the content of the house and the preparation time. Hence, uncertainties in the damage functions are not dealt with in this analysis.

The maximum damage values are here only indicative and are based on the average price per m^2 for a house or an apartment. These information are provided by the European Commission

(Directorate General for Regional Policy - DG Regio) and EUROSTAT (NEW CRONOS database) and are collected in the web-databases named Urban Audit.

The damage function used in this study depends on several components: different land used classes, flood depth factors, economical value per square meter.

The study area corresponds to a part of the historical centre of Prague close to the river Vtlava, which was severely flooded on August 2002, and is equal to almost 1000 hectares.

The MOLAND Land Use database for the year 1998 (which is the closest available date to 2002, when the flooding occurred) was used. The database is generated at a resolution of 50m pixel-size. The flooded area was individuated and considered according to the map of the flooded area provided by the Prague City Council.

The flood damage depends on the land use type: in urban areas floods produce as a consequence much more damage than floods in a rural area. The land use classes, which are used to calculate the flood damage, correspond to the land use classes of the MOLAND legend, that are the same of CLC European database but with a more detailed level of land use class. In this analysis only the damage for built-up areas is evaluated.

In the flood of 1993 in Holland (Kok, 2001), it was calculated that 75% of the damage to industry was related to property and 25% was related to productivity loss. There are three different ways to calculate the damage: per firm, per hectare and per employee.

In this kind if assessment, the most suitable method is to evaluate flood damage in industrial area. The maximum damage cost of industry has to be assessed per hectare. The following damage function is used by Kok (with linear interpolation between these step values):

Inundation depth	Damage factor
0 m	0
1 m	0.4
2 m	0.8
3 m	0.9
4 m	1

Table 8.1*: Damage factor for industrial and commercial areas*

The damage function for roads and railroads present 5 meter as a maximum inundation depth. The maximum damage values vary depending on the type of road. In the floodplain there are 12 hectares of mainly roads and rails. The damage function proposed by Kok is the following:

Inundation depth	Damage factor
0 m	0
5m	1

Table 8.2*: Damage factor for roads and rails*

Linear interpolation can be used between these points.

Flood damage in urban areas is calculated per hectare of surface covered by urban fabrics. The applied flood damage function is based on damage data of the Commissie Watersnood Maas provided for assessing damage in the floodplain of the Meuse River (in Kok, 2001) where three types of damage are considered: the house itself, the content of the house and the

car. Damage to cars is not taken into account because there is usually enough time to move these cars onto the higher parts of the area.

Two different databases are considered to estimate the *hazard flood depth*:

- the actual flood map for the 2002 event as provided by the Prague City Council
- a high resolution Digital Elevation Model (DEM), in order to define the water depth of the flood.

***Figure 8.4**: Digital Elevation Model (DEM) and Prague flooded area 2002.*

The damage factors for each of the different impact categories and different depths are listed below in table 8.3:

Depth (metres)	**Damage factor houses**	**Damage factor Content**
0	0	0
1	0.05	0.47
2	0.11	0.50
3	0.35	0.66
4	0.68	0.83
5	1	1

***Table 8.3**: Damage functions used in calculations of the Commissie Watersnood Maas (in Kok, 2001).*

Linear interpolation is used to obtain the complete function of damage factor for the house and its content that is presented in Table 8.4:

Depth (metres)	Damage factor
0	0
0.5	0.06
1	**0.08**
1.5	0.10
2	**0.44**
3	**0.62**
4	0.78
5	0.80
6	1

***Table 8.4**: Proposed damage function for houses (property and content).*

The study area includes the following residential MOLAND Land Use classes, which are separated depending on their water level:

AREA (square meters)	*MOLAND Land Use classes*	Water depth and damage factor
427500	Residential continuous dense	3 (0,62)
260000	Residential continuous dense	2 (0,44)
142500	Residential continuous dense	1 (0,08)
150000	Residential continuous medium dense	3 (0,62)
20000	Residential continuous medium dense	2 (0,44)
77500	Residential discontinuous urban fabric	3 (0,62)
10000	Residential discontinuous urban fabric	2 (0,44)
325000	Residential discontinuous sparse urban fabric	3 (0,62)
52500	Residential discontinuous sparse urban fabric	2 (0,44)

***Table 8.5**: Residential areas and different water depth in the study area.*

According to Urban Audit database, the average price per m^2 for an apartment (2001) is € 827,21 and the average price per m^2 for a house (2001) is € 1562,5[7]. For the purpose of the damage evaluation method herein proposed, these figures should be considered like a *reconstruction cost*, namely the costs for rebuilding to a standard responding to local conditions.

In residential continuous dense, medium dense and residential discontinuous, built-up areas are expected to be formed of buildings with apartments, while in residential discontinuous sparse areas artificially surfaced areas cover between 10% and 50% of the total surface and so they are assumed to be constituted of single houses.

Then, all the necessary data are available to propose an assessment for the different urban categories of land use. The generic formula used is:

$$DAMAGE = p * A * H * V$$

Where:

[7] Data available at the web site www.urbanaudit.org (DG REGIO/EUROSTAT).

- p= % of urban fabric covered surface in a X land use
- A= area (m^2) of the X land use
- H= water depth damage factor
- V= average price for m^2 for an apartment/a house

As an example of application of the above formula, let's consider the class named "Residential continuous dense urban fabric" which corresponds, according to the MOLAND definition[8], to a class where residential structures cover more than 80% of the total surface. Therefore the formula to evaluate the damage is:

80% (427500) * € 827.21* 0.62 → € 175401608
80% (260000) * € 827.21* 0.44 → € 75706259
80% (142500) * € 827.21* 0.08 → € 7544155

The formula is then applied to all land use classes and the final total damage computed.

The proposed approach provide final figures that should not be considered as a detailed cost assessment of the damage, since they are strongly depending on the quality of the damage functions and the availability of detailed datasets. In this case, the evaluation was limited by the economical (market) value per m^2 for houses. Also, the final figure might not necessarily reflect the reconstruction costs because of the land-use based approach (as opposite to the single building approach)

The method, with damage function properly developed for each Country of the European Union, is hereinafter applied to compute European Maps of Flood Risk.

[8] See http://moland.jrc.it

9 ANNEX 3 European Flood Risk Maps

9.1 Accumulated Risk maps on spatial grids

The maps in figures 9.1 to 9.7 present the results of the integration of flood direct damages on a 50km grid, for the four return periods respectively. The value of each grid represents the accumulated value of damage computed as if the flood event is occurring simultaneously all over the grid.

The grid width was chosen according to the resolution of the climate change scenario models that are dealt with in other tasks of the project.

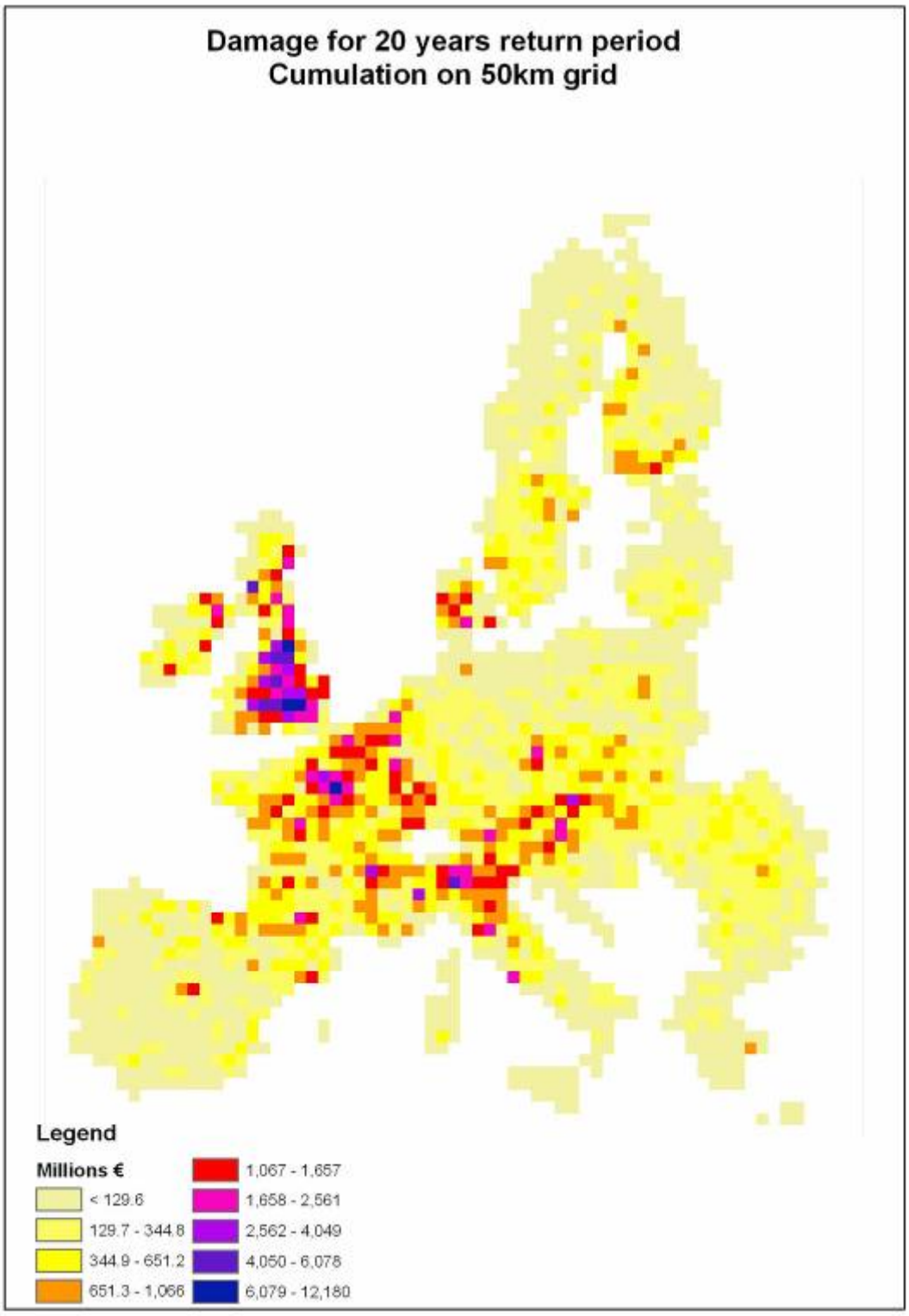

***Figure 9.1**: Direct risk (monetary impact) for flood hazard with return period of 20 years.*

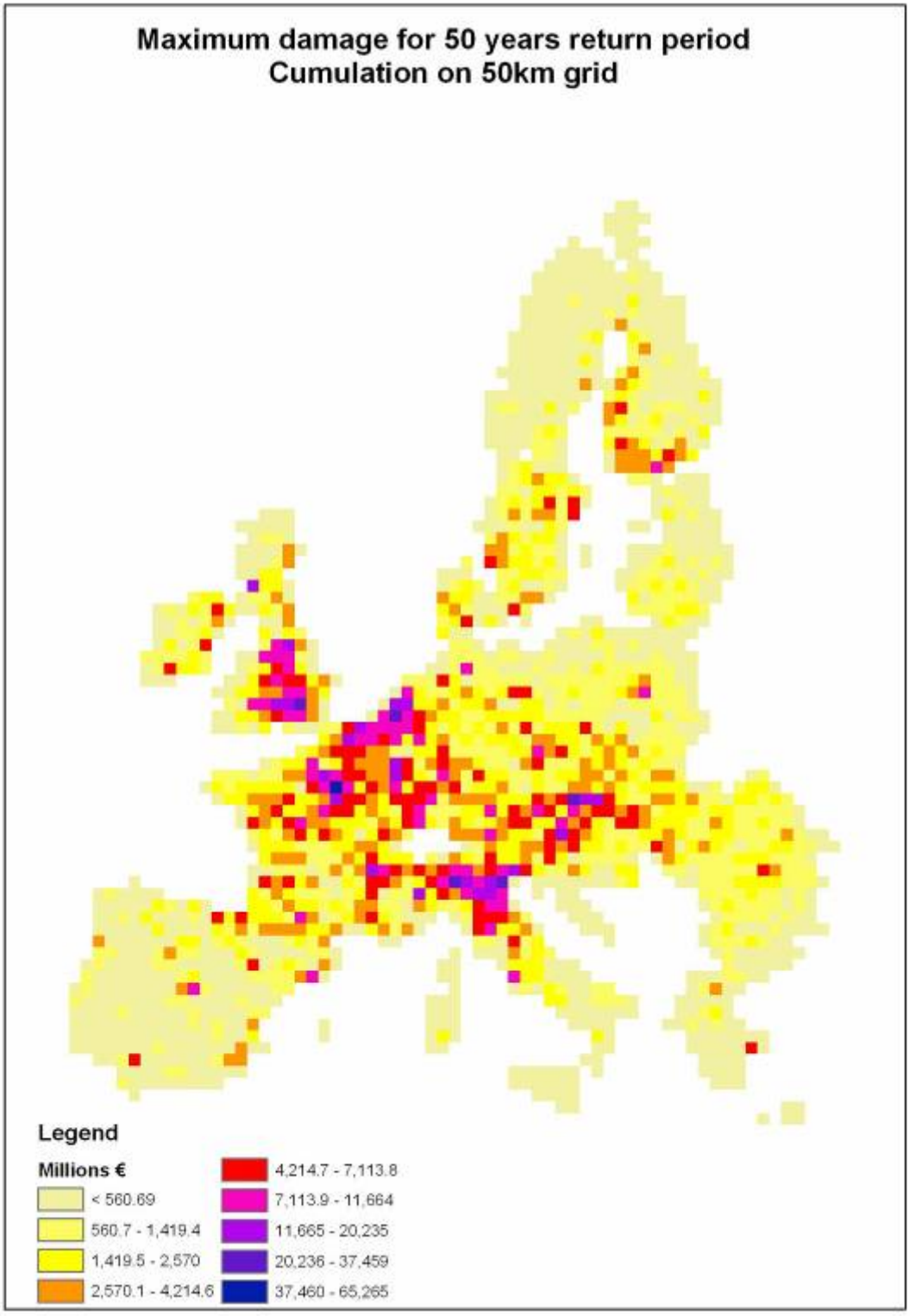

***Figure 9.2**: Direct risk (monetary impact) for flood hazard with return period of 50 years. Maximum value*

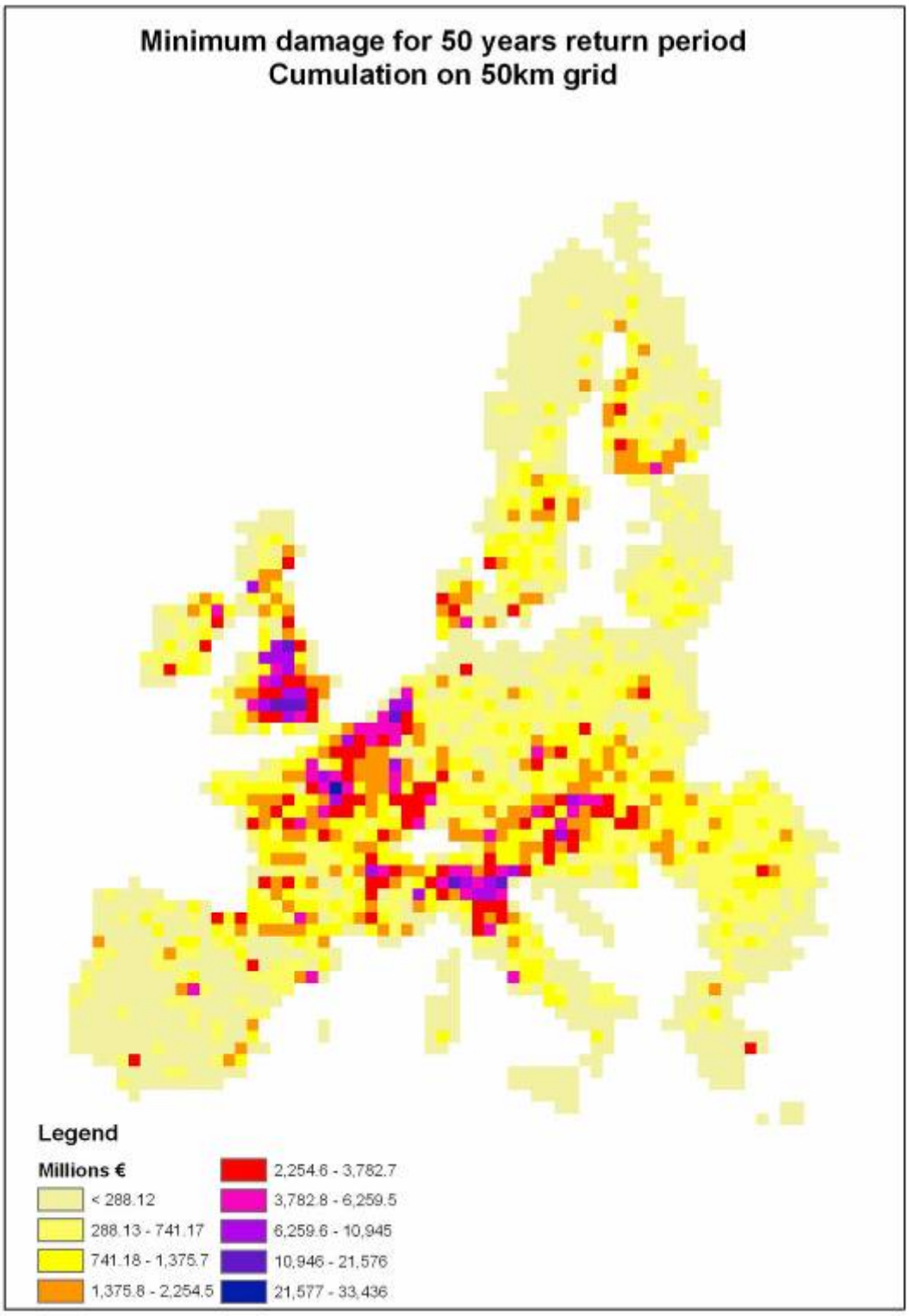

***Figure 9.3**: Direct risk (monetary impact) for flood hazard with return period of 50 years. Minimum value.*

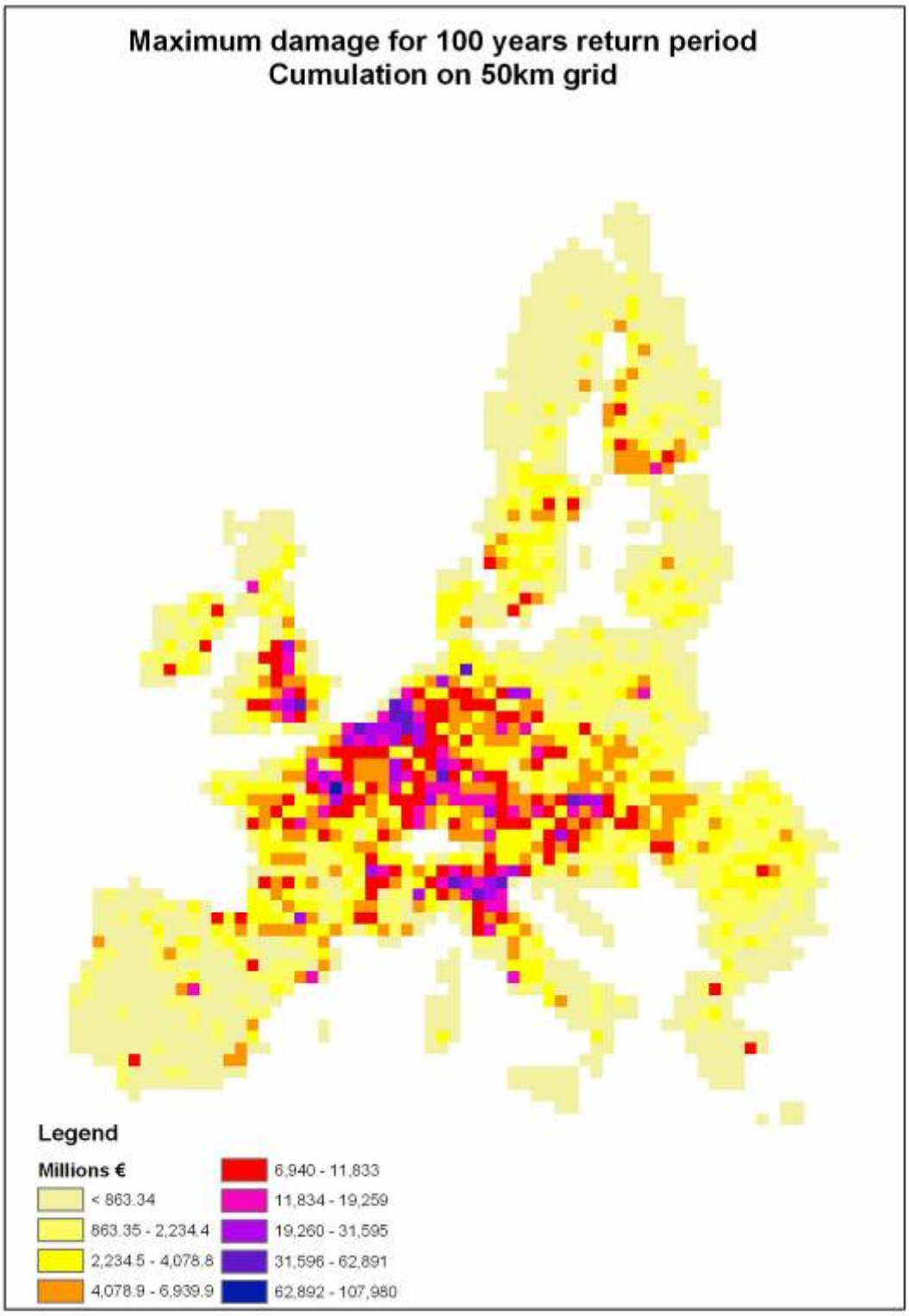

***Figure 9.4**: Direct risk (monetary impact) for flood hazard with return period of 100 years. Maximum value*

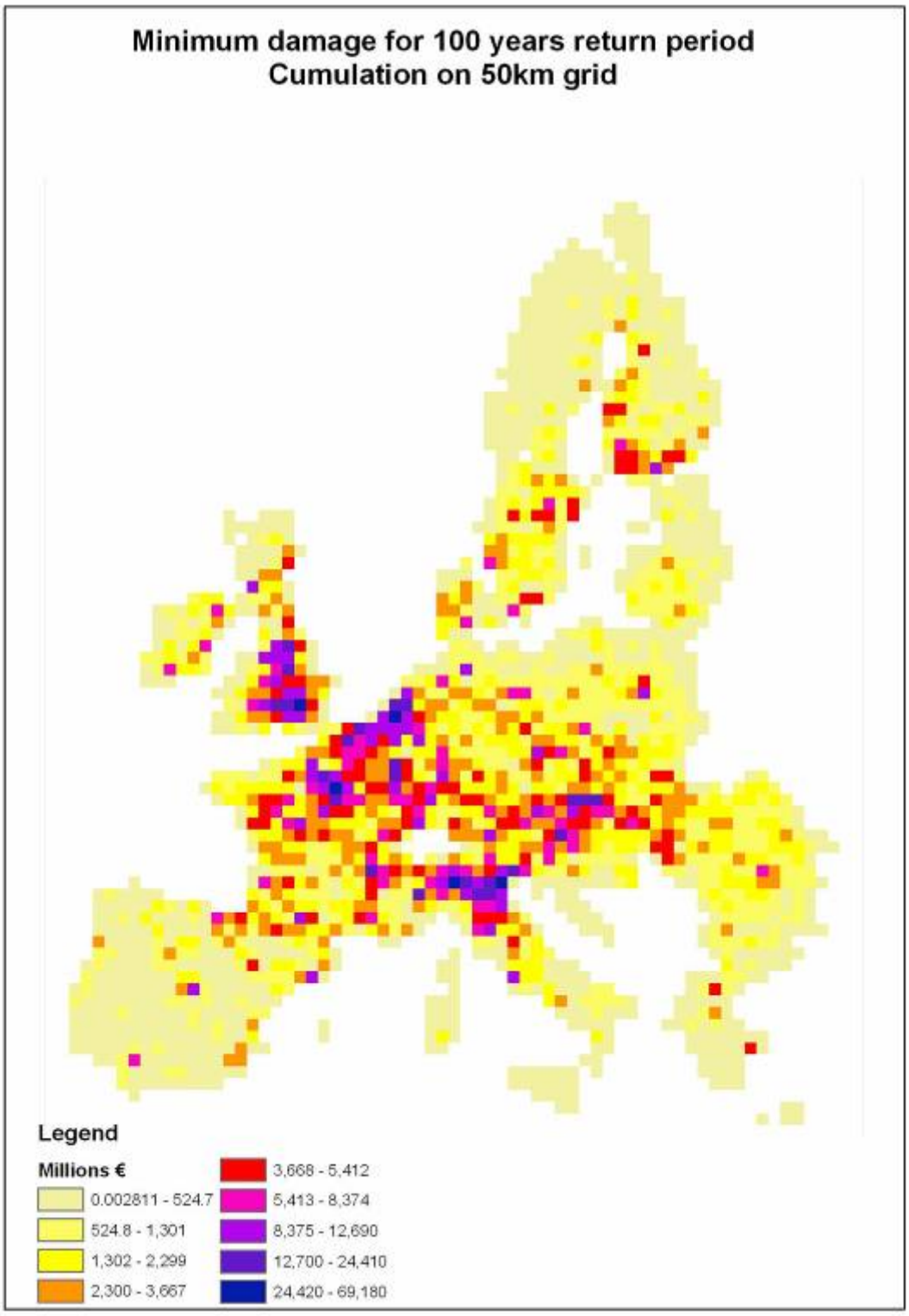

Figure 9.5*: Direct risk (monetary impact) for flood hazard with return period of 100 years. Minimum value.*

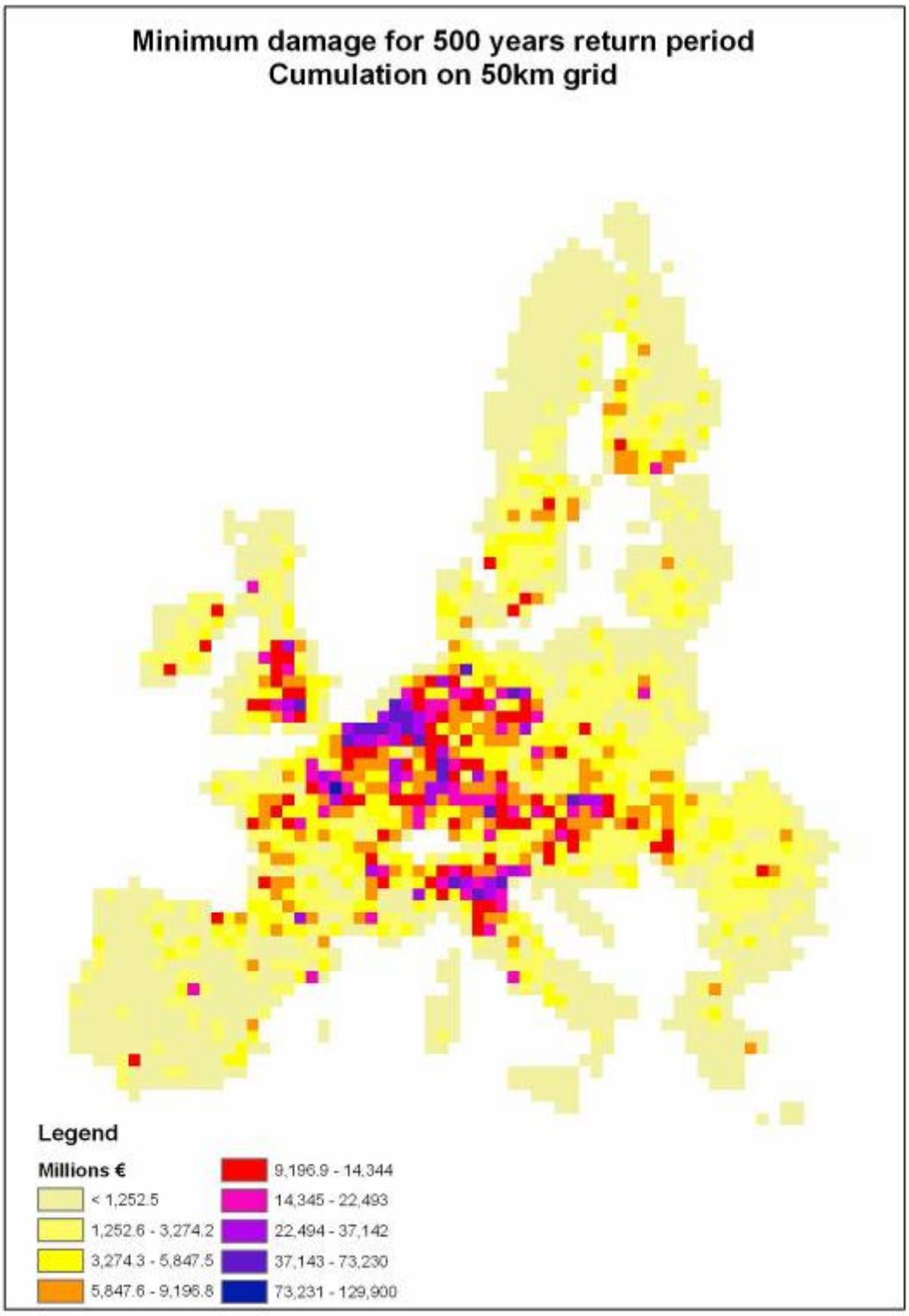

***Figure 9.6**: Direct risk (monetary impact) for flood hazard with return period of 500 years. Minimum value./*

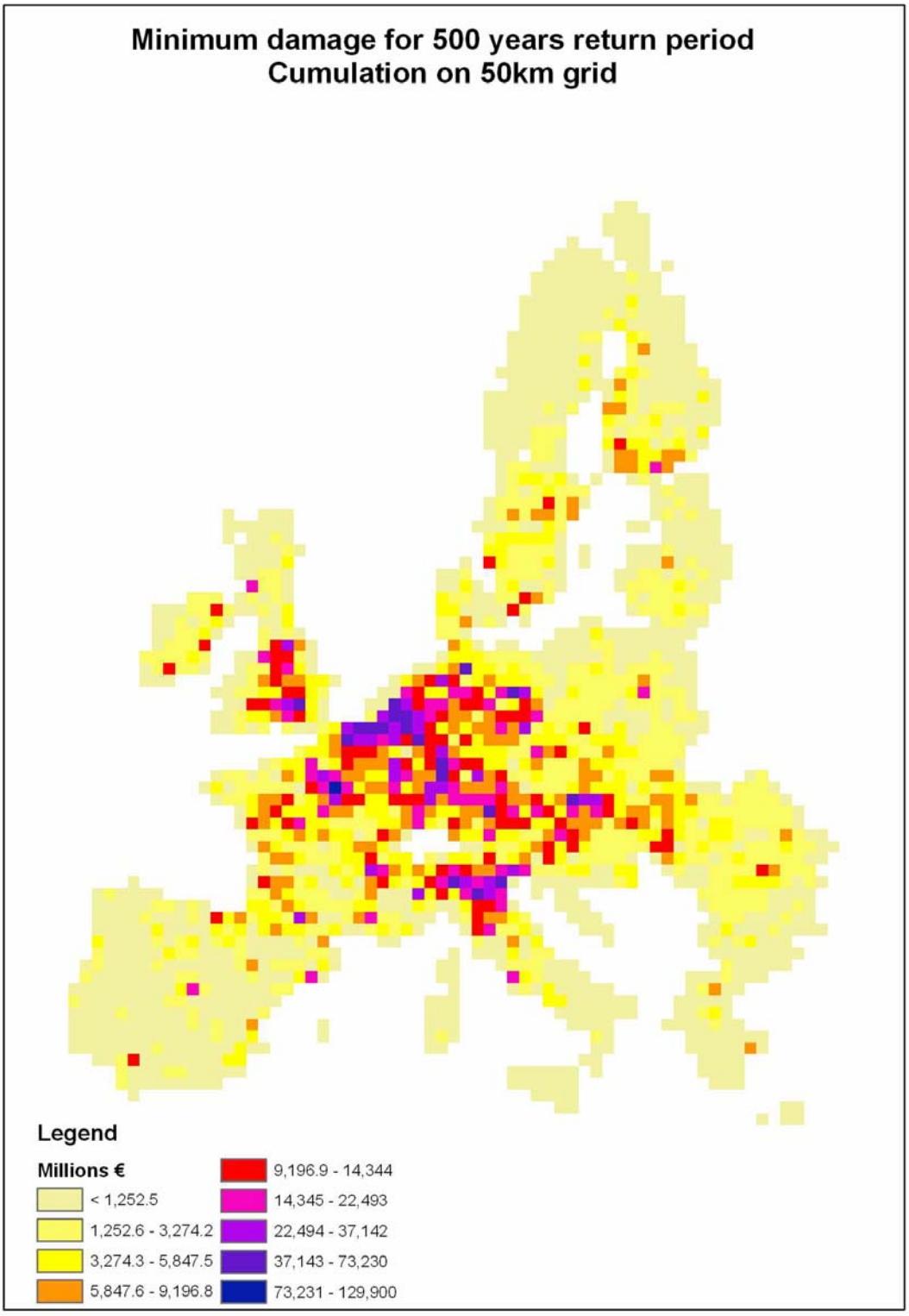

***Figure 9.7**: Direct risk (monetary impact) for flood hazard with return period of 500 years. Maximum value*

9.2 Accumulated Risk maps on administrative boundaries (NUTS level 2)

The maps in figures 9.8 to 9.14 present the results of the integration of flood direct damages on NUTS-2 aggregation (regional level), for the four return periods respectively. The value of each unit represents the accumulated value of damage computed as if the flood event is occurring simultaneously all over the NUTS-2 region.

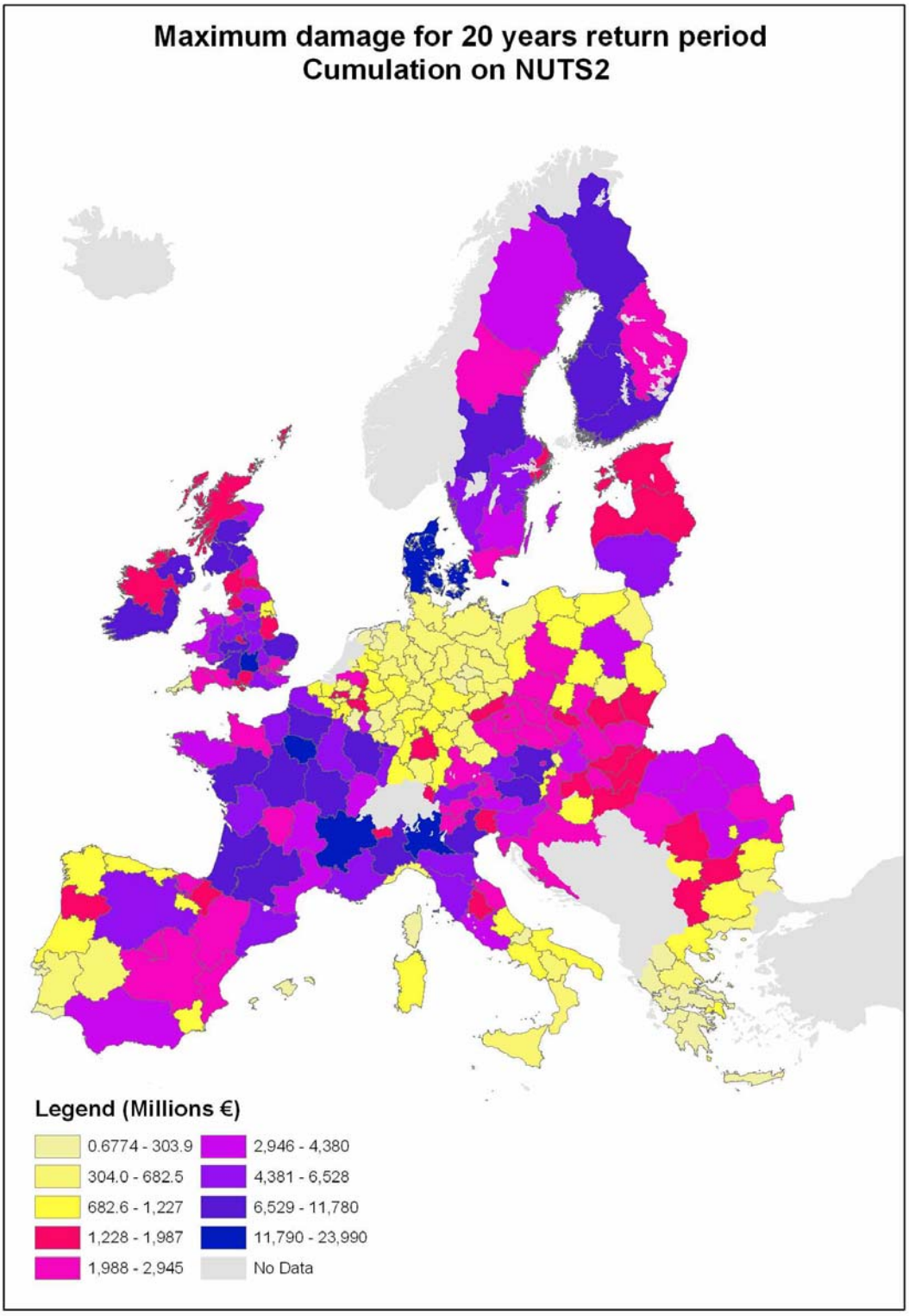

***Figure 9.8**: Direct risk (monetary impact) for flood hazard with return period of 20 years. Maximum value*

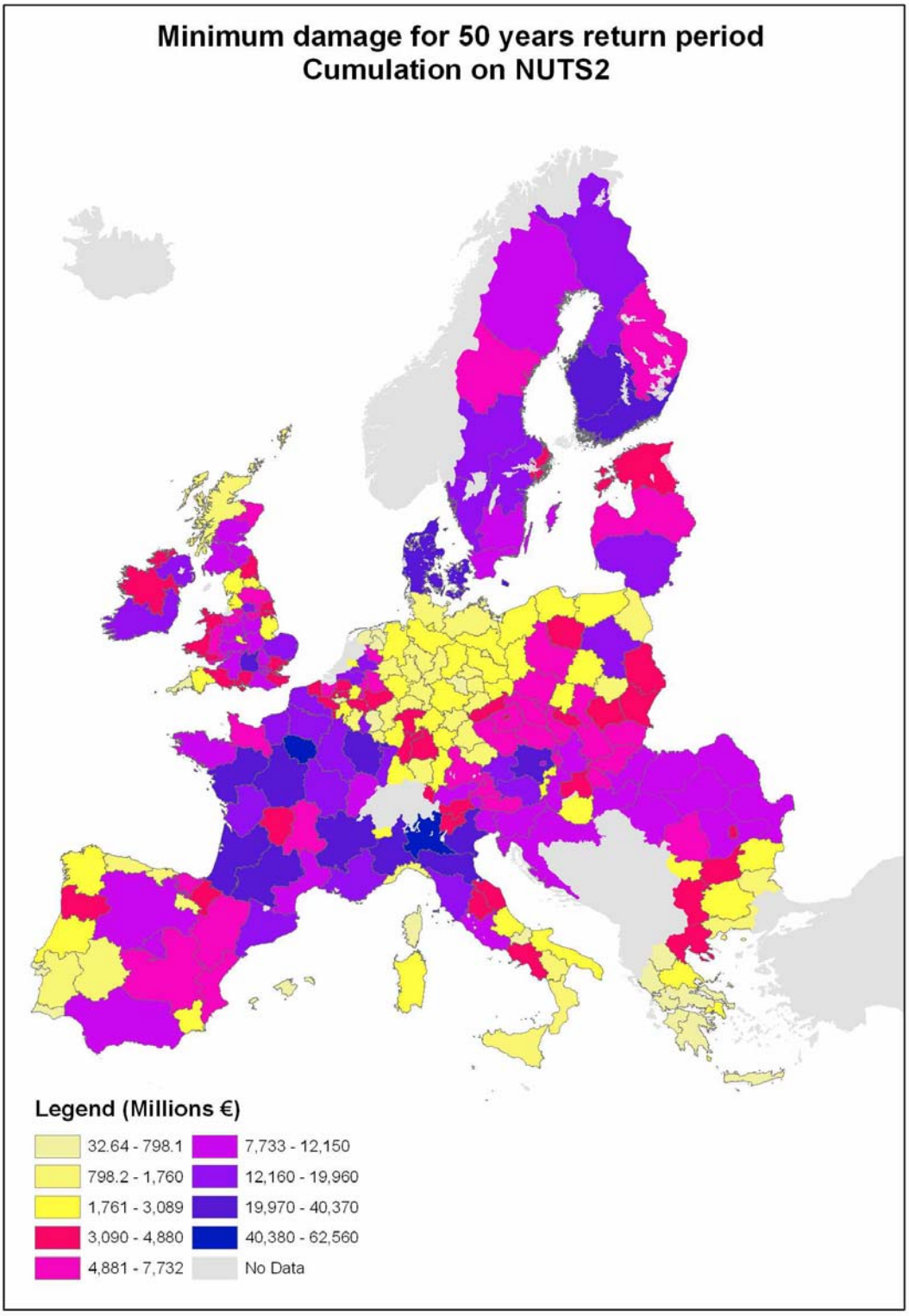

***Figure 9.9**: Direct risk (monetary impact) for flood hazard with return period of 50 years. Minimum value*

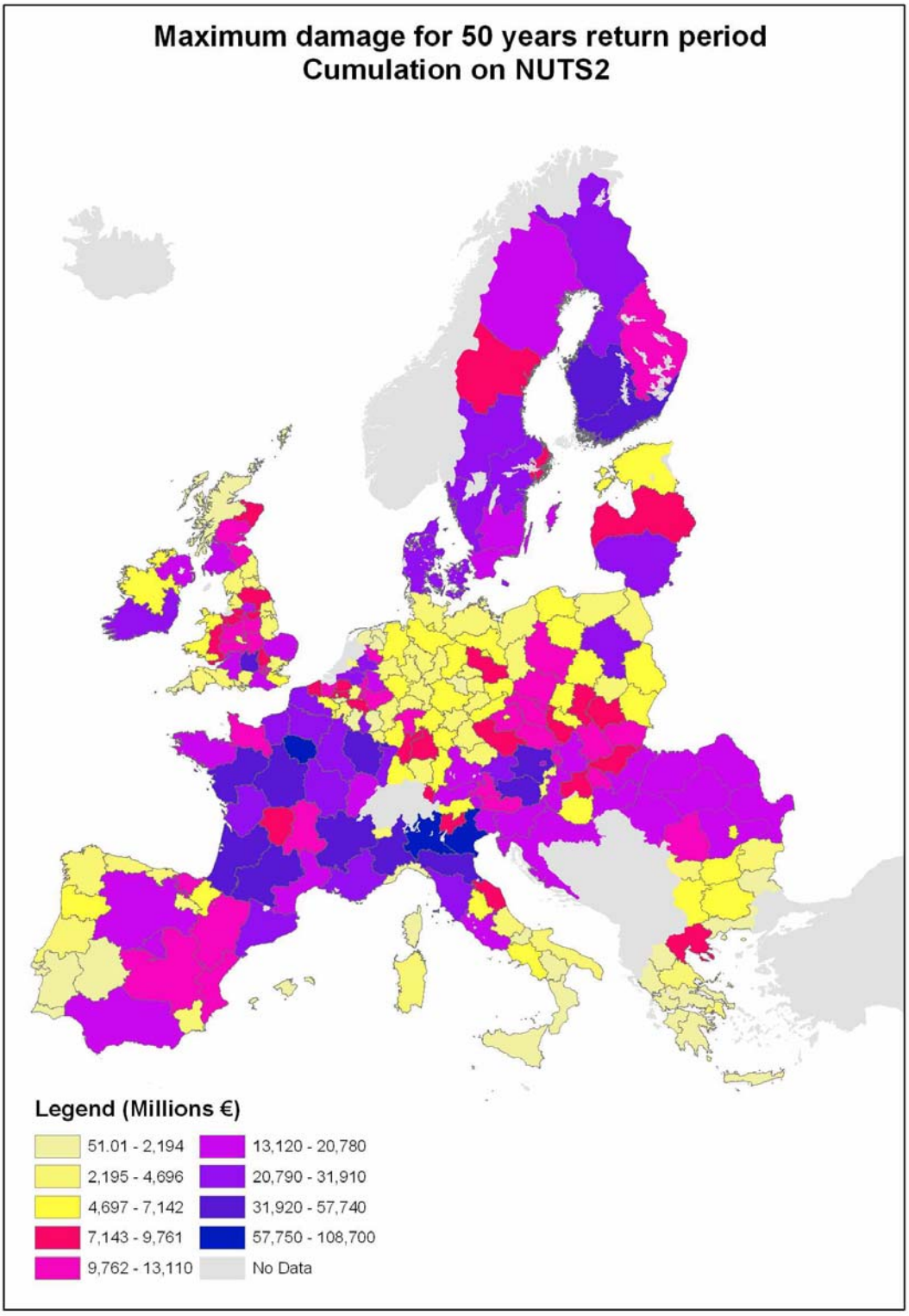

***Figure 9.10**: Direct risk (monetary impact) for flood hazard with return period of 50 years. Maximum value*

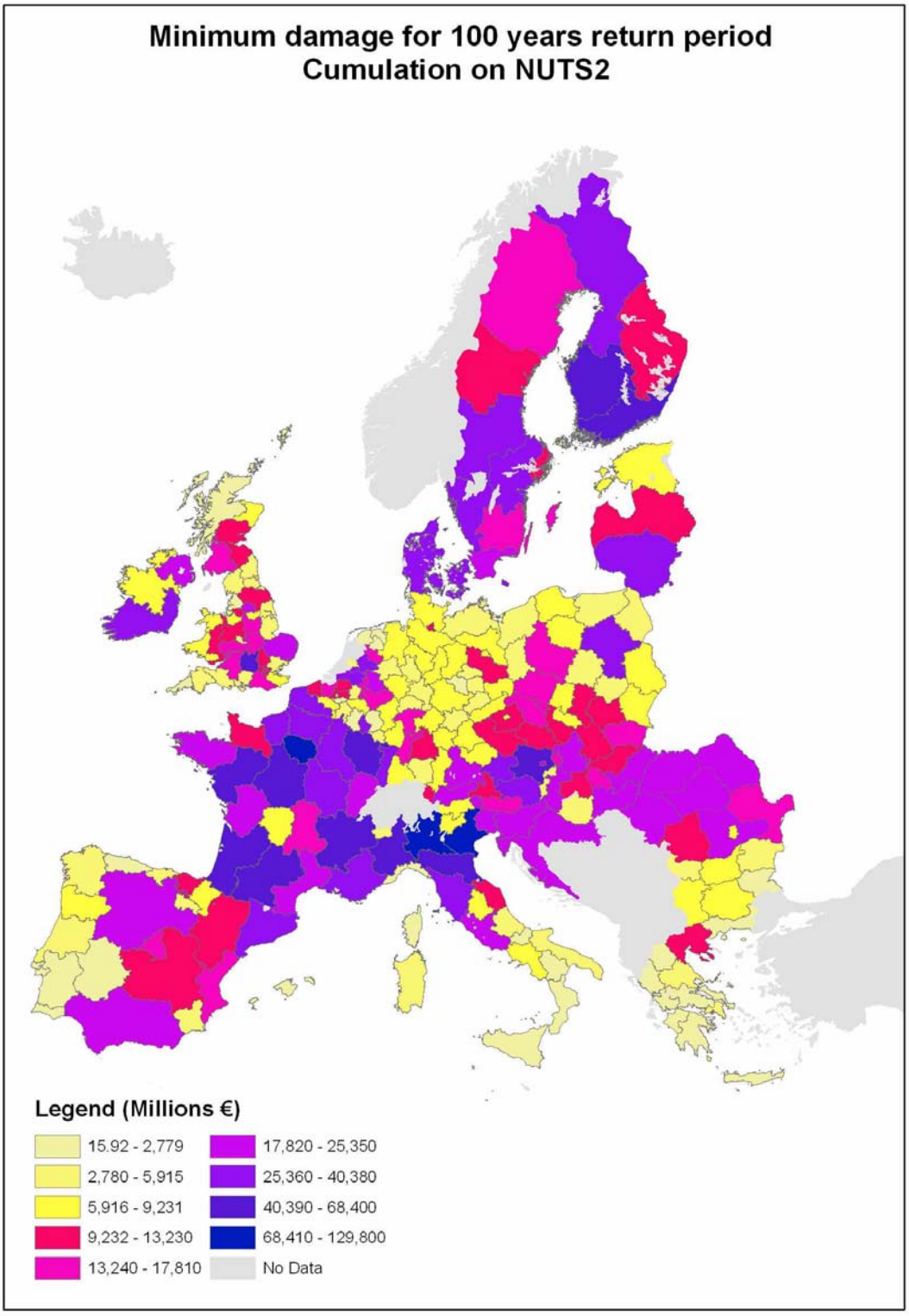

***Figure 9.11**: Direct risk (monetary impact) for flood hazard with return period of 100 years. Minimum value*

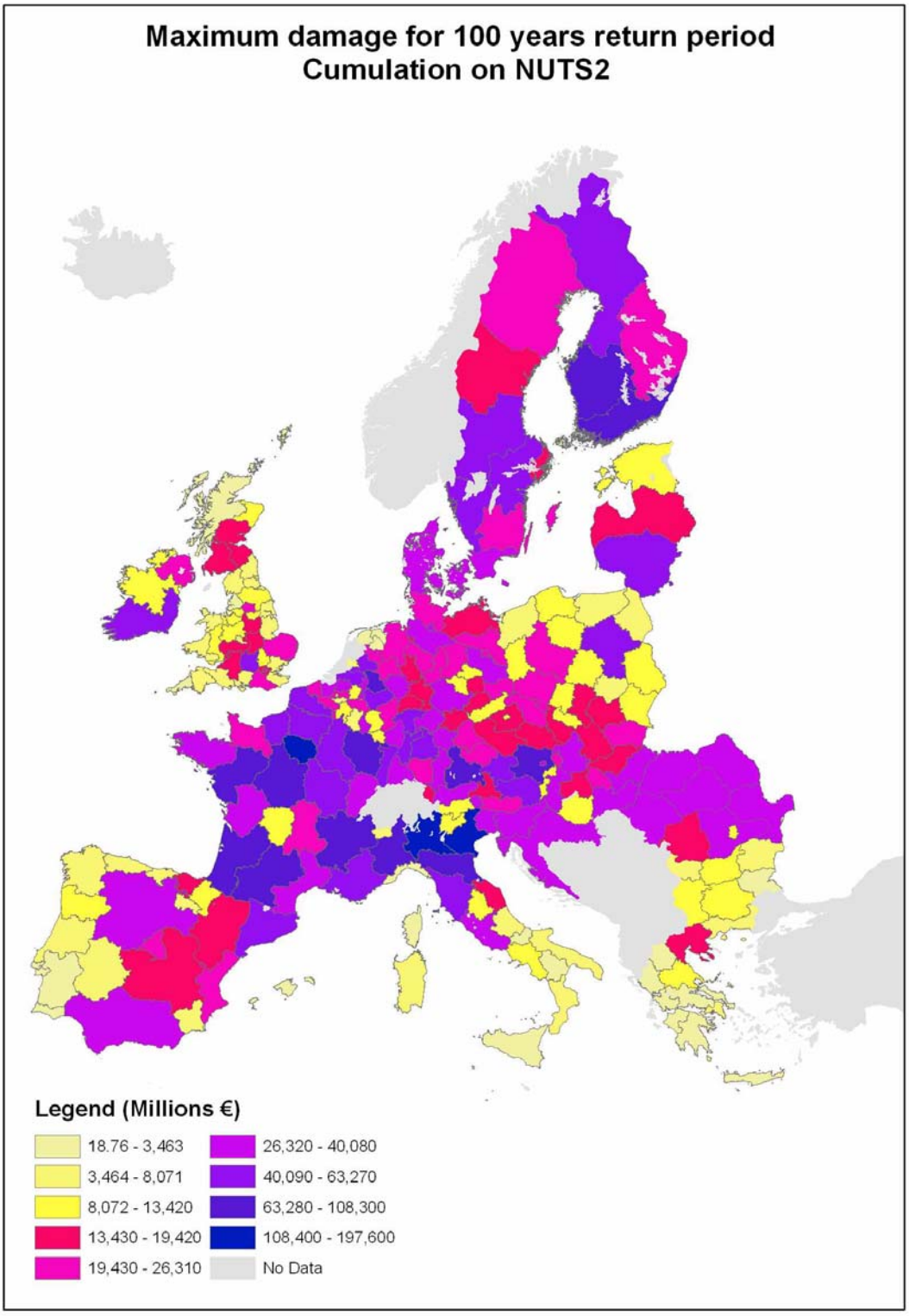

***Figure 9.12**: Direct risk (monetary impact) for flood hazard with return period of 100 years. Maximum value*

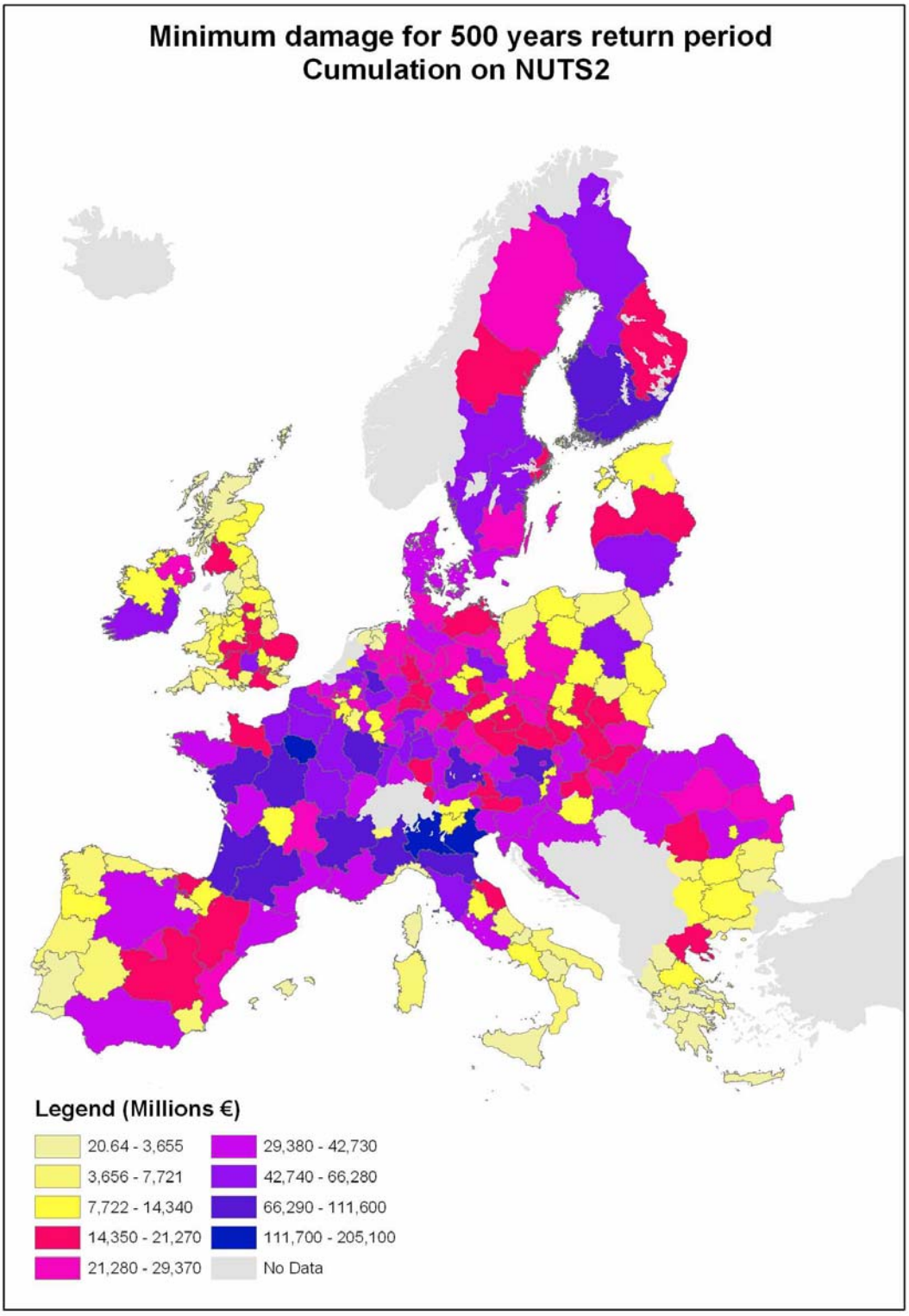

***Figure 9.13**: Direct risk (monetary impact) for flood hazard with return period of 500 years. Minimum value*

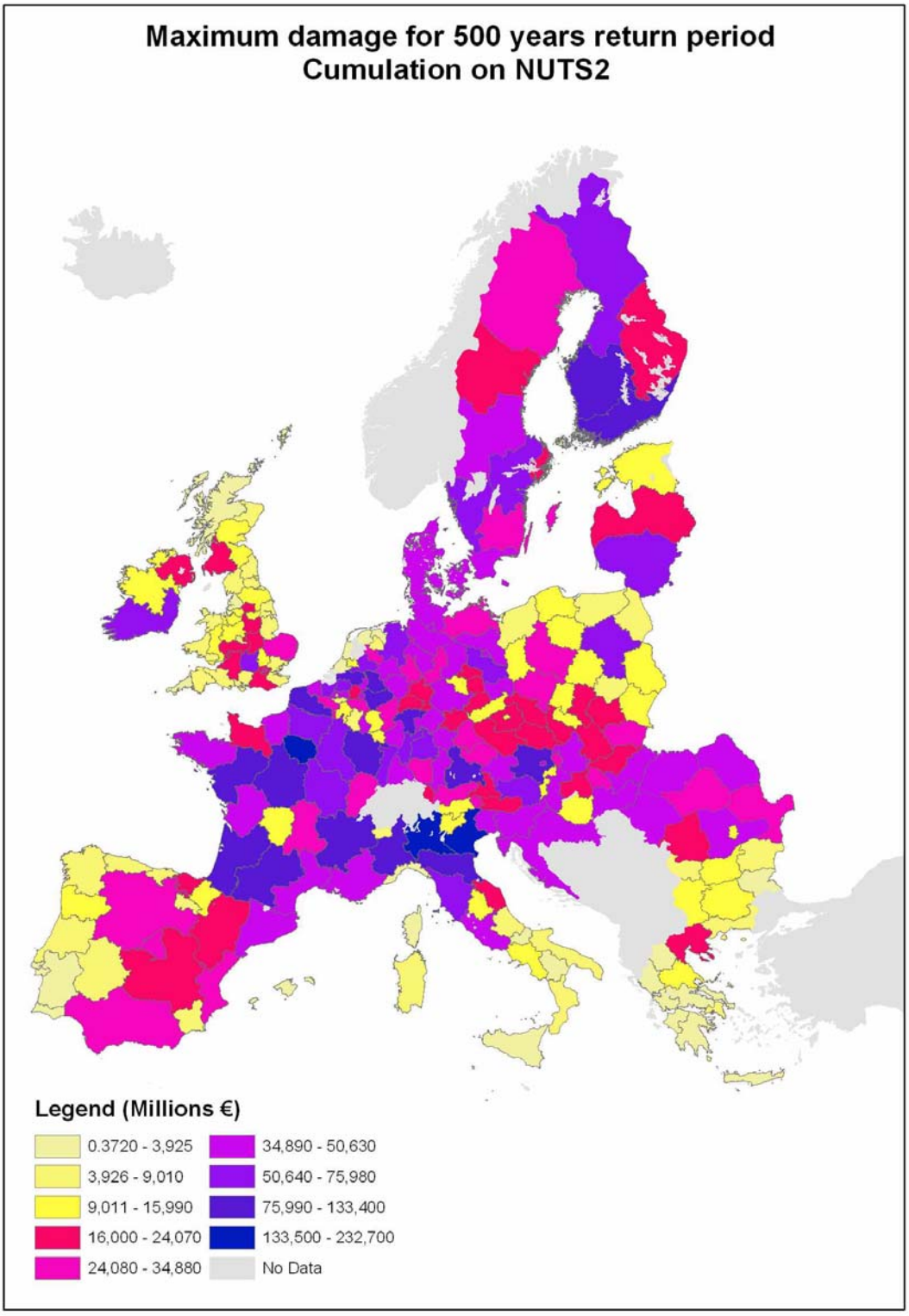

***Figure 9.14**: Direct risk (monetary impact) for flood hazard with return period of 500 years. Maximum value.*

10 ANNEX 4: preliminary European Heat/Drought Hazard and Risk Maps

In this section are shown the preliminary results of the "work in progress" over the Mediterranean domain. The study about the impact of extreme events in agriculture includes at this stage a complete analysis of extreme events frequency occurring during crop growing cycle and their effect on final yield. Cropsyst growth model, driven by RCM HadRM3P for the present period (1960-1990), was run over the whole European domain to simulate potential and actual yield of winter crops (barley) and summer crops (sunflower, maize, sorghum, soybean). All the grid points included in the dataset were used for crop growth simulations. All the pixels where the growing cycle was not completed by Cropsyst (i.e. a complete simulation from sowing to harvest time) were discharged so that the presented maps may be intended as potential cultivated areas of each crop.

According to the procedure described in the first section, the number of heat stress events was computed for each crop in a period including pre and post anthesis, where the impact of temperature is higher. The crop included in this analysis may have different sensibility to heat stress but generally the maximum tolerance threshold ranges between 31°C-33°C. The number of events per year was averaged over the period (1961-1990).

Drought stress events were derived directly from Cropsyst model, which includes subroutines simulating soil water content for each soil layer. A wilting point=-1600 J kg^{-1} at anthesis stage was considered the threshold below which crops reduce their potential yield. The frequency of soil water content below the wilting point at anthesis stage was then calculated. Maize was not included in this analysis since it was considered an irrigated crop.

10.1 Average of number of heat stress at anthesis stage

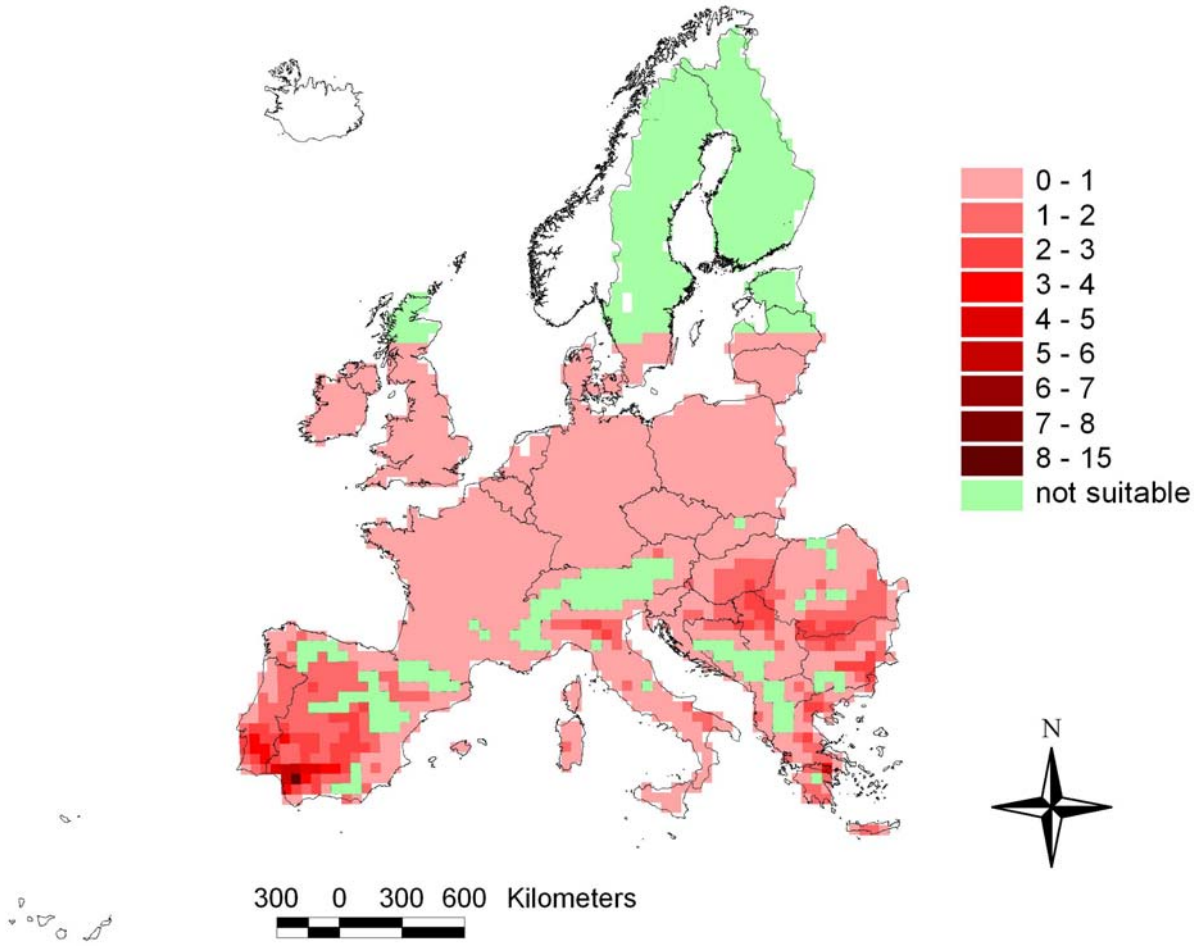

***Figure 10.1**: Barley. Number of heat stress events (Tmax>31°C) averaged over 30 years, at anthesis stage. A period of ±7 days around the date of anthesis (pre-anthesis and post anthesis phase) was included for this analysis*

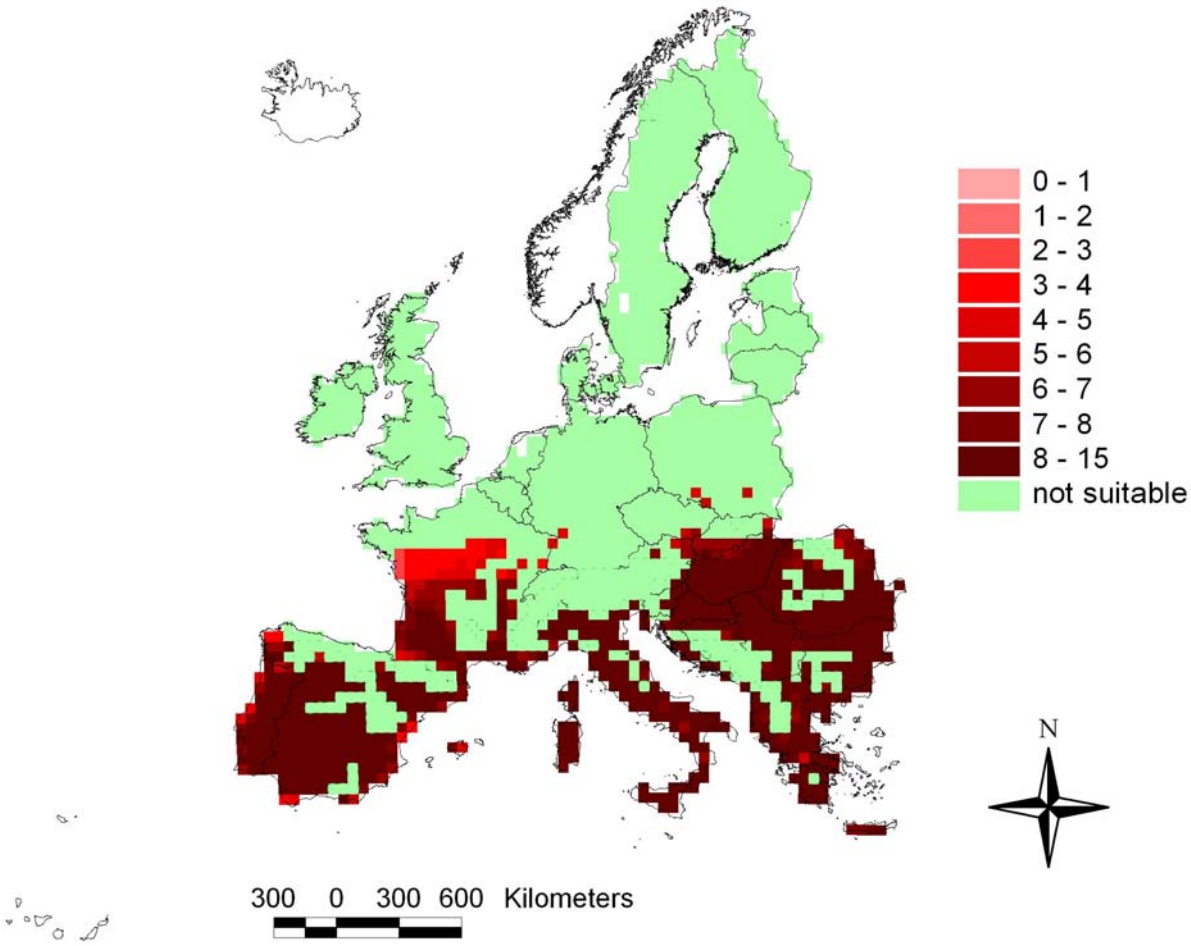

***Figure 10.2**: Maize. Number of heat stress events (Tmax>31°C) averaged over 30 years, at anthesis stage. A period of ±7 days around the date of anthesis (pre-anthesis and post anthesis phase) was included for this analysis*

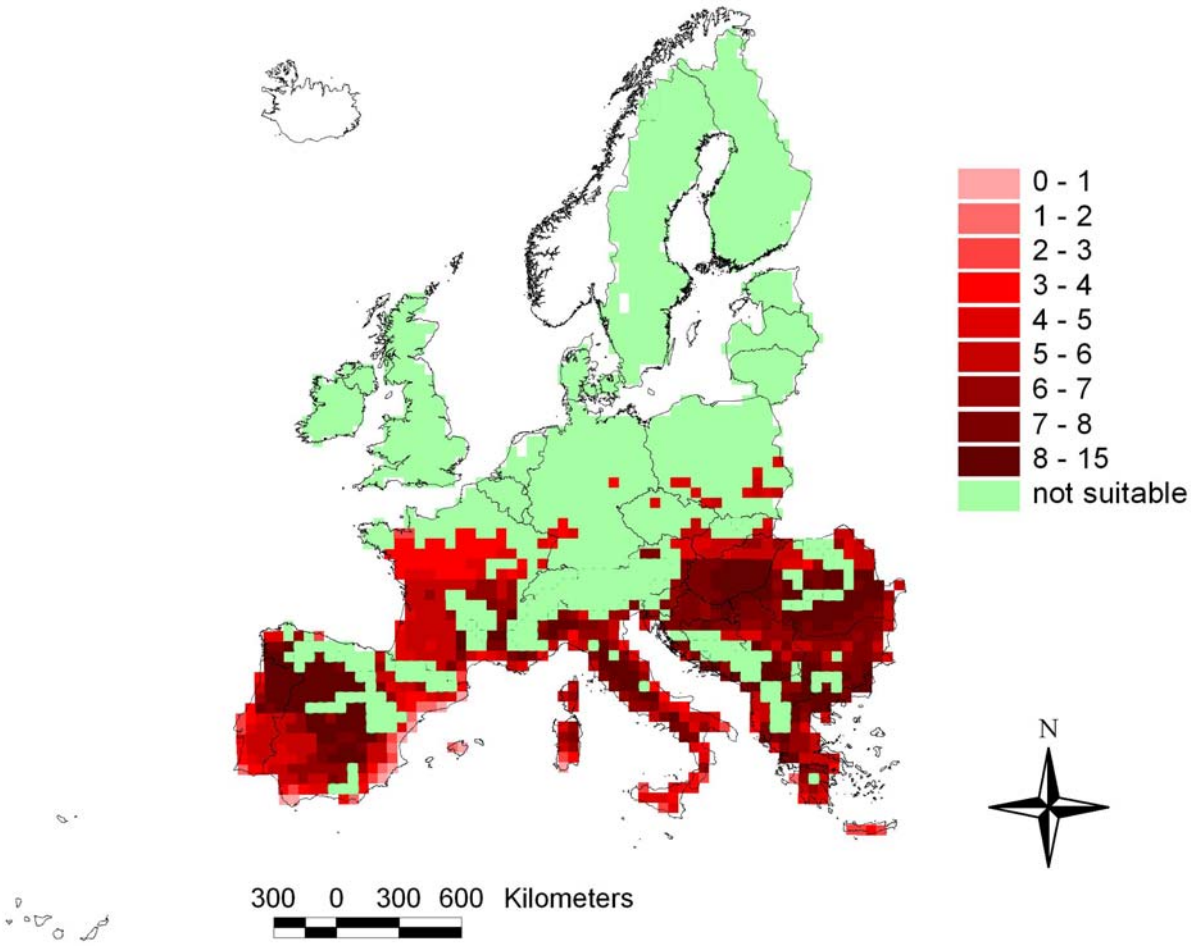

***Figure 10.3**: Sunflower. Number of heat stress events (Tmax>31°C) averaged over 30 years, at anthesis stage. A period of ±7 days around the date of anthesis (pre-anthesis and post anthesis phase) was included for this analysis*

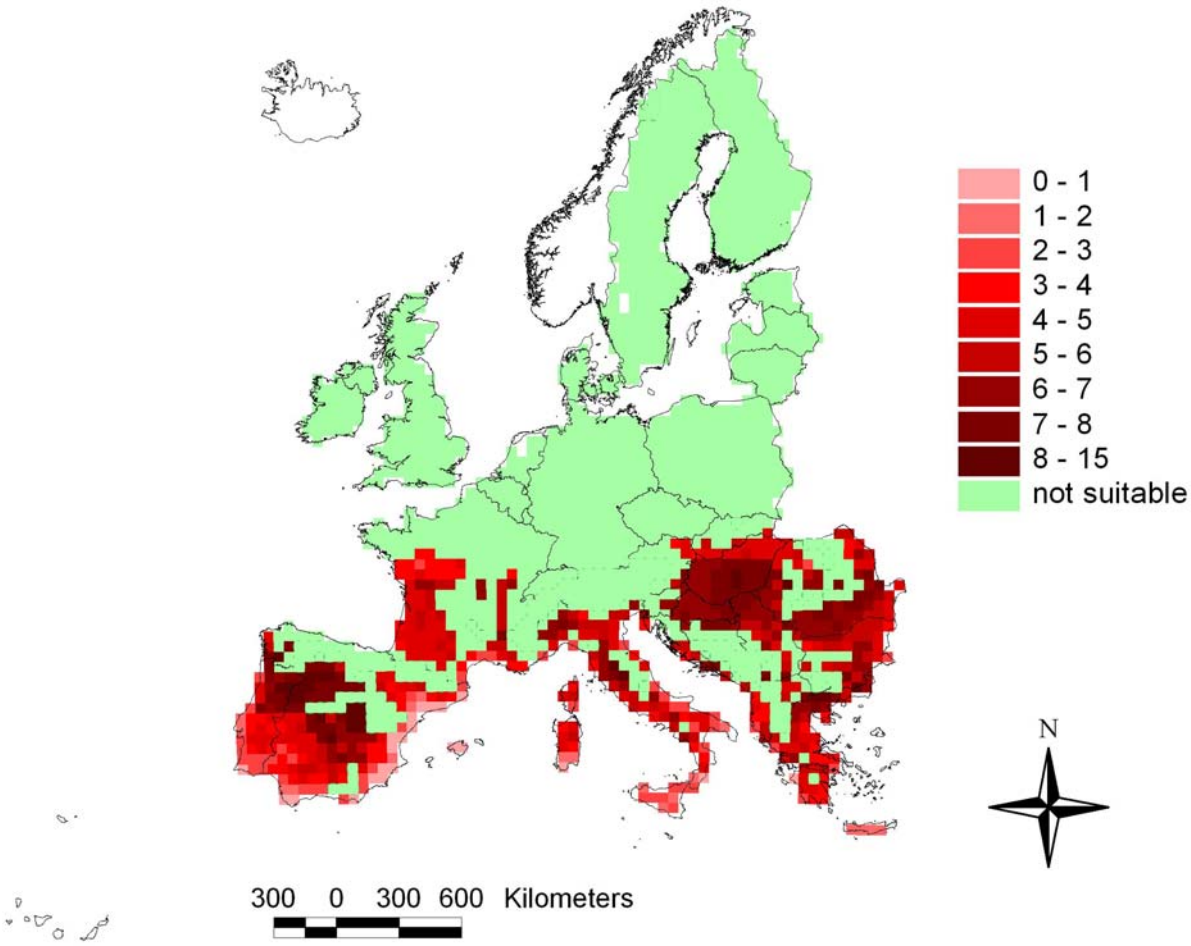

***Figure 10.4**: Soybean. Number of heat stress events (Tmax>31°C) averaged over 30 years, at anthesis stage. A period of ±7 days around the date of anthesis (pre-anthesis and post anthesis phase) was included for this analysis*

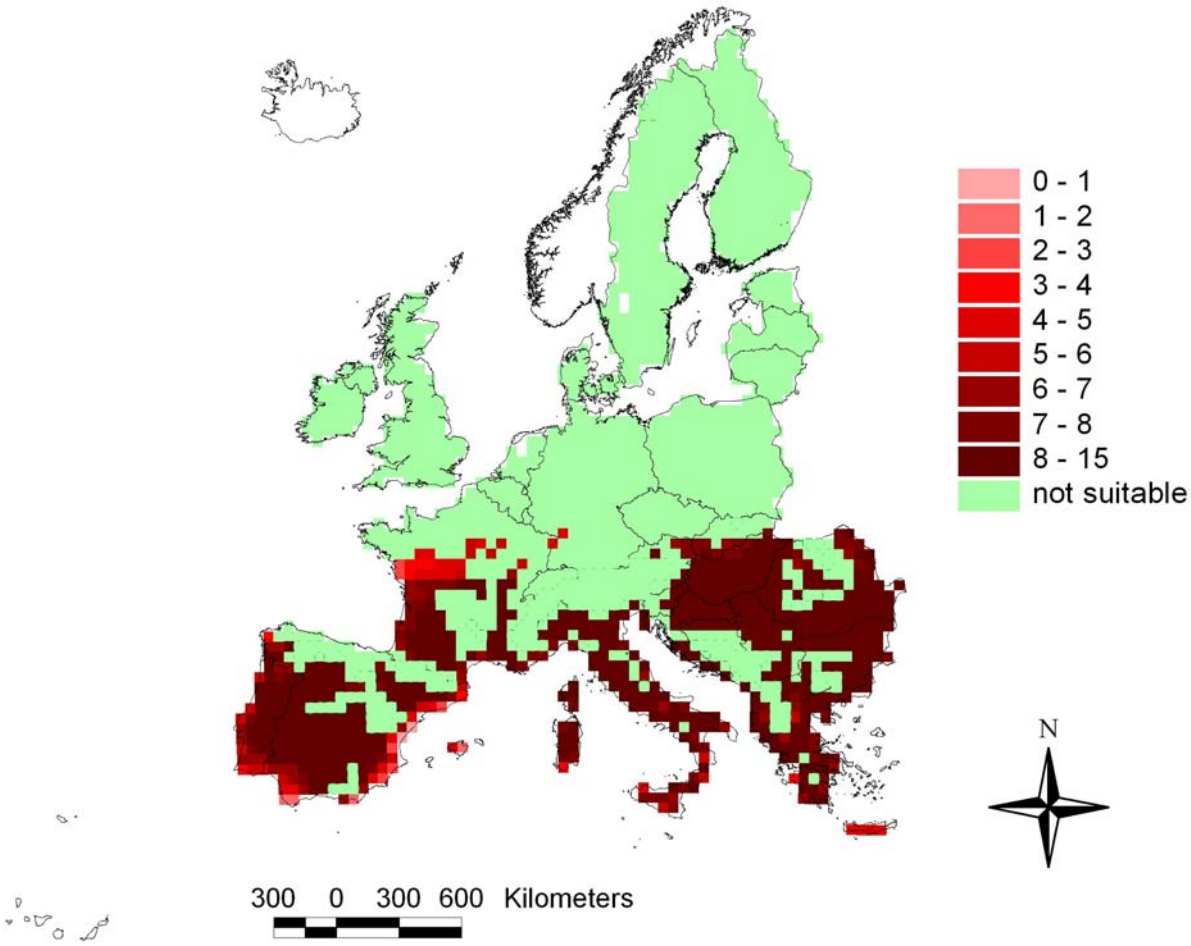

***Figure 10.5**: Sorghum. Number of heat stress events (Tmax>33°C) averaged over 30 years, at anthesis stage. A period of ±7 days around the date of anthesis (pre-anthesis and post anthesis phase) was included for this analysis*

10.2 Frequency of water stress at anthesis stage

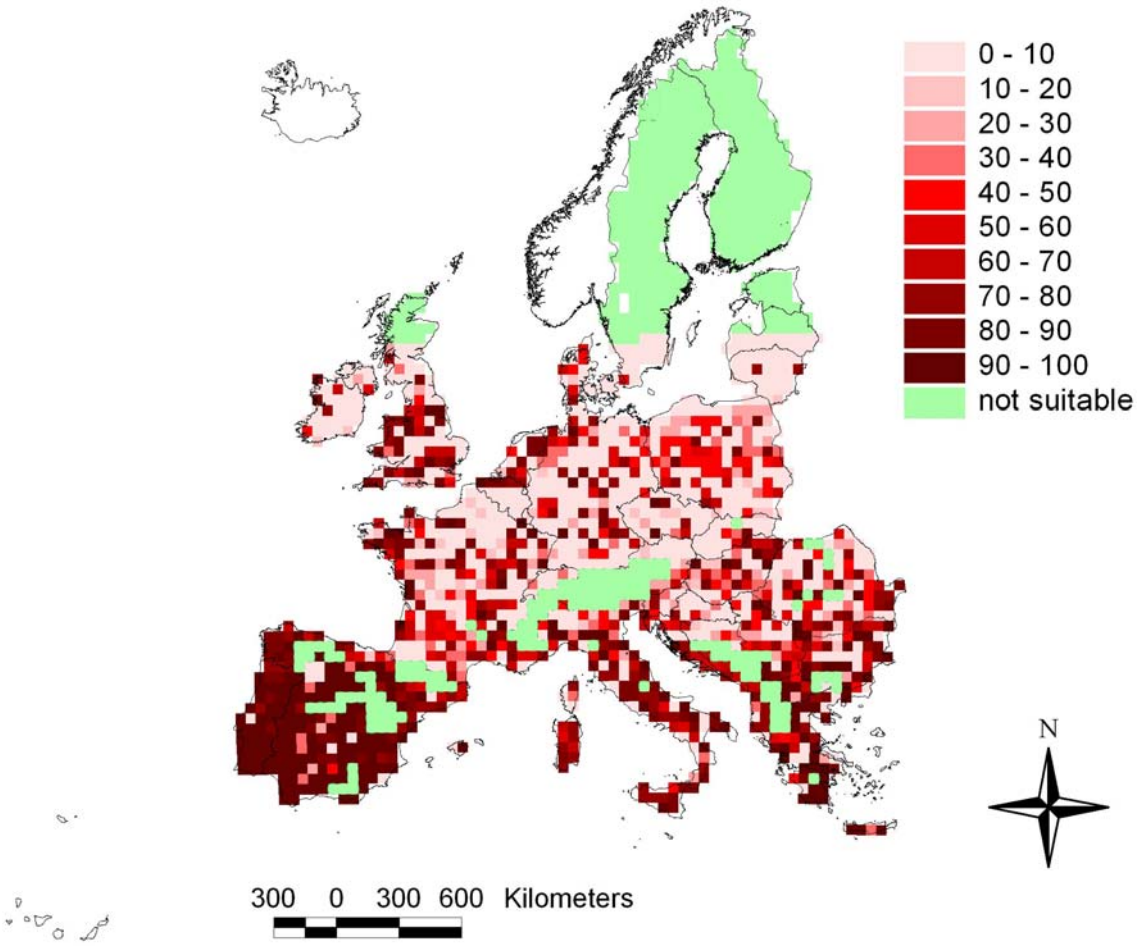

***Figure 10.6**: Barley. Percentage of drought periods (soil water content lower than wilting point) at anthesis stage calculated over a period of 30 years.*

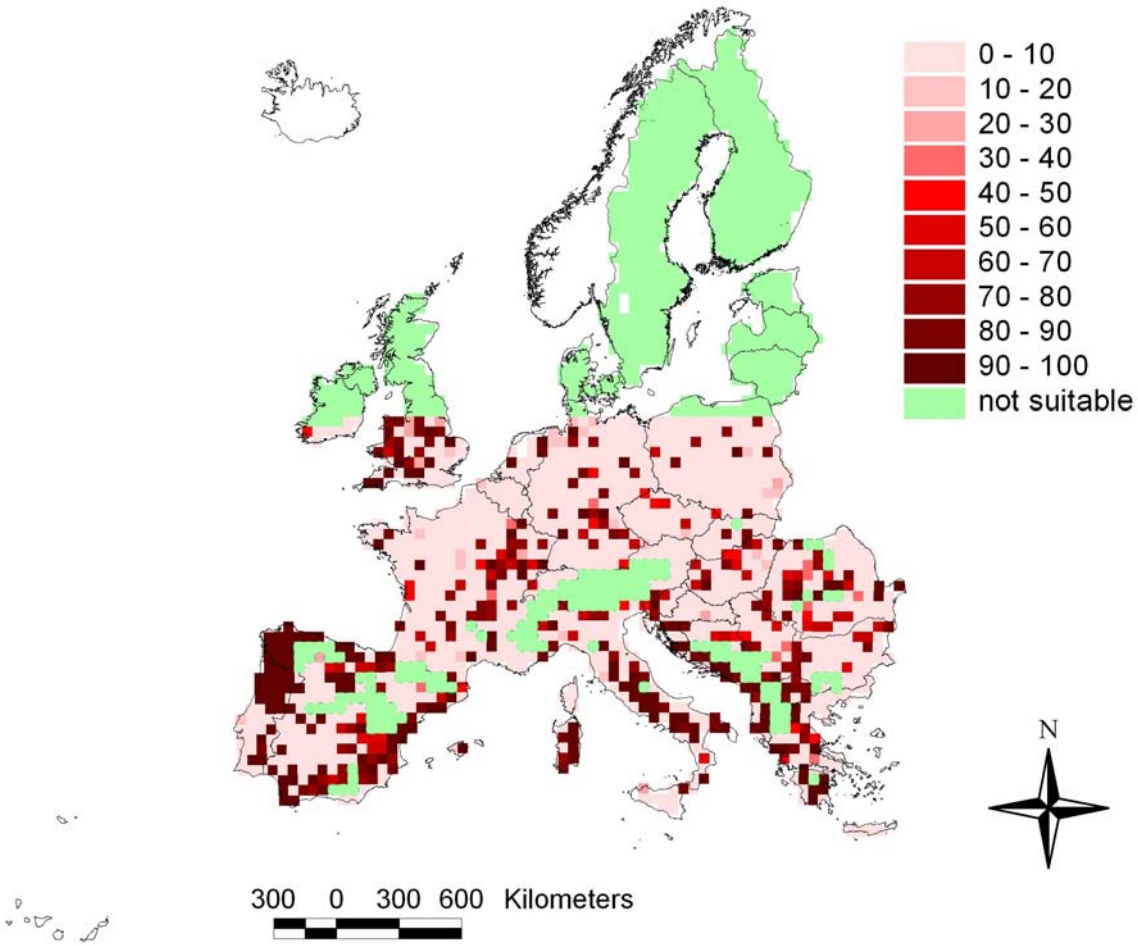

***Figure 10.7**: Sunflower. Percentage of drought periods (soil water content lower than wilting point) at anthesis stage calculated over a period of 30 years.*

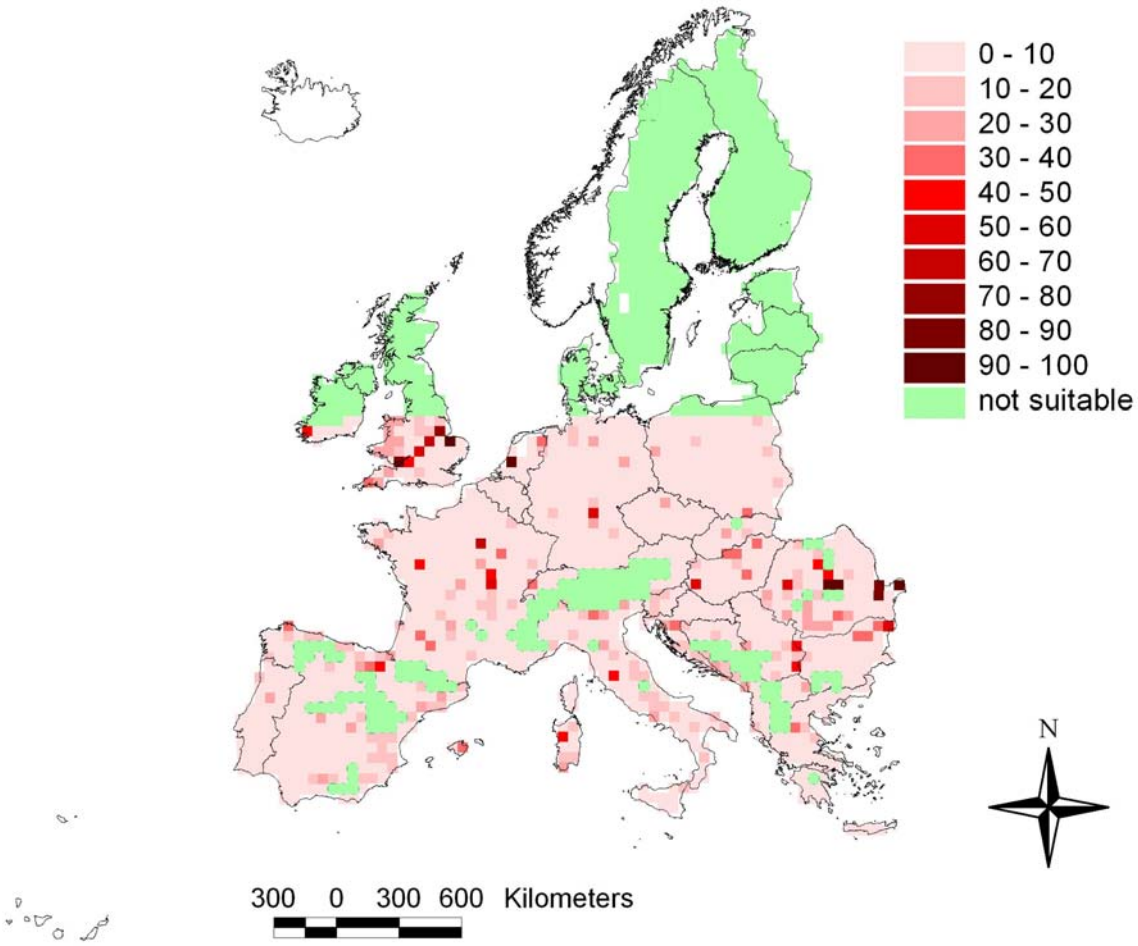

***Figure 10.8**: Soybean. Percentage of drought periods (soil water content lower than wilting point) at anthesis stage calculated over a period of 30 years.*

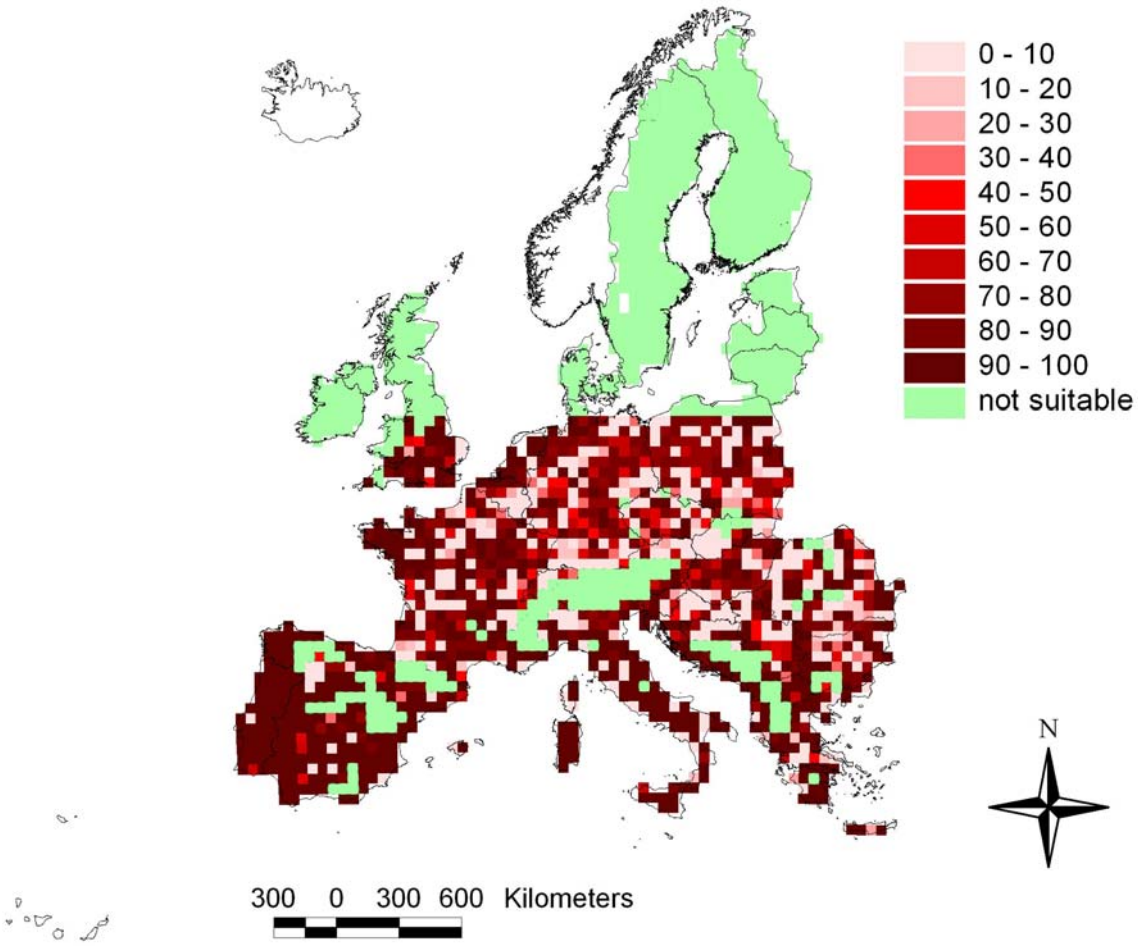

***Figure 10.9**: Sorghum. Percentage of drought periods (soil water content lower than wilting point) at anthesis stage calculated over a period of 30 years.*

10.3 Average yield loss due to extreme events (heat stress and water stress) at anthesis stage

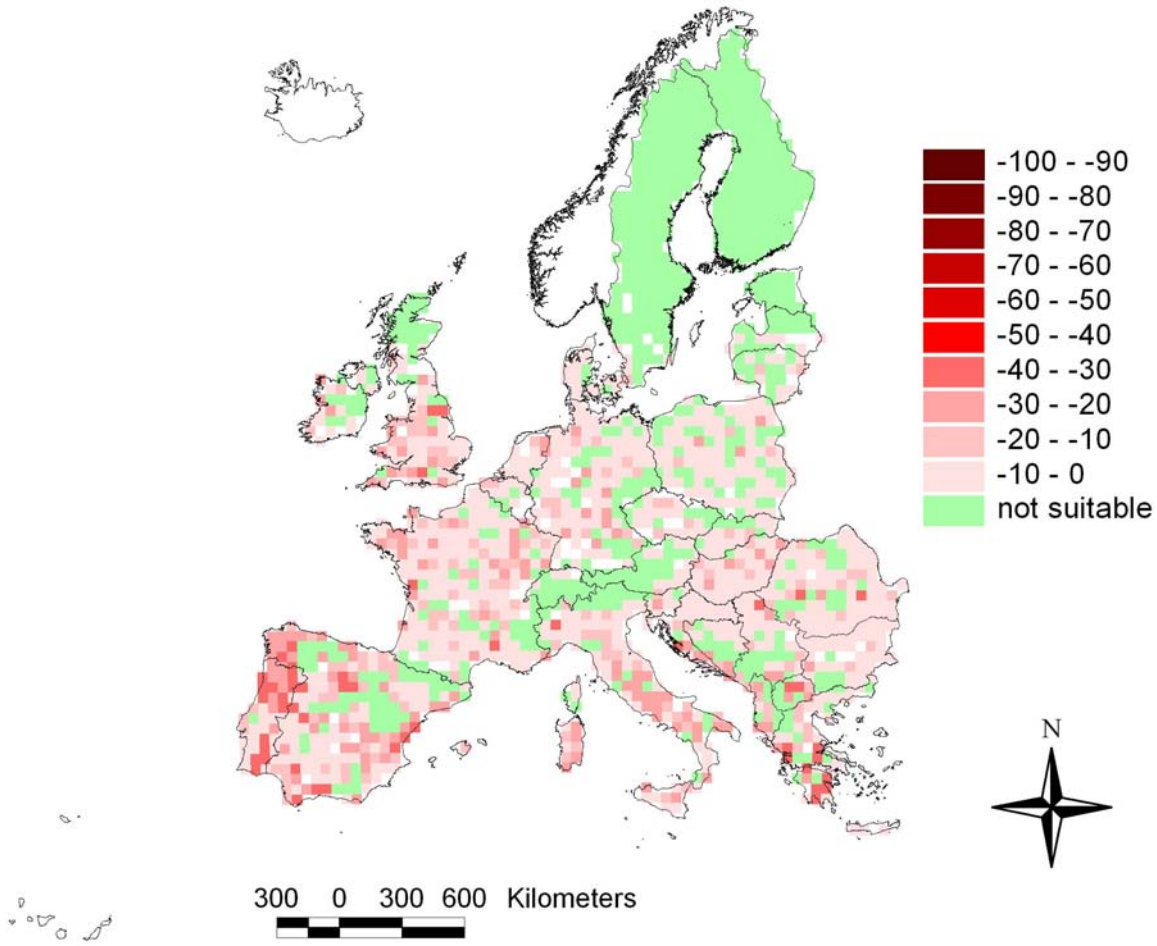

***Figure 10.10**: Barley. Yield loss due to both heat stress and heat events at anthesis expressed as percentage on potential biomass (simulated not including the impact of extreme events - average over 30 year)*

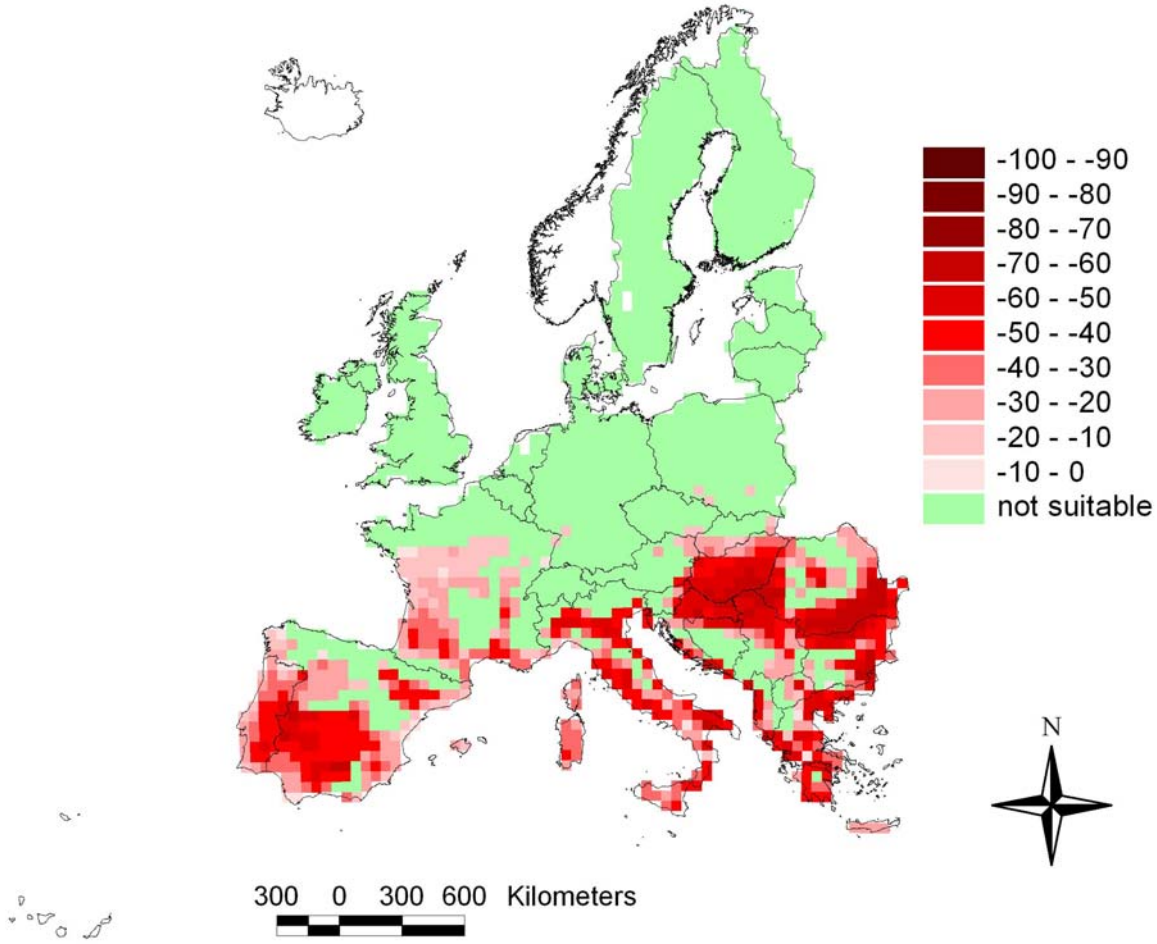

***Figure 10.11**: Maize. Yield loss due to both heat stress and heat events at anthesis expressed as percentage on potential biomass (simulated not including the impact of extreme events - average over 30 year)*

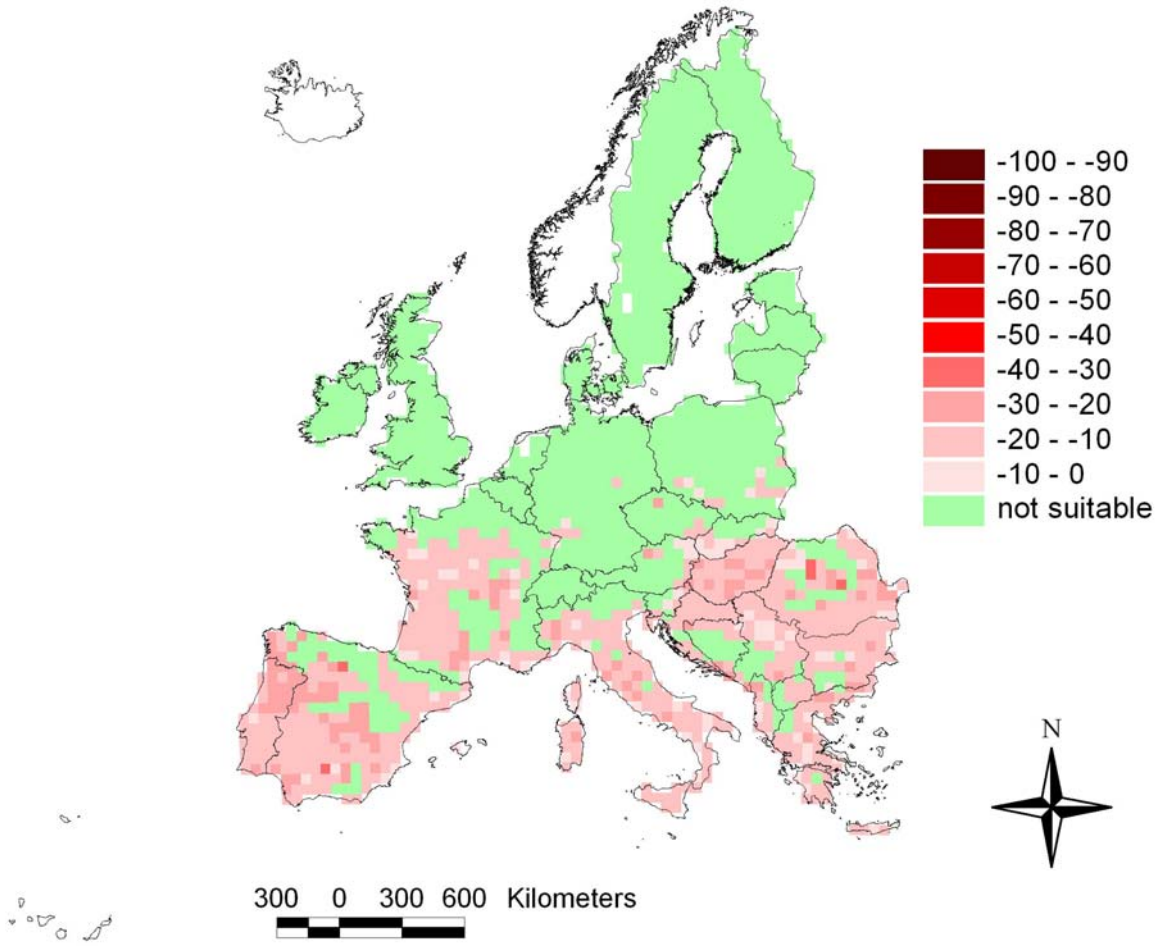

***Figure 10.12**: Sunflower. Yield loss due to both heat stress and heat events at anthesis expressed as percentage on potential biomass (simulated not including the impact of extreme events - average over 30 year)*

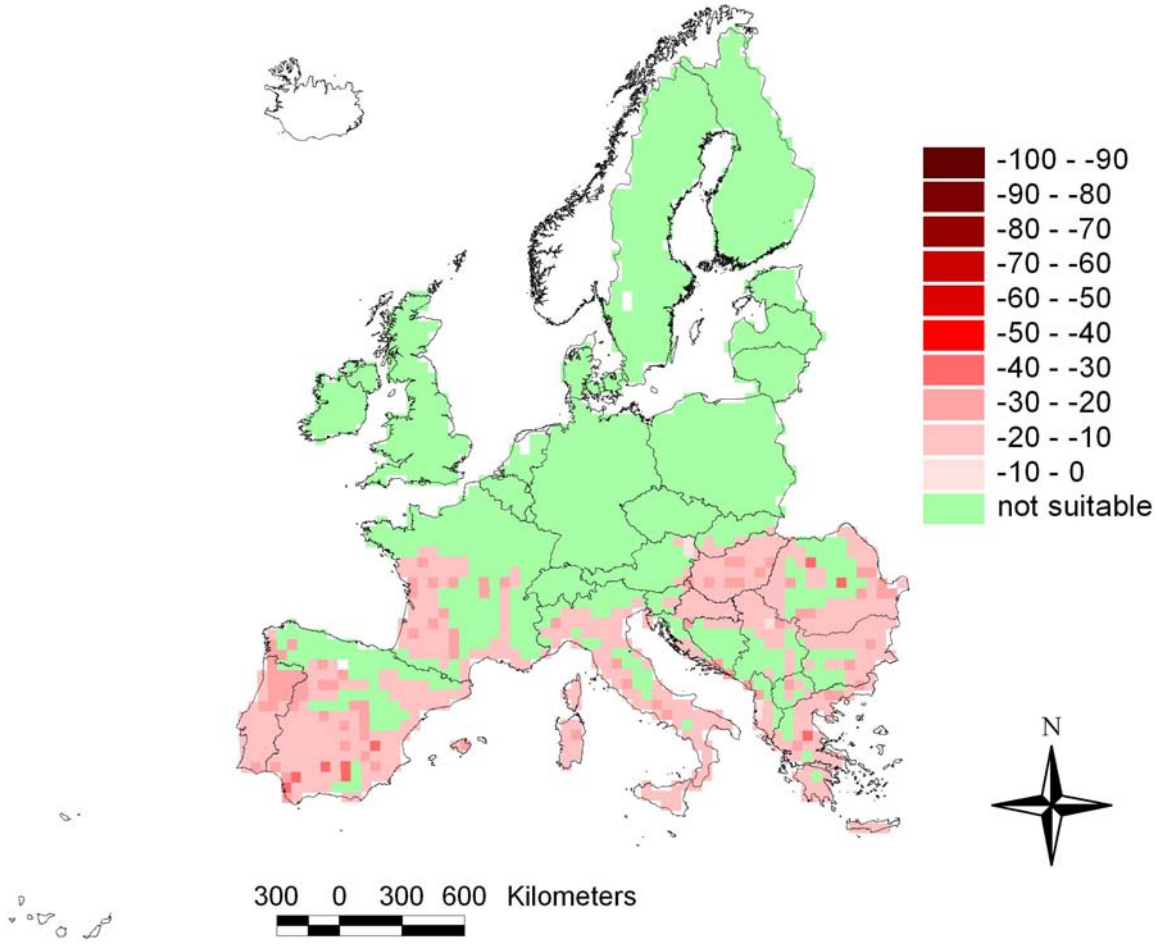

Figure 10.13:*Soybean. Yield loss due to both heat stress and heat events at anthesis expressed as percentage on potential biomass (simulated not including the impact of extreme events - average over 30 year)*

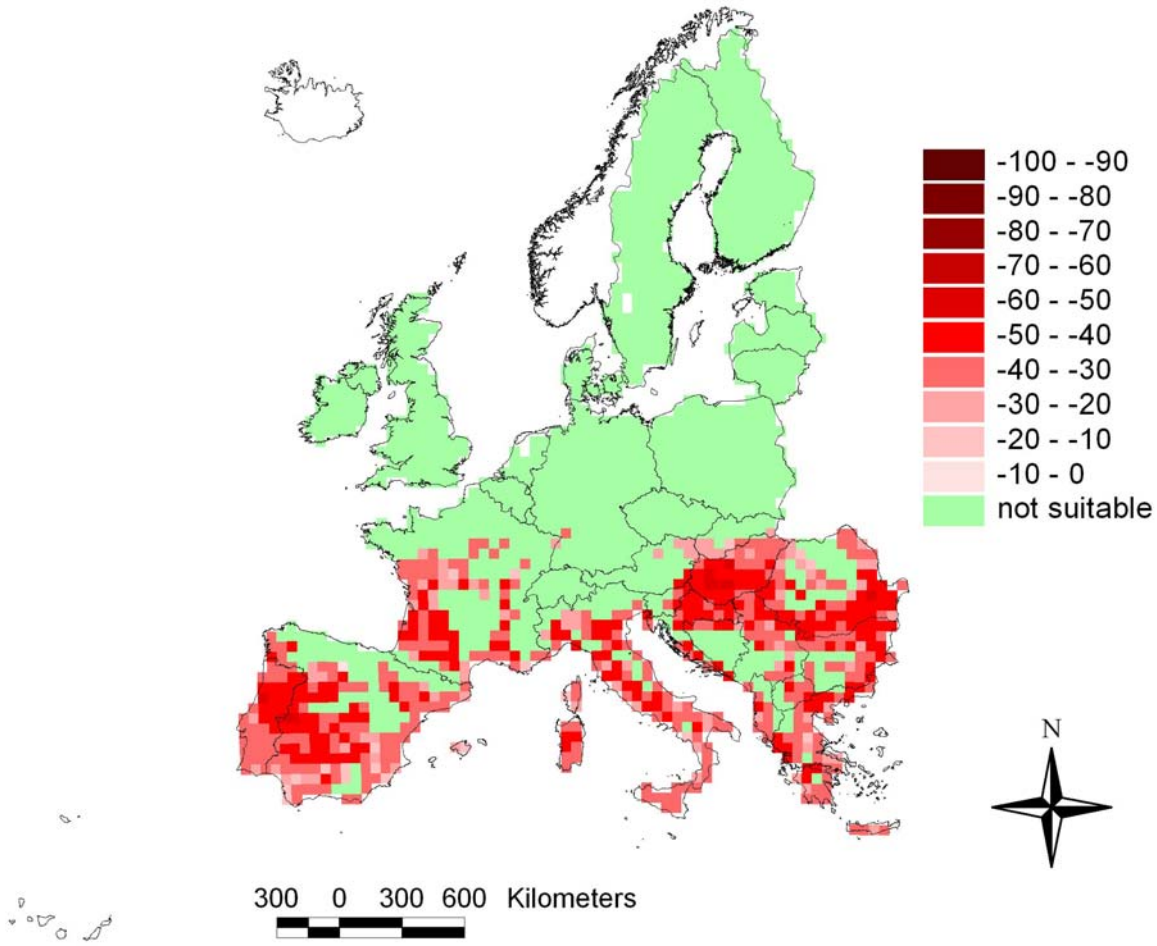

***Figure 10.14**: Sorghum. Yield loss due to both heat stress and heat events at anthesis expressed as percentage on potential biomass (simulated not including the impact of extreme events - average over 30 year)*

European Commission

EUR 23208 EN – Joint Research Centre – Institute for Environment and Sustainability

Title: **An assessment of weather-related risks in Europe: maps of flood and drought risks (Interim report for ADAM FP6 Integrated Project**

Author(s): **Elisabetta Genovese, Nicola Lugeri, Carlo Lavalle, José I. Barredo (JRC)**

Marco Bindi, Marco Moriondo (DISAT - University of Florence)

Luxembourg: Office for Official Publications of the European Communities

2007 – 116 pp. – 21 x 29.7 cm

EUR – Scientific and Technical Research series – ISSN 1018-5593

Abstract

This technical report describes the adopted methodology and the outputs produced during the first 18 months of life of the "ADAM" project. ADAM (Adaptation and Mitigation Strategies: Supporting European Climate Policy) is an Integrated Project financed under thematic priority "Global Change and Ecosystems" of the 6th framework programme (for further information, see www.adam.info)

The task 'A2.1 - An assessment of weather-related risks in Europe' has the following main objective:

"*Quantify and map weather-related extreme-event risks to public and private capital assets, human lives, and agriculture/forestry/tourism, and identify high-risk areas ("hot spots") on which to focus more detailed analysis.*"

The key innovative aspects of the work herein presented are manifold:

- the quantification of the probabilistic monetary impact of extreme events;
- the combined use of modelling techniques and of observed data to supply the lack of information at the various scales of relevance of the study;
- the estimation of uncertainty arising from limitations in data availability and modelling assumptions;
- the geographical scale (continental) of the exercise.

The key outputs of task A2.1 are digital maps of risks from natural extremes at European scale identifying monetary/economic losses. The maps are furnished as input to other tasks of package A2 for successive modelling exercises and analysis.

As defined in the project work-plan, task A2.1 has duration of 24 months. The 18-month deliverables are maps of flood and drought risks.

The report focuses on inland river flood damage to properties and infrastructures and on climatic stresses (drought and heat waves) in agriculture. Population exposure has only been addressed in a partial study and it's therefore not included in the final monetary losses assessment.

The work on floods has been carried out by the Institute for Environment and Sustainability of the Joint research Centre; the work on droughts and heat waves by the Department of Agronomy and Land Management – University of Florence.

The methodology is centred on the risk paradigm of the research community. The risk is defined as a product of hazard, exposure and vulnerability where:

- Hazard is the threatening natural event including its probability/magnitude of occurrence;
- Exposure is the values/humans that are present at the location related to a given event;
- Vulnerability is the lack of resistance to damaging/destructive forces (damage function).

This definition has been applied to extreme events such as floods and heat/water stresses, with the due adjustments required by data availability and specific modelling techniques.

The mission of the JRC is to provide customer-driven scientific and technical support for the conception, development, implementation and monitoring of EU policies. As a service of the European Commission, the JRC functions as a reference centre of science and technology for the Union. Close to the policy-making process, it serves the common interest of the Member States, while being independent of special interests, whether private or national.